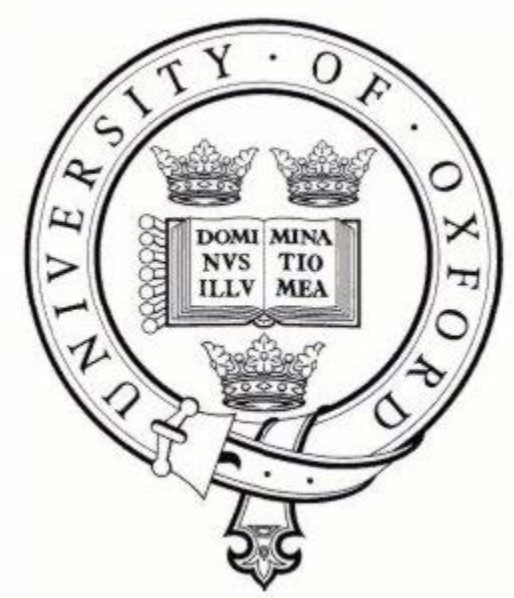
Modulation of the PD-1 pathway by inhibitory antibody superagonists



Billur Akkaya

Christ Church College

Supervisors: Richard J. Cornall, Simon J, Davis

Thesis submitted for the degree of Doctor of Philosophy

Trinity Term, 2012

Abstract

Modulation of the PD-1 pathway by inhibitory antibody superagonists

Billur Akkaya, Christ Church College

Thesis submitted for the degree of Doctor of Philosophy
Trinity Term, 2012

In metozoans, most of the key events that lead to cell activation and inhibition are controlled by tyrosine phosphorylation. Extracellular signals are transmitted by membrane bound receptors, which have intrinsic kinase activity or themselves recruit intracellular kinases to specialised inhibitory or activating phosphorylation motifs. In this way, the pattern of kinase activation creates its own turnover and can rapidly generate amplified signals by positive feedback, or recruit inhibitory proteins to counteract the signals. This process of inhibition is also constitutive since it requires continuous counter-inhibition by phosphatases at the cell surface and intracellularly even in the absence of ligands. The absence of phosphatase activity results in unbridled protein phosphorylation and form this and other data it has been proposed that the triggering of the T cell receptor and other co-receptors may result simply by physical exclusion of the large phosphatases such as CD45 from the vicinity of the receptors. Superagonist monoclonal antibodies may work in a similar way, by binding receptors close to the plasma membrane and excluding extracellular phosphatases. The work described in this thesis seeks to discover if antibody superagonists can be generated against the T cell inhibitory cell surface receptor PD-1 and test if this approach can attenuate the immune response. Using in vitro assays of lymphocyte activation and a mouse model expressing human PD-1, this study characterises a series of anti-PD-1 antibodies and shows how patterns of inhibitory activity varying according to binding sites. The inhibitory effects of the anti-PD1 antibodies are seen in the humoral, cellular and transplant immune responses. Agonistic anti-PD1 antibodies induce regulatory T cells and may have role in suppression of autoimmune disease. The thesis suggests that superagonism may be harnessed clinically to dampen the immune response, through activation of inhibitory receptors.

Acknowledgements

I completed this thesis under very exciting circumstances such as being about to move to the other side of the ocean and expecting a new baby. Although very challenging, there were wonderful people who helped and supported me to prepare a nice thesis.

First of all, I would like to express my gratitudes to my supervisors Simon Davis and Richard Cornall for their guidance and generous support. Their teaching method along with their expertise in T cell biology and immune regulation has helped me to deepen my understanding of immunology and prepared me for a future career in that field. This thesis would never be complete without their useful advices.

I am grateful to Felix Scholarship who gave me the opportunity to read for a Dphil in University of Oxford, thus made me achieve the most important milestone of my education.

I would like to thank Davis Lab and Cornall Lab members for all the fruitful discussions, technical help and also for the very friendly working environment they created. I thank Heather Brouwer and Jan Fennelly for their assistance during my first year in Davis Lab. My special thanks go to Tanya Crockford, who has always been warm and caring, for her gracious help during every step of my PhD. I must not forget Sophia Bennet, Greg Crawford, Delphine Baup, Consuelo Anzilotti, Daian Cheng and Katherine Bull for their nice personalities and supports. Finally, I should thank Olivier Morteau for his friendship and contributions to my studies.

I would not have finished this thesis without the support of my parents Ifakat Gungor, Abdullah Onur Gungor, and parents-in-law Ayse Akkaya, Sebahattin Akkaya who dedicated themselves to my wellbeing and success. Last but not least, I would like to thank my husband Munir Akkaya, my eternal love and best friend, who made the Oxford dream come true. My son Nazim Erdem Akkaya and daughter Ayse Ahenk Akkaya deserve the biggest “thank you” for the joy they have brought to every aspect of my life and for making this Oxford story even more memorable…

Contents

Abstract **i**
Acknowledgements **ii**
Contents **iii**
Abbreviations **vii**
1 Introduction
1.1 Overview of the immune system 1
1.1.1 Innate immunity 2
1.1.2 The interface between innate and adaptive immunity 5
1.1.3 Overview of the concepts relating to adaptive Immunity 7
1.2 Homeostasis of the adaptive immune system 10
1.3 The concepts of self-tolerance and autoimmunity 12
1.3.1 Central tolerance and associated autoimmune conditions 13
1.3.2 Peripheral tolerance and associated autoimmune conditions 14
1.3.3 Targeting costimulatory pathways for treating autoimmunity 16
CD28, B7-1 and B7-2 17
CTLA-4 19
ICOS 20
PD-1 21
B7-H3 22
B7-H4 22
BTLA 23
Alternative strategies: superagonist antibodies against inhibitory co-receptors 24
1.4 Role of PD-1 in regulating T cell responses 26
1.4.1 Structure of PD-1 and its ligands 26
1.4.2 PD-1 signalling 27
1.4.3 Reverse signalling by PD-L1 and PD-L2 30
1.4.4 Regulation of PD-1 expression 31
1.4.5 Biological significance of PD-1 32
PD-1 in chronic viral infections 32
PD-1 in anti-tumor immunity 34
PD-1 in autoimmunity 34
PD-1 in transplantation immunity 37
1.5 Models of T cell receptor triggering 39
1.5.1 Aggregation 40
1.5.2 Conformational change 43
1.5.3 Segregation and redistribution based models of TCR Triggering 45
1.5.4 Implications for antibody induced signalling of segregation

and redistribution-based models of receptor triggering 48
1.6 Work preceding the project 51
1.7 Objectives of this thesis 54

2 Materials and Methods
2.1 Reagents and solutions 55
2.1.1 General reagents 55
2.1.2 Cell culture media 57
2.2 Cellular methods 58
2.2.1 Hybridoma culture for large scale antibody production 58
Detection of the antibody secretion 58
2.2.2 Transfection of HEK-293T cells to analyse antibody Binding 59
2.2.3 Human peripheral blood mononuclear cell proliferation assay 59
Preparation of Dynalbeads™ 59
Preparation of antibody-coated plates 60
Preparation of the human peripheral blood polymorphonuclear cells 60
2.2.4 Stimulation assay for upregulating humanized PD-1 protein expression on the T cells of hPD-1KI mice 61
2.2.5 iTreg formation assay 61
Preparation of Dynalbeads™ and antibody coated plates 61
Preparation of the cultures 62
2.2.6 Mouse mixed lymphocyte reaction 63
2.3 Localizing the targets of anti-PD-1 antibodies in human lymphoid tissue by immunohistochemistry 64
2.4 Mice and immunizations 64
2.4.1 Humanized PD-1 knock-in mice 65
Generation of the mice 65
Genotyping strategy for the identification of mouse PD-1 and humanized PD-1 genes 65
Immunizations for the immune response models 67
Immunizations for adoptive transfer experiments 68
Immunizations for inducing experimental autoimmune encephalomyelitis (EAE) 69
2.4.2 Foxp3-GFP-hPD-1KI reporter mice 69
Genotyping strategy for the identification of the reporter allele 69
2.4.3 OT-1-GFP-hPD-1KI mice 70
Genotyping strategy for the identification of the GFP reporter allele and the TCR transgene 70
2.5 Analysis of the cellular assays and immune responses 71

2.5.1 Flow cytometry and fluorescence activated cell sorting 71
Detection of PD-1 expression on 293T cells 71
Quantification of the antibody levels on Dynalbeads™ 71
Analysis of human PBMC proliferation assay 72
Detection of the upregulation of humanized PD-1 on cultured mouse splenocytes 72
Fluorescence activated sorting of naïve $CD4^+$ T cells and analysis of iTreg formation 73
Analysis of the mixed lymphocyte reaction assays 73
Initial characterization of the immune system of hPD-1KI mice 74
Characterization of the immune responses in models of Immunity 75
Detection of SRBC induced primary germinal centre reaction *75*
Detection of the immune response to MVA challenge *75*
Analysis of the antigen specific responses in adoptive transfer experiments 75
Characterization of the time course of PD-1 expression at the onset of EAE 76
2.5.2 ELISA 76
Sheep red blood cell specific ELISA 76
2.6 Protein Methods for antibody purification 77
2.6.1 Protein G purification 77
2.6.2 Gel filtration 78
2.6.3 SDS-PAGE for detecting the purity of the antibody 78

3 Analyzing the effects of anti-PD-1 antibody agonists on human PBMCs
3.1 Introduction 79
3.2 The strategy used for the bead preparation 80
3.3 The effects of the bead-bound anti-PD-1 antibodies on primary human T cells 83
3.4 Analysis of the proliferative responses using an alternative antibody immobilization strategy 85
3.5 Discussion 87

4 Characterization of a humanized PD-1 knock-in mouse model
4.1 Introduction 89
4.2 Analysis of the expression of humanized PD-1 protein on T cells 90
4.3 Analysis of the upregulation of humanized PD-1 protein upon in vivo stimulation 90
4.4 Characterization of the immune system of naïve hPD-1KI mice 92
4.5 Testing the ability of hPD-1KI mice to mount a normal immune response 96
4.6 Discussion 98

5 The effects of PD-1 agonists on humoral and cellular immunity

5.1 Introduction 99
5.2 Effects of in vivo administration of PD-1 agonists on primary GC reactions 100
5.3 Effects of the anti-PD-1 antibodies on cellular immunity 105
5.4 The effect of anti-PD-1 antibody administration on the antigen specific $CD8^+$ T cell response 107
5.5 Effects of the anti-PD-1 antibodies on the in vitro allogeneic response 109
5.6 Discussion 114

6 Effects of PD-1 agonism on the induction of Treg formation

6.1 Introduction 116
6.2 In vitro induction of Treg formation using bead-bound antibodies against CD3, CD28 and PD-1 117
6.3 The differentiation of naïve $CD4^+$ T cells into Tregs after unlinked activation of the TCR and coreceptors 119
6.4 Discussion 130

7 The use of PD-1 agonist antibodies in experimental autoimmune encephalomyelitis

7.1 Introduction 131
7.2 Investigating a possible regulatory role for clone 19 in EAE 132
7.3 Time course of the PD-1 expression during the disease onset 133
7.4 The disease profile following the late injection of PD-1 agonists 134
7.5 Discussion 141

8 General discussion

8.1 Inhibitory effects of anti-PD-1 antibodies on human PBMCs 143
8.2 The hPD-1KI mouse model has the immunological features of WT C57BL/6 mice 145
8.3 Inhibition of the in vitro allogeneic response by clone 19 147
8.4 Effects of stimulating the PD-1 pathway during the germinal centre reaction 148
8.5 Inhibitory effects of PD-1 agonists on $CD8^+$ T cell driven immune Responses 150
8.6 Tolerogenic effect of PD-1 agonists by induction of regulatory T cells 151
8.7 Use of PD-1 agonists in models of autoimmunity 153

Bibliography 155

Abbreviations

APC	Antigen presenting cell
CD	Cluster of differentiation
CFSE	Carboxyfluorescein succinimidyl ester
CTLA-4	Cytotoxic T-Lymphocyte Antigen 4
EAE	Experimental autoimmune encephalitis
EM	Electron microscopy
Fab	Fragment antigen-binding
Fc	Fragment-crystallizable
GC	Germinal centre
GFP	Green fluorescent protein
hPD-1 KI	Humanized PD-1 knock-in
ICOS	Inducible T cell Costimulator
ICS	Intracellular cytokine staining
IFN-γ	Interferon-gamma
ITIM	Immunoreceptor tyrosine-based inhibition motif
ITSM	Immunoreceptor tyrosine-based switch motif
Koff	Dissociation rate constant
LAMP-I	Lysosomal-associated membrane protein 1
Lck	Lymphocyte-specific Tyrosine Kinase
mAb	Monoclonal antibody
MHC	Major Histocompatibility Complex
MVA	Modified Vaccinia Ankara
PBMC	Peripheral blood mononuclear cell
PD-1	Programmed Death 1
PD-L1/ 2	Programmed cell death 1 ligand 1/ 2
SAg	Superagonist
SH-2	Src Homology Domain 2
SHP-1/ 2	SH2 domain-containing protein tyrosine phosphatase- 1/ 2
SPR	Surface plasmon resonance
SRBC	Sheep red blood cell
TCR	T cell antigen receptor
Tfh	T follicular helper cells
TGF-β	Transforming growth factor beta
TNF-α	Tumor necrosis factor-alpha
Treg	Regulatory T cell

Chapter 1:

General introduction

1.1 Overview of the immune system

With the emergence of the first unicellular organism more than 3.5 billion years ago, a series of adaptations for “the survival of the fittest“ began and almost at the same time the earliest form of immunity started to develop [1-2]. The most primitive form of immunity, which presumably allowed ameoba to distinguish between food and other ameobas, has evolved into a major mechanism of host defence over time. Genomic analysis of multicellular organisms revealed that a sophisticated mechanism of host defence existed before plants and animals diverged [3]. That highly conserved mechanism among the multicellular organisms (metazoans) is the recognition of “microbial nonself” through sensing pathogen associated molecular patterns (PAMPs) which are conserved products of different classes of pathogens [4]. A second and more complex mechanism of host defence which appeared first in jawed vertebrates provided the organisms with the ability of distinguishing different nonself elements from each other by germline encoded rearrangement of their specific sensors. The major breakthrough in illuminating the occurrence of that highly specific arm of immunity was the discovery of RAG proteins (*RAG-1, RAG-2*), which orchestrate the recombinatorial gene rearrangement processes of T- cell receptors and immunoglobulins [3, 5]. The more primitive arm of the evolving immune system, which relies on constitutively produced, highly conserved sensing mechanisms and rapidly acting effector cells, is called innate immunity. The other arm, which introduces diversity to the immune system is called adaptive immunity.

1.1.1 Innate immunity

Innate immunity, the first mechanism of host defense, relies on a limited number of germline-encoded receptors that discriminate “infectious non-self” from “self”. These receptors are activated by generic products of pathogens and are called pattern recognition receptors (PRRs). In vertebrates, there are also inhibitory mechanisms which function through recognition of self molecules and sense the pathogens through their “lack of self” [6].

Invasion of the host by pathogens triggers a series of immune processes through interactions between the pattern recognition receptors and a diverse array of pathogen-associated molecules that are highly conserved and essential for the pathogen’s life cycle. Toll-like receptors (TLRs) are the most widely studied PRRs and are considered to be the primary sensors of pathogens [7]. TLRs are type 1 transmembrane glycoproteins with extracellular leucine-rich repeats that play a role in PAMP recognition, and a cytoplasmic Toll/Interleukin-1 receptor (TIR) domain that is responsible for downstream signalling. To date, in humans there are ten and in mice there are twelve TLRs identified. TLR 1, 2, 4, 5 and 6 are expressed on the cell surface and interact with extracellular components of PAMPs derived from bacteria, fungi and protozoa. TLR 3, 7, 8 and 9 are expressed on endosomal membranes and primarily recognize nucleic acid PAMPs from viruses and bacteria that have been phagocytosed by cells [7-10]

In addition to TLRs, there are several other membrane-bound, soluble and cytosolic PRRs present in the innate immune system. C-type lectins, scavenger receptors and N-formylmethionyl receptors are other transmembrane PRRs. C-type lectins recognize carbohydrate structures on the cell walls of microorganisms. Some of the C-type lectins play a role in phagocytosis of the microbes and some of them, such as Dectin-1, assist TLR signalling. Scavenger receptors and N-formylmethionyl receptors are expressed by phagocytes and allow

these cells to detect microbes and respond against them [11]. Soluble PRRs, also known as acute phase proteins, are essential for the clearance of apoptotic cells and their components from blood and mucosal tissues by phagocytosis. They can also opsonize microbial cells for facilitating their phagocytosis and complement mediated destruction. Soluble PRRs are divided into three groups: collectins, ficolins and pentraxins [12-13]. RLRs (RIG-I-like receptors) and NLRs (NOD-like receptors) constitute the two major cytosolic PRRs [11]. Two well-known members of RLRs, RIG-I and MDA5 recognize different types of viral RNAs in the cytosol, whereas the recently identified member DAI recognizes viral DNA. NLRs are categorized into three subfamilies according to possession of one of the three major domains: a caspase recruitment domain (CARD) present in the NOD subfamily, a pyrin domain present in the NALP subfamily and a BIR domain (Baculoviral inhibitor-of-apoptosis-protein repeat-containing domain) present in the NAIP subfamily. Members of the NOD subfamily are involved in recognizing bacterial peptidoglycan and are also responsible for production of antimicrobial peptides. NALP and NAIP subfamilies are involved in the induction of an inflammatory response mediated by the IL-1 family of cytokines [12, 14-18].

In vertebrates there are other mechanisms for distinguishing infected cells as well as cells that are malignantly transformed. NK cells are the unique innate effector cells of the vertebrates which provide a special defense against intracellular pathogens, particularly viruses [12]. They express two types of receptors, activating and inhibitory, which regulate the function of NK cells. It's the balance between the activity of these two receptor types which determines the outcome of the NK cell response [19].

Mouse Ly49 family receptors specifically recognize MHC-I and related molecules and the majority of them are inhibitory. Inhibitory members transmit signals through their immunoreceptor tyrosine-based inhibition motifs (ITIM) whereas the activating receptors bear immunoreceptor tyrosine-based activation motifs (ITAM) and function through an adapter called

DAP12 [20]. In humans and primates, Ly 49 family is replaced by the killer immunoglobulin-like (KIR) family of receptors which also consists of activating and inhibitory receptors with ITAMs and ITIMs, bind MHC-I and related molecules, and are highly polymorphic [21]. The inhibitory receptors generally interact with self proteins and provide a mechanism to limit NK cell activity against self tissue [19]. On the other hand, the function of the activating members of these receptors is less clear and they are thought to evolve as part of a defense mechanism against the pathogens which express surface proteins mimicking self proteins of the host [22]. Although it has long been thought that all NK cells recognize self-MHC by the inhibitory Ly49/KIR family of receptors and stay tolerant to self-tissue, and are in this way “licensed”, it has recently been shown that a population of NK cells which do not recognize self MHC also exists [23]. These “unlicensed” NK cells were shown to be hyporesponsive in the steady state but since their activity is not restricted by the inhibitory receptors that recognize self MHC, they control viral infections better than the “licensed” NK cells [24]. There are also CD94–NKG2A/C/E heterodimers that recognize non-classical MHC molecules, HLA-E in humans and Qa1 in mice. HLA-E and Qa1 bind peptides derived from the leader sequence of classical MHC class I molecules, so they may reflect and help monitor the levels of MHC-I expression indirectly [25-26]. KLRG1 is another ITIM bearing inhibitory NK cell receptor that recognizes E-, N- and R-Cadherin positive targets [27]. It is thought to prevent damage to healthy tissue expressing normal levels of Cadherins and also to help NK cells detect malignant tissue with reduced Cadherin expression [28].

NKG2D is an activating NK cell receptor that exists as a homodimer and recognizes “stressed” cells [29]. It binds to the MHC-I related molecules whose expression is regulated by DNA damage and heat shock response pathways which are often activated in malignantly transformed cells [30]. Signalling through either DAP10 or DAP12, NKG2D induces cytokine secretion and cytotoxicity [31]. It may also induce cytotoxic T cell (CTL), Th1 and Th2 cell

responses against immunogenic tumors [32]. Natural cytotoxicity receptors (NCR) are other activating receptors present on NK cells [33] thought to recognize tumor cells and regulate anti-tumor immune responses; however, their mechanism of action is yet to be clarified [23].

The 2B4 receptor (CD244), which is present on all human and mouse NK cells, binds CD48 expressed on all hematopoietic cells [34]. It has been postulated that CD244 could be a multifunctional receptor since it may be either activating or inhibitory depending on the adapter it recruits [23]. In humans although it was shown to play an important role in rejection of melanoma cells expressing CD48, its involvement in the rejection of other tumor types is unknown [35]. NK cells also express some costimulatory molecules that provide further stimulation. These are DNAM-1, NKR-P1 and PIL receptors. Some recent reports suggest that DNAM-1 and NKR-P1 may be more than just costimulatory receptors and may present unique MHC independent self/nonself discrimination properties and may play crucial roles in tumor immunity [23]. PIL receptors are suggested to recognize carbohydrate chains on target cells, which therefore broadens the range of the target molecules that NK cells can recognize [36].

1.1.2 The interface between innate and adaptive immunity

Discrimination of self and non-self is a key requirement of the immune system. Although PRRs provide a fast detection mechanism for pathogens, the innate immune system has also evolved other receptors to recognize pathogens such as the specialized receptors that enable NK cells to sense “non-self”, “missing-self” and “induced self” [37]. However, these sensing mechanisms are not sufficient to develop a fully specialized response consisting of memory, which required the development of adaptive immunity.

Specific responses against protein antigens are generated by T cells of the adaptive immune system that recognize the antigens presented on other cells in the context of MHC. Antigen

presentation is therefore one of the most important functions of the innate immune system which is executed by highly specialized cells such as dendritic cells (DCs) and also by macrophages, B cells and non-professional antigen presenting cells such as epithelial cells and fibroblasts [3]. Immature myeloid and plasmacytoid DCs are the phagocytic cells, which are derived from the same bone marrow precursors as macrophages and are of unclear ontogenic origin, respectively, perform most of the antigen presentation at the steady state [38-39]. They are mainly responsible for scanning the peripheral tissues by continuous macropinocytosis as well as for detecting pathogens via the PRRs on their surface [3]. Upon binding pathogens by TLRs they mature through upregulating MHC-I, MHC-II molecules and the costimulatory molecules B7-1 and B7-2 to establish an optimal interaction with naïve T cells [37]. In addition to their role in the discrimination of self from infectious non-self, TLRs on the surface of DCs provide an adjuvant effect upon binding the PAMPs and therefore are essential for the initiation of the adaptive immune response [40] .

There are several modes of pathogen recognition that help DCs to present antigens and activate the adaptive immune response. These are: cell-extrinsic recognition of pathogens by TLRs, cell-intrinsic recognition of pathogens by RLRs/NLRs and cell-intrinsic recognition of infected cells by endosomal TLRs [41]. Cell extrinsic recognition of pathogens is facilitated through surface TLRs that detect bacteria and are internalized into the phagosome where bacterial antigens are processed for presentation on MHC-II. Bacterial antigens and PAMPs are co-localized in the same phagosome, so that the DC recognizes their common origin. TLR-mediated recognition of bacterial PAMPs promotes the selection of bacterial antigens for optimal presentation on MHC-II and leads to the induction of costimulatory molecules and cytokines necessary for activation and differentiation of T lymphocytes [42]. DCs directly infected by viruses implement cell-intrinsic recognition mediated by the recognition of viral PAMPs within the cytosol by RIG-I like receptors (RLRs) [43]. Cytosolic viral proteins are

processed and presented on MHC-I (via the conventional endoplasmic reticulum pathway) or MHC-II (via autophagy) [41, 44]. RLR signaling induces costimulatory molecules and cytokines necessary for activation and differentiation of T lymphocytes. In this mechanism, how the origin of antigen is established is unclear. In the case of the MHC-I pathway, this may depend on the abundance of viral antigens [41]; for MHC-II, it may depend on targeting of viral antigens by the autophagy machinery [45]. Cell-extrinsic recognition of infected cells starts with recognition of the viral PAMPs in the cytosol via the RLRs [46]. This leads to secretion of type I interferons (IFNs) and other factors that activate DCs. Infected dead cells are then phagocytosed by noninfected DCs, and viral PAMPs are recognized through endosomal TLRs which in turn induce costimulatory molecules and cytokines necessary for activation and differentiation of T lymphocytes [12]. Viral antigens are processed and presented on MHC-II (via the conventional endosomal pathway) or MHC-I (via cross-presentation) [41].

1.1.3 Overview of the concepts relating to adaptive Immunity

Effector cells of the adaptive immune system, namely lymphocytes, which are specific for a large number of antigens, exist prior to exposure to the antigen and when the lymphocyte, which bears only one type of antigen receptor, encounters the specific antigen, it gets selected and activated. This fundamental concept is called the “clonal selection hypothesis” [47]. An early and incomplete form of this idea was first proposed by Niels Jerne, in 1955, in the form of a natural selection theory, hypothesizing that a large number of randomly diversified immunoglobulins existed in all individuals [48]. However, he was postulating that “protein replication” is the reason for the increasing titer of the antigen-specific antibodies. In 1957, Macfarlane Burnet published a modified version of Jerne's theory of antibody formation but incorporating the concept of clonal selection. Burnet proposed that the antibody-producing cells, rather than individual antibody

molecules, were the unit of selection, undergoing rounds of selection against antigen [49]. Further evidence for the clonal selection theory was produced by Nossal and Lederberg who showed that single plasma cells produced antibodies with a single specificity [50]. Although it was widely accepted, the clonal selection theory raised a mechanistic issue: if an organism can produce antibodies against almost any protein that is derived from any other organism, how can its genome encode for more individual antibody molecules than the total of its proteins [51]? In 1959, Talmage proposed a quantitative model of immune specificity and postulated that the recognition of near-infinite number of antigens did not require an equally large primary antibody repertoire. In this way he made germline recombination as a source of antibody diversity seem plausible [47, 51-52].

Until the early 1960s, the thymus had not been recognized as an immunological organ and the distinction between T and B lymphocytes had not yet been introduced [53]. Towards the late 1960s, Miller demonstrated the existence and functional difference of thymus derived lymphocytes (later known as T cells) and bone marrow derived lymphocytes (later known as B cells) by using irradiated adult thymectomized mice to which genetically different mouse cells were transferred. He showed that thymus-derived cells could be activated specifically by antigen, that they were not the precursors of antibody-forming cells, and that they were essential to provide help for other lymphocytes that are derived from bone marrow so that those lymphocytes can respond to antigen by producing antibody [54-58]. In the mid 1970s, discovery of MHC restriction clearly indicated that T cells recognize a fundamentally different form of antigen from B cells and in a different context [59]. However, the antigen receptor on T cells could not easily be identified partly due to the limited technology and partly due to the misdirected debates on whether T cells express a membrane-bound form of immunoglobulins and whether TCRs share common idiotypic determinants with immunoglobulins [60].

Contrary to the studies carried out on the T-cell antigen receptor (TCR) in the 1970s, studies on antibody diversity provided fruitful evidence for germline recombination. Tonegawa showed that variable and constant regions of antibodies are encoded by different gene segments in the germline DNA which become adjacent in the mature B cells [61]. This was the evidence of somatic gene rearrangement. Finally, in the late 1980s and early 1990s, the factors responsible for the gene rearrangement, recombination activating gene 1 and 2 (RAG-1 and 2) were isolated by Schatz and Baltimore [62]. The 1980s were also successful years for studies on T cells. In the first half of the decade, the TCR protein was identified by Allison, Reinherz, and by Kappler and Marrack who used monoclonal antibodies against T cell clones for detecting the TCR [63-65]. In the rest of the decade, the MHC structure was solved by Bjorkman [66] and TCR α, β, γ, δ genes were characterized by Davis and Hedrick and also by Tak Mak using subtractive hybridization methods [67-68]. Identification of TCR cDNAs led to an understanding of how the TCR repertoire is generated. It has also paved the way for the development of TCR transgenic mice, transfected cell lines and hybridomas, which helped clarify our understanding of how T cells can recognize both peptide and MHC molecules with a single receptor and provided insights into the thymic selection process [60].

Through all these studies and many more beginning more than fifty years ago, the major characteristics of the adaptive immune system, namely specificity and diversity, have been illuminated.

1.2 Homeostasis of the adaptive immune system

The immune system has the ability of maintaining a state of equilibrium, even during the immune responses against diverse pathogens, despite the continuous interaction of the immune effector cells with self-antigens. This balance is called immune homeostasis. For immune homeostasis to be achieved, three conditions must be met: maintaining the survival of naïve lymphocytes, terminating immune responses properly and eliminating autoreactivity [69].

The survival stimulus for naïve lymphocytes is given through antigen receptors. A continuous, low–affinity interaction with self-antigens together with the anti-apoptotic signals induced by IL-7 for T cells and B cell activation factor (BAFF) for B cells seem to be enough to promote survival of naïve cells [70-71]. It is also suggested that homeostasis of memory lymphocytes is maintained by an antigen independent mechanism similar to that of naïve lymphocytes which requires self–recognition rather than antigen exposure [70].

Immune activation requires two important signals. The first signal is antigen, which determines the specificity of the response and the second signal is provided by costimulatory molecules in the case of T cell activation and most commonly by the complement product C3d in the case of B cell activation. Other accessory signals such as secretion of cytokines are also important for further enhancing and modifying effector cell function [69]. CD28-B7 family members are the best-defined costimulatory molecules. B7 molecules, B7-1 and B7-2, are upregulated on antigen presenting cells (APCs) by the cytokine milieu generated during innate immune responses against pathogens. CD28 acts as a receptor for those costimulatory molecules and provides the necessary signals for T cell activation and survival [72]. ICOS, which belongs to the CD28 family of co-receptors, is upregulated upon T cell activation and its interaction with the constitutively expressed ICOS ligand (ICOSL, also known as LICOS, B7-H2, GL50, B7RP-1, B7h) also promotes T cell activation and effector function [73]. CD21 is a costimulatory receptor

expressed on mature B cells and follicular dendritic cells (FDCs). It enhances signaling through the B cell receptor in response to T cell dependent, complement tagged antigens as well as antigen transport in B cells and antigen retention in FDCs [74-75]. The CD40-CD40L interaction also provides a costimulatory second signal for B cells [76].

There are passive and active mechanisms for preventing and terminating immune responses. When the main antigenic stimulus disappears or the second signal is absent, the passive mechanisms that result in either functional inactivation of the lymphocyte or programmed cell death are implemented [69]. Antigen recognition in the absence of second signals or in the presence of negative costimulatory signals, such as CTLA-4 and PD-1, may result in a state of functional unresponsiveness, called anergy [77-79]. It is also suggested that suboptimal antigenic stimulus leads to T cell anergy even in the presence of a second signal [80]. Anergy may also be a common mechanism for both B cells and T cells for limiting the responsiveness against self-antigens and foreign antigens administered without adjuvants as both conditions lack a second signal [81-82]. “Death by neglect” is another passive mechanism that is probably responsible for the rapid elimination of a huge number of effector lymphocytes by programmed cell death when an immune response is in decline. It is mediated by decreased expression of anti-apoptotic molecules such as Bcl-2 and Bcl-XL due to lack of essential survival stimuli [69]. The pool of naïve and memory cells is not affected by this process. This may be because they are less dependent on antigen and the second signal, therefore, they continue to express anti-apoptotic molecules [83]. Active mechanisms for terminating immune activation are mainly described for T cells and can be grouped into three types: activation induced cell death (AICD) mediated by negative costimulatory molecules, Fas mediated AICD and regulatory T-cell (Treg) mediated AICD. Inhibitory members of the CD28 family, i.e. CTLA-4, PD-1 and BTLA are upregulated on T cells upon activation. Upon triggering their intracytoplasmic tyrosine residues recruit phosphatases and terminate the T cell activation signal [84].

The activation of T cells also causes co-expression of death receptor Fas (CD95) and its ligand FasL on T cells. Fas-FasL interactions between neighbouring cells result in apoptosis. Fas mediated apoptosis is distinguished from passive cell death by some unique features. It is induced by repetitive encounters with antigen, potentiated by IL-2 and not affected by decreased Bcl-2 or Bcl-XL expression [85]. IL-2 may have a dual effect on lymphocytes depending on the stage of the immune response. This has been suggested by the observation that IL-2 deficient mice develop autoimmunity rather than immunodeficiency. In the early stages of the immune response IL-2 may display its growth promoting effects and towards the end accumulated IL-2 may induce Fas mediated apoptosis, helping to maintain homeostasis [86-88]. Upon antigen exposure, the pool of naïve lymphocytes differentiates into both effector and regulatory cells. Regulatory T cells release two important anti-inflammatory cytokines, TGFβ and IL-10, which limit inflammatory processes and the expansion of effector T cells. They have a crucial role especially in suppressing self-reactive T cells in the periphery [69].

Maintaining self-tolerance is another aspect of immune homeostasis. It is still debated whether there is an overlap or a clear distinction between the mechanisms used for limiting normal immune responses against foreign antigens and preventing the action of self-reactive lymphocytes.

1.3 The concepts of self-tolerance and autoimmunity

Despite being continuously exposed to self-antigens, effector cells of the immune system are capable of maintaining their non-responsive state against self, in a process called self-tolerance. It is maintained by controlling the generation of self-reactive lymphocytes in the central lymphoid organs and further controlling their activation, expansion and survival in the periphery [89]. Autoimmunity, which means reactivity against self, is the most inevitable outcome of broken

self-tolerance. Transgenic mouse models of autoimmunity and the phenotype based modelling of human diseases by N-ethyl N-nitrosourea (ENU) mutagenesis have provided effective tools for deciphering the underlying mechanisms of both monogenic and complex autoimmune disorders [90].

1.3.1 Central tolerance and associated autoimmune conditions

Central tolerance is achieved by successful positive selection, negative selection and receptor editing processes and allows development of a self-tolerant lymphocyte repertoire in bone marrow and thymus. There are a number of autoimmune diseases that can be ascribed to genetic abnormalities in the thymus. Since proper antigen expression and presentation play important roles in intrathymic selection processes, any defect in either of the processes results in overt autoimmune phenotypes. This may be the explanation for the link between certain HLA alleles and autoimmunity. Reduced expression of self-antigens in thymus is the underlying mechanism for several autoimmune diseases [90].

AIRE encodes a transcription factor that regulates expression of a variety of self-antigens in the thymus. In humans, its deficiency leads to a monogenic disease called autoimmune polyendocrinopathy candidiasis ectodermal dystrophy (APECED). APECED patients and AIRE deficient mice display a similar phenotype with multiple tissue specific antibodies, lymphocytic infiltration and autoimmune destruction of multiple endocrine and non-endocrine organs. The possible mechanism of autoimmunity is that in the absence of AIRE, tissue specific antigens are not expressed in the thymus and thymocytes specific for those antigens that cannot be deleted, escape to the periphery [91]. For example, polymorphisms of the insulin gene which lead to a decreased expression of insulin in the thymus lead to type 1 diabetes [92]. The presence of insulin specific T cells in the pancreatic draining lymph nodes further indicates the reason for

pathology. Although the exact mechanism is yet to be confirmed, a similar etiopathogenesis is ascribed to Myasthenia Gravis and Graves Disease [90].

Parallel to the defects in antigen expression and presentation, defective TCR signalling may also result in a lack of central tolerance. For example, mice carrying a missense ZAP-70 mutation which causes a partial defect in TCR signalling, were shown to display an autoimmune phenotype similar to rheumatoid arthritis [93]. Although both positive and negative selection processes are altered in these mice, the overall effect is probably due to impaired negative selection which leads to an escape of autoreactive clones to the periphery where dysfunction of thymus derived natural Tregs may also contribute to the pathology [94]. This is an important observation that shows the link between the decreased responsiveness of thymocytes and autoimmunity [93].

1.3.2 Peripheral tolerance and associated autoimmune conditions

Presentation of self-antigens in the periphery poses a risk for the propagation of autoreactive clones that escape from negative selection. However, there are several mechanisms for preventing the action of autoreactive lymphocytes in the periphery. Peripheral tolerance is maintained mainly by the suppressive action of Tregs and tolerogenic APCs using several mechanisms. As will be discussed, inhibitory members of the CD28 family co-receptors play crucial roles in these mechanisms.

APC maturation is skewed towards a tolerogenic phenotype in the presence of abundant apoptotic cells in the environment. The main function of tolerogenic APCs is to uptake the debris of apoptotic cells and constantly present self-antigens to T cells. This interaction may induce anergy in T cells through upregulation of CTLA-4 and PD-1. Chronic interactions with self-

antigens may also result in peripheral deletion of autoreactive cells upon Fas-FasL interaction and through apoptosis mediating Bim-dependent processes [83].

Tregs constitute a group of regulatory cells with heterogeneous phenotypes for which it is difficult to attribute a universal mechanism of action to their regulatory function [95]. However, accumulating evidence suggests that the possible core mechanism of thymus-derived Treg (natural Treg) mediated suppression depends on CTLA-4 and IL-2. CTLA-4 may mediate suppression of APCs through downregulation of surface B7-1 and B7-2 and also by occupying those ligands on APCs therefore outcompeting CD28 expressed by effector T cells [96]. In parallel to the CTLA-4 mediated effects, Tregs may absorb IL-2 using their high affinity IL-2 receptors and leave the surrounding cells deprived of the essential survival stimulus, or they may directly inhibit IL-2 mRNA expression in Foxp3- T cells (non-Tregs) [97]. The effector T cells which contact with the Treg-conditioned APCs may either become anergic due to lack of costimulation or die through apoptosis due to lack of IL-2 [89, 96-97].

Treg formation can also be induced in the periphery in the presence of sub-immunogenic doses of antigen and TGF-β. Similar to nTregs, induced Tregs (iTregs) express high levels of CD25, CTLA-4, GITR, PD-1 and PD-L1. However, the crucial molecules for the function of iTregs may be PD-1 and PD-L1 rather than CTLA-4. Ligation of PD-1 has been shown to induce iTreg formation and enhance their suppressor functions. Studies of PD-L1 suggested that it may condition the DCs and impose a tolerogenic phenotype on them by decreasing B7-1 and B7-2 expression. Furthermore, PD-1 expression on DCs may also negatively regulate DC function [98]. In contrast to inhibitory receptors, the activating costimulatory receptor CD28 may not be crucial for the function of Tregs. However, it constitutes an essential element for the differentiation of nTregs in the thymus, and therefore can be considered to have an indirect role in peripheral tolerance [99].

Defects in the components of peripheral tolerance may also result in autoimmunity. Several mutations in the Foxp3 gene cause a rare X-linked recessive disorder that has been linked to a lack of Tregs. That syndrome is called IPEX (immune dysregulation, polyendocrinopathy, enteropathy, X-linked syndrome) and leads to severe, multi-organ, autoimmune phenomena including enteropathy, chronic dermatitis, endocrinopathy and other organ-specific diseases such as anemia, thrombocytopenia, hepatitis and nephritis [100].

A variety of CTLA-4 polymorphisms have been associated with a diverse array of human autoimmune diseases and so the CTLA-4 gene is considered to be a general susceptibility locus [90]. The importance of CTLA-4 has also be proven by the phenotype of CTLA-4 deficient mice which display severe autoimmunity and die at 2-3 weeks of age due to massive lymphocytic infiltration of the major organs [101]. PD-1 polymorphisms have also been associated with human autoimmune diseases but PD-1 deficient mice develop a less severe autoimmune phenotype compared to the CTLA-4 deficient mice [90, 102-103]. This could be due to overriding positive costimulation through CD28 in the absence of CTLA-4.

1.3.3 Targeting costimulatory pathways for treating autoimmunity

According to the paradigm of costimulation, T cells require two signals in order to exert their functions [104]. Interaction of TCR with peptide-MHC complex provides the first signal which is modified by the second signal produced by the CD28 family of costimulatory receptors [105]. Costimulatory receptors can either increase the strength of the first signal and sustain the activated status of T cells, as in the example of CD28 and ICOS, or they can limit or attenuate the signal as in the case of CTLA4 and PD-1 [84]. Therefore, biological agents targeting costimulatory molecules have great therapeutic potential.

Currently, there are several modalities for treating the human autoimmune diseases using biological agents. These are cell depletion strategies, strategies targeting the inflammatory cytokines and strategies influencing cell signalling [106]. In this section, strategies influencing cell signalling will be discussed from a costimulaton related perspective. This section will focus on the members of CD28/B7 family since they are closely related molecules that are likely to be triggered in the same way.

CD28, B7-1 and B7-2

CD28 is constitutively expressed on T cells and plays a critical role in T cell activation. It has been shown that the deficiency of CD28 or the blockade of the CD28/B7 axis decreases the disease severity in mouse models of lupus, multiple sclerosis, myocarditis, arthritis, thyroiditis and myasthenia gravis [107-112] and confers resistance to EAE induction and progression in NOD mice [113]. However, administration of the blocking agent late in the disease process had no effect on progression of the ongoing autoimmune reaction in NOD mice (ref. [114]). This suggests that the beneficial effect of CD28 blockade in mouse models of autoimmunity may be limited to the inhibition of the primary autoreactive responses and that the CD28 pathway plays a less prominent role if antigen expression continues and memory cells are the cause of autoimmunity [115-116]. Since this type of continuous exposure and memory phenotype of the autoreactive cells is the common features of many autoimmune processes, blockade of CD28 may not be the ideal therapeutic option.

Stimulation of the CD28 pathway has also been attempted as an unusual strategy for treating autoimmune disorders. It was shown that a special class of monoclonal antibodies against CD28, called CD28 superagonists, effectively promoted expansion of Tregs and therefore inhibited immunopathology in mouse models of autoimmunity [117]. Further studies on non-

human primates provided consistent results. However, healthy human subjects each developed massive cytokine storm during a phase I clinical trial, whereupon the study was stopped [118]. The reason for the cytokine storm was probably the activation of the human effector memory $CD4^+$ T cells which express CD28. This was not anticipated after pre-clinical trials since this $CD4^+$ T cell subset does not express CD28 in mice and non-human primates [119].

B7-1 and B7-2 are the first-described members of the B7 family of costimulatory ligands. They regulate various immune processes mainly through their interactions with the activating costimulatory receptor CD28 and the inhibitory costimulatory receptor CTLA-4 [84]. Strategies for blocking B7-1 and B7-2 have been tried in EAE and diabetes models. Anti-B7-1 monoclonal antibody (mAb) treatment inhibited the clinical signs of EAE whereas anti-B7-2 mAb exacerbated the disease [120]. The relapsing-remitting EAE model utilizing some other mouse strains showed that anti-B7-2 treatment has no effect on relapses however anti-B7-1 mAb caused exacerbation of the relapses. In the same study, it was also demonstrated that treatment with the Fab fragment of anti-B7-1 antibody results in clinical remission [121]. This difference between the intact antibody and the Fab fragment may be attributed to the cross-linking effect of the whole antibody, which may trigger intracellular signalling events. Indeed, this type of reverse signalling has been demonstrated in CTLA-4-Ig and CD28-Ig treated DCs [122-123]. In contrast to the EAE studies where B7-2 blockade did not have any effect, anti-B7-2 treatment was shown to prevent clinical disease in NOD mice if it was given early in the disease process [124]. Altogether, evidence suggests that B7 molecules may not be reliable targets for the therapy of autoimmune diseases due to blocking of the regulatory B7- CTLA-4 interaction, their intrinsic signalling properties and unpredictable actions in different animal models of autoimmunity. Furthermore, the inhibitory effects of the bidirectional signalling between programmed death ligand-1 (PD-L1) and B7-1 has to be taken into account while targeting the B7-1 molecule by blocking agents [125]. Nevertheless, there are still some ongoing clinical trials

testing anti-B7-1 and anti-B7-2 mAbs for psoriasis and the prevention of graft vs. host disease [126].

CTLA-4

CTLA-4 is an inhibitory member of CD28 family of costimulatory receptors, which is rapidly upregulated on T cells upon T cell activation and CD28 engagement. It is probably the most well-known costimulatory candidate for treating autoimmune disorders. It is used in the soluble Ig form for blocking B7-1 and B7-2 molecules, thus preventing their interaction with CD28. CTLA-4-Ig also has the potential to inhibit DC function through reverse B7-1 signalling [127]. Although it has been shown to decrease the number of nTregs in transplant models [128-129], some studies suggested that this effect may be countered by improved regulatory function [130] and enhanced iTreg formation in the periphery [131]. The effect of the CTLA-4-Ig treatment on Tregs has to be re-addressed by further studies.

An ameliorating effect of CTLA-4-Ig has been demonstrated in a variety of animal models of human diseases such as lupus, EAE and allergic contact dermatitis [107, 132-133]. Furthermore, it has been shown that it prevents rat cardiac allograft rejection, improves graft survival, prevents autoimmune glomerulonephritis, and suppresses collagen-induced arthritis and clinical disease in NOD mice [133-135]. Although CTLA-4-Ig administration is widely accepted as a potential therapy option, in an EAE study a disease exacerbating effect was observed with multiple CTLA-4-Ig injections [136]. In the same study, blockade of B7-2, but not B7-1 also resulted in exacerbation of the actively induced EAE. The enhanced disease caused by the multiple injections of CTLA-4-Ig or the single injection of anti-B7-2 suggests an inhibitory function for the interaction of B7-2 with its counter-receptors CD28 and CTLA-4 in EAE. Therefore, proper timing for the intervention is a crucial factor for this mode of treatment. CTLA-

4-Ig has been tested in clinical trials for rheumatoid arthritis and demonstrated to increase remission rate in patients [137]. It is currently available on the market and a second generation CTLA-4-Ig has also recently been approved by the FDA for the prevention of acute rejection in renal transplant patients [138].

Targeting CTLA-4 by agonist antibodies might be another strategy for inhibiting immune responses, however, it has long remained under-valued among the other strategies. In one study, allogeneic T cell responses were shown to be inhibited when the recipients were transferred with the allogeneic tumour cells that were engineered to express a dimeric scFv against CTLA-4 [139]. The same group also generated a transgenic mouse model expressing a CTLA-4 specific scFv on B cells and showed that expression of this CTLA-4 agonist inhibited the autoreactive T cell responses and protected NOD mice from spontaneous diabetes [140]. They suggested that membrane bound CTLA-4 antibodies cross-link CTLA-4 and therefore lead to a strong inhibitory signal despite the observation that the soluble antibodies which are also capable of cross-linking CTLA-4 are rather blocking [139, 141]. One possible explanation for this discrepancy might be that the short membrane-bound scFv acts in an analogous way to CD28 superagonists (see 1.6.3) and induces strong signalling due to the size dependent exclusion of the large tyrosine phosphatases from the immune synapse.

ICOS

ICOS is a second positive costimulatory molecule of the CD28 family, with different characteristics to CD28. In contrast to CD28, ICOS is inducibly expressed upon T cell activation and its deficiency does not impair the activation of naïve T cells [142]. Its deficiency instead leads to hypogammaglobulinemia and defective germinal centre formation in mice and humans [143-144]. Recent studies have also demonstrated a role for ICOS in the maintenance of the

effector memory T cell pool [145]. These observations suggest that ICOS may be essential in perpetuating ongoing immune responses. Since elimination of the memory responses is a crucial strategy for treating autoimmunity, blockade of the ICOS pathway may provide a potential option for therapy. Blocking antibodies against ICOS have provided disease amelioration in GVHD in mouse models [146-147]. There are also ongoing in vivo trials for the fully humanized mAbs against ICOS and ICOSL [148-149].

PD-1

PD-1 plays critical roles in autoimmunity, tumour immunity, transplantation immunity and immune privilege. In the last decade, the potential benefits of blocking PD-1 action have been extensively investigated and a fully humanized blocking antibody against PD-1 has already been approved for clinical trials in cancer and chronic infectious diseases [150]. However, the advantage of triggering PD-1 has not yet been widely studied except for a few studies carried out on mouse models of autoimmunity. Genetically modified DCs that overexpress PD-L1 together with the myelin oligodendrocyte glycoprotein (MOG)-MHC-II were generated and tested in an EAE model. Mice treated with those DCs had less central nervous system inflammation with a notable clinical remission [151]. Furthermore, a recombinant adenovirus expressing full length PD-L1 administered to BXSB mice displayed a moderate suppression in the lupus like syndrome with lower frequency of proteinuria, reduced amount of anti-dsDNA and improved renal pathology [152]. The roles of the PD-1 pathway in immune regulation and a PD-1 agonism-based therapeutic strategy are discussed below.

B7-H3

B7-H3 is also a member of the B7 family of costimulatory ligands which has a wide tissue expression. Although its receptor has not yet been identified, it is probably expressed on activated T cells and is distinct from CD28, ICOS, CTLA-4 and PD-1 [153]. The treatment of T cells with B7-H3-Ig was shown to reduce proliferative responses to anti-CD3 antibodies in vitro [154]. In an EAE model, its blockade resulted in increased CNS inflammation and exacerbation of the disease [155]. Although it could be considered to be a potential candidate for immune modulatory strategies, there is still some controversy with regard to its actual role. In two different studies carried out on transplant models, its blockade has been shown to both prevent and accelerate graft rejection [156-157]. One of the reasons for this discrepancy may be the presence of different activating and inhibitory receptors for this ligand [157]. Therefore, its mechanism of action needs more detailed study.

B7-H4

B7-H4 is yet another recently described member of the B7 family. Signalling through an unknown receptor, B7-H4 was shown to inhibit T cell proliferation [158-159] and its increased expression has been associated with a tolerogenic phenotype of APCs [160]. Its blockade led to accelerated disease onset and increased disease severity in EAE models [158]. Furthermore, early treatment with B7-H4-Ig increased Treg numbers in pancreas and reduced the insulitis scores in NOD mice [161]. Overall, the current evidence suggests that B7-H4 may be a potential therapeutic target.

BTLA

B and T cell lymphocyte attenuator (BTLA) is an unusual co-inhibitory receptor of the CD28 family insofar as it also acts as one of the ligands of a TNF receptor superfamily protein, called Herpes virus entry mediator (HVEM) [162]. HVEM acts as a bi-directional switch for regulating various innate and adaptive immune responses. Upon binding the Ig superfamily (IgSF) members CD160 and BTLA, it induces inhibition on NK cells and T cells [163]. Its engagement with LIGHT (short for “lymphotoxin-like, exhibits inducible expression, and competes with herpes simplex virus glycoprotein D for HVEM, a receptor expressed by T lymphocytes”), and lymphotoxin α (LTα) results in positive costimulatory signals leading to T cell activation and inflammatory responses [164-165]. BTLA deficient mice are prone to develop autoantibodies and develop liver inflammation in old age [166]. Those mice are also susceptible to EAE and allergic airway inflammation [84, 167]. HVEM deficiency also leads to autoimmunity suggesting that co-inhibitory signalling through HVEM/BTLA and HVEM/CD160 pairs may play a superior role compared to the positive costimulation provided by the LIGHT/HVEM interaction [168]. Furthermore, polymorphism of the human BTLA gene was shown to increase the risk of rheumatoid arthritis [169]. However, recent data emphasizing the costimulatory effect of BTLA-HVEM engagement, which leads to increased NF-κβ activation and survival signals downstream of HVEM but not BTLA, suggests that strategies for augmenting signalling through HVEM may not result in inhibition [170]. Therefore, a safer alternative therapy option would be directly targeting BTLA by agonist antibodies. Indeed, in a human GVHD model, treatment with an agonistic BTLA antibody prevented GVHD while maintaining responses against viral and bacterial pathogens through selectively inhibiting effector T cells and expanding nTregs [171]. This suggests that BTLA agonists could be used to preventing the aberrant immune responses without causing global immunosuppression.

Alternative strategies: superagonist antibodies against inhibitory co-receptors

In contrast to the idea that T cell activation requires two indispensible signals, through the TCR and the costimulatory receptor CD28 [104], a class of monoclonal CD28 agonists has been shown to induce T cell activation in the absence of a TCR derived signal [172]. This process is called antibody superagonism. Structural studies demonstrated that conventional (i.e. costimulatory) CD28 agonists bind to the membrane distal epitopes on CD28 that are close to the ligand binding site whereas CD28 antibody superagonists bind to membrane proximal epitopes [173]. Since both types of antibodies are capable of cross-linking CD28, their distinct activities may be attributed to the topology of the antigen-antibody complexes they form. Formation of a relatively compact complex upon binding of an antibody superagonist presumably results in a closer association of T cell and APC membranes. This may lead to the size-dependent reorganization of the signalling elements at the cell-cell contact from where the large phosphatases, such as CD45, are passively excluded. Thus, small kinases such as Lck are enriched at the immune synapse and the net effect would be a strong phosphorylation of CD28 [173-174].

Although the antibody superagonists were first described against CD28, they may target any receptor that is capable of signalling through the intracytoplasmic tyrosine motifs. Receptors with those motifs require extrinsic kinases to become phosphorylated and to effectively recruit intracytoplasmic signalling molecules. Most of the cell surface receptors are negative co-receptors with immunoreceptor tyrosine-based inhibition motif (ITIMs; Table 1.1). Therefore inhibiting immune activation and autoimmune processes may be possible by directing antibody superagonists against those receptors.

ITAM	ITSM	ITIM	Unclassified
CD3γ; CD3δ; CD3ε;	19A; BTLA; CD84;	BTLA; CD5; CD31;	CD28;
TCRζ; CD66d?;	CD244(2B4); NTBA;	CD66a; CD72; CMRF35H;	CTLA-4; ICOS;
CD79A; CD79B;	CD229(Ly9); PD-1;	DCIR; EPO-R;	CD200R
DAP12; Dectin-1;	SLAM(CD150)	FcγRIIB/CD32;	
FcεRIb; FcR1γ;		G6B; IL4R;	
Hypothetical FLJ46519;		IRTA1; IRTA2;	
SPAP2?		KIR2DL1; KIR2DL2;	
		KIR2DL3; KIR2DL4;	
		KIR2DL5; KIR3DL1;	
		KIR3DL2; LIR1; LIR2	
		LIR3; LIR5; LIR8;	
		LAIR-1; MAFA;	
		NKG2A; NKp44;	
		NTB-A; PD-1; PILRa;	
		SPAP1; SPAP2; SIGLECL1;	
		SIGLEC2/CD22; SIGLEC3/CD33;	
		SIGLEC5; SIGLEC6;	
		SIGLEC7; SIGLEC10;	
		SIGLEC11; SIGLEC4;	
		SIGLEC8; SIGLEC9;	
		PECAM-1; SIRPα2; SIT	

Table 1.1 Receptors with immunoreceptor-based tyrosine motifs, adapted from [175]

1.4 Role of PD-1 in regulating T cell responses

The Programmed Death-1 (PD-1) gene was first isolated from a T cell hyridoma undergoing cell death upon stimulation with phorbol 12-myristate 13-acetate (PMA) and ionomycin [176]. However, its relation to programmed cell death was not confirmed in subsequent experiments and its function remained unclear until the observation of autoimmunity in PD-1 deficient mice ($Pdcd1^{-/-}$) [150]. The spontaneous development of age related lupus like glomerulonephritis and arthritis in PD-1 deficient C57BL/6 mice suggested an inhibitory role for PD-1. At 14 months of age, half of the mice displayed signs of glomerulonephritis with IgG3 and C3 deposition in the glomeruli. Most of the mice also developed arthritis by this age [102]. When this model was backcrossed into the Balb/c background, a much more severe phenotype was observed with mice dying as early as 5 weeks of age from severe congestive heart failure. Echocardiographic examination revealed the reason of the congestive heart failure as dilated cardiomyopathy with pathological examinations revealing cardiac inflammation and immune complex deposition. Autoantibodies against cardiac troponin I were isolated from the serum of PD-1 deficient Balb/c mice. However, no autoantigen has been identified for the lupus like disease in PD-1 deficient C57BL/6 mice [103, 150]. PD-1 ligands were identified subsequently by the detection of interactions between recombinant PD-1-Ig and the newly identified B7-like molecules. These ligands were called PD-L1 (B7-H1) and PD-L2 (B7-H2) [177-178].

1.4.1 Structure of PD-1 and its ligands

PD-1 is a 50-55 kDa type 1 transmembrane glycoprotein which is composed of an extracellular IgV-like domain that shares 21-33% amino acid identity with CD28, CTLA-4 and ICOS. As it lacks the membrane proximal cysteine residue required for dimerization, it probably exists as a monomer [179]. It has two immunoreceptor-based tyrosine motifs in the cytoplasmic region. The

membrane proximal motif is an ITIM, and the second motif, which is probably responsible for PD-1 signalling is an immunoreceptor tyrosine-based switch motif (ITSM) [180-181]. PD-L1 and PD-L2 are type 1 transmembrane glycoproteins composed of IgV- and IgC-like domains. They share 40% amino acid identity with each other and 20% with B7 molecules [150].

Analysis of the crystal structure of PD-1 and PD-Ls revealed that, in contrast to the CTLA-4 molecule which uses hydrophobic MYPPPY sequence located in the FG loop as the B7 binding site, PD-1 uses its AGFCC' β-sheet to bind to the equivalent faces of PD-Ls. This face-to-face interaction makes the contact area of PD-1 and PD-Ls larger and gives a more compact structure to the complex [179, 182]. However, the long linker segment connecting the PD-1 IgV-like domain and the transmembrane region probably adjusts the total size of the complex and makes it comparable to the size of TCR-MHC and CTLA-4-B7 complexes.

1.4.2 PD-1 signalling

The inhibitory mechanism of PD-1 was first investigated in a B cell line using a chimeric PD-1 protein that contains the cytoplasmic region of PD-1 and extracellular portion of the inhibitory receptor FcγRIIB (FcPD) [183]. Upon simultaneous cross-linking of the BCR and FcPD, strong suppression of calcium mobilization was observed. BCR triggering resulted in phosphorylation of both ITIM and ITSM motifs, however only the ITSM recruited SH2 domain containing tyrosine phosphatase 2 (SHP-2). SHP-2 dephosphorylated BCR-proximal signalling molecules including Igα/β (CD79a/b) and spleen tyrosine kinase (Syk) which attenuated activation of phospholipase Cγ2 (PLCγ2), phosphotidylinositol-3-kinase (PI3K), vav and extracellular signal regulated kinase 1/2 (ERK1/2). Thus, among the two tyrosine motifs, only the ITSM seems to have an indispensible role in PD-1 signalling.

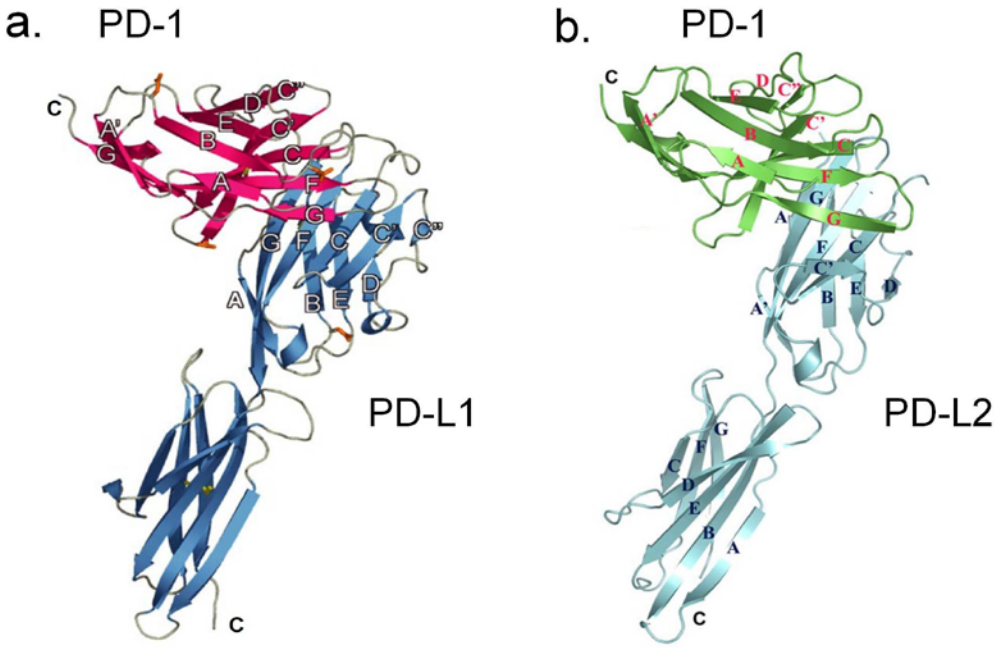


Figure 1.1 Crystal structures of PD-1 and PD-L complexes, adapted from [179,182]. The face-to-face interaction between the β-sheets of PD-1 and its ligands make the complexes more compact. **a.** The structure of the PD-1-PD-L1 complex. The strands of the two β-sheets of PD-1 are labelled as ABED and AGFCC'C". The strands of the two β-sheets of PD-L1 IgV-like domain are labelled AGFCC'C" and BED. It is the AGFCC'C" β-sheets of each molecule that interact. **b.** The structure of the PD-1-PD-L2 complex revealing a very similar mode of interaction.

Upon T cell activation, PD-1 engagement decreases the phosphorylation of TCR downstream elements CD3ζ, zeta associated protein of 70kDa (ZAP70) and PKC-θ. In addition to the TCR, PD-1 engagement inhibits CD28 signalling by reducing PI3K phosphorylation by SHP-2 and therefore inhibiting serine threonine kinase Akt activity [184]. SHP-1 has also been shown to associate with PD-1, however at a later stage when the mature synapse is formed where it may play a role in the direct dephosphorylation of CD28 downstream elements in the c-SMAC [185]. CTLA-4 also inhibits CD28 signalling. Previously it was proposed that PD-1 recruits protein phosphatase 2A (PP2A) for blocking Akt activity; therefore, PD-1 and CTLA-4 both inhibit CD28 signalling but with different mechanisms [186-187]. However, some other findings suggested that CTLA-4 also recruits PI3K, SHP1 and/or SHP2, thus differential recruitment of phosphatases may not account for the mechanism that differentiates PD-1 and CTLA-4 pathways [185, 188]. Imaging studies have recently started to illuminate the mechanisms of PD-1 and CTLA-4 mediated inhibition. It has been demonstrated that during early T cell activation events, PD-1 and PI3K co-localize at TCR microclusters whereas CTLA-4 remains in vesicles and is translocated to the central supramolecular activation cluster (c-SMAC) at a later activation phase [189-190]. Furthermore, it was demonstrated that PKC-θ downstream of CD28 is directly inhibited by CTLA-4 whereas PD-1 inhibits it indirectly [185]. Recently, Qureshi et al. showed that CTLA-4 can capture B7-1 and B7-2 from opposing cells by trans-endocytosis [191]. This appears to be an additional mechanism distinguishing the CTLA-4 and PD-1 pathways.

PD-1 signal has also been shown to play a critical role in iTreg development, maintenance and suppressive function [192]. Although it has not been extensively studied yet, current evidence suggests that PD-1 promotes iTreg development by antagonizing the Akt-mTOR signalling pathway [192]. Another important function of PD-1 is anergy induction, the mechanism of which has long remained unclear. Recent findings suggest that the level of IL-2 production may set the

threshold for anergy resistance and PD-1 may provide a regulatory mechanism for inhibiting IL-2 production in response to anergy induction [78, 193].

1.4.3 Reverse signalling by PD-L1 and PD-L2

The first evidence for reverse signalling by PD-L1 and PD-L2 came from experiments with *in vitro* cultured bone marrow derived DCs. When PD-L1 and PD-L2 were blocked by administration of soluble PD-1 Fc fusion protein (PD-1-Ig), DCs acquired a suppressive phenotype and increased their IL-10 production. This may be an indication for a reverse signalling through PD-1 ligands. However, it is not clear whether PD-L1 or PD-L2 is more effective in this setting [194].

It has also been suggested that bi-directional signalling may be possible between PD-L1 and B7-1. Initial surface plasmon resonance based assays demonstrated that PD-L1 binds to B7-1 with an intermediate affinity (~1.7μM) between B7-1 for CD28 (4 μM) and B7-1 for CTLA-4 (0.2 μM). Functional assays on the T cells lacking other binding partners of B7-1 (CD28 and CTLA-4) showed that B7-1 coated beads are able to inhibit anti-CD3 antibody mediated T cell proliferation. Moreover, when PD-L1, CD28 and CTLA-4 deficient cells are used, B7-1 mediated inhibition disappears. Similarly, in the presence of PD-L1 coated beads, T cells lacking PD-1 displayed decreased proliferation in response to anti-CD3 antibody whereas PD-1- B7-1 double deficient cells were no longer inhibited. Altogether, these findings suggest that PD-L1 and B7-1 expression on T cells may have functional consequences and their possible bi-directional signalling may provide an additional control over T cell activation. This additional mechanism will need to be kept in mind when modulating the activities of PD-L1 and B7-1 molecules for therapeutic purposes [195].

1.4.4 Regulation of PD-1 expression

PD-1 can be inducibly expressed on T cells, B cells, monocytes, NK cells, NKT cells and myeloid DCs in the periphery [152]. It is also expressed on α/β as well as γ/δ CD4-CD8- DN thymocytes probably starting from the DN stage when TCR-β rearrangement occurs. It negatively regulates positive selection and promotes negative selection through controlling the TCR signalling thresholds [196-197]. Surface expression of PD-1 may act as a marker for distinguishing freshly isolated ($CD4^+CD25^+PD\text{-}1^{low}$) resting peripheral Tregs from ($CD4^+CD25^+PD\text{-}1^{high}$) activated T cells. Resting Tregs retain PD-1 intracellularly and translocate it to the surface in response to TCR stimulation [198]. Stimulation of the PD-1 pathway in naïve $CD4^+$ T cells synergizes with TGF-β for inducing Treg formation in the periphery [192]. Furthermore, PD-1 is expressed on follicular helper T (Tfh) cells in the germinal centres and may regulate the selection and survival of GC B cells presumably through interaction with PD-L2 expressed on GC B cells [199-200].

In the periphery, PD-L1 is constitutively expressed on T cells, B cells, DCs, macrophages and bone marrow derived mast cells. It is also expressed on a variety of non-hematopoietic cells including lung, vascular endothelium, liver non-parenchymal cells, mesenchymal stem cells, pancreatic islets, microglia, astrocytes and keratinocytes [201-202]. However, PD-L2 expression is restricted to activated DCs, macrophages, bone marrow derived mast cells, 50-70% of peritoneal B1 cells and human vascular endothelial cells [201, 203]. Recently, it has been shown that PD-L2 is also expressed on activated $CD4^+$ and $CD8^+$ T cells as well as on polarized Th2 cells after TCR triggering [204-205]. In the thymus, PD-L1 is extensively expressed on cortical and medullary epithelial cells as well as DCs and its interaction with PD-1 is crucial for the positive selection of DP thymocytes [206]. On the other hand, PD-L2 expression in the thymus is confined to medullary stromal cells with no suggested role in T cell repertoire formation [152]. It has however been shown that the PD-1 pathway is important for tolerance at

immune privileged sites. During implantation of the embryo, PD-L1 and PD-L2 are expressed on syncytiotrophoblasts and vascular endothelium, respectively. PD-L1 is differentially expressed at the placenta across the gestation period and it plays an important role in fetal-maternal tolerance. PD-L1 is also expressed constitutively in the cornea and the PD-1-PD-L1 interaction protects the eye from T cell mediated damage [152]. Altogether, these findings imply that PD-1 plays crucial roles in central and peripheral tolerance as well as in the protection of immune privileged organs.

Although the exact mechanisms still remain unclear, some transcription factors and cytokines have been implicated in regulating inducible expression of PD-1 and its ligands. It has recently been demonstrated that NFATc1 may be an important transcription factor for inducible upregulation of PD-1 upon TCR cross-linking [207]. In macrophages, interferon (IFN)-sensitive responsive element and STAT1/2 are suggested to be crucial for constitutive and IFN-α induced PD-1 expression [208]. PD-L1 expression is dependent on two IFN regulatory factor-1 binding sites and the essential stimuli are IFN-α, IFN-β and IFN-γ as well as IL-10 for macrophages. MyD88, MEK, TRAF6 and JAK2 have also been implicated in PD-L1 induction. Inducible expression of PD-L2 on DCs requires granulocyte-monocyte colony stimulating factor (GM-CSF) and IL-4 [152].

1.4.5 Biological significance of PD-1

PD-1 in chronic viral infections

During chronic viral infections, CD8+ T cells acquire a state of impaired functionality, which is called exhaustion. It occurs probably due to chronic antigenic stimulation and is characterized by a loss of cytotoxicity and cytokine production [209]. In a murine model of chronic LCMV

infection, it was demonstrated for the first time that PD-1 expression is upregulated on virus specific $CD8^+$ T cells in the acute period and it remains high in those cells exhibiting an exhausted phenotype as the infection extends into its chronic phase. However, in the acute infection, a rapid increase in PD-1 expression is followed by a sharp decrease as the disease resolves [210]. A similar phenomenon was observed in the subsequent studies investigating T cell exhaustion in simian immunodeficiency virus (SIV), human immunodeficiency virus (HIV), hepatitis B virus (HBV), hepatitis C virus (HCV) infections [211-214]. In those studies, it was also shown that the percentage of PD-1 expressing cells and the expression levels correlate with viral load and the decline in T cell function. Therefore, PD-1 may serve as a useful marker for the disease severity and the degree of T cell exhaustion in chronic viral infections [152].

It has also been observed that PD-1 expression declines following HIV-1 escape whereas it remains high on T cells that are specific for conserved epitopes [215]. This indicates that a continuous antigen specific T cell stimulation may be responsible for exhaustion. In addition to this, a TCR independent mechanism has also been suggested: PD-1 upregulation may be triggered by viral proteins such as the Nef protein of HIV and the core protein of HCV in a TCR independent manner [216-217].

Since PD-1 may provide crucial signals inducing T cell exhaustion, blocking the PD-1-PD-L1 interaction has been tested for reversing the exhausted phenotype in the chronic viral infections. These studies revealed that blocking PD-1 improves the functionality of the virus specific T cells [211, 218-220]. A cooperative action of PD-1 and other inhibitory molecules such as signalling lymphocyte activation molecule (SLAM)-related receptor CD244, T-cell Ig- and mucin domain-containing molecule-3 (Tim-3) and lymphocyte activation gene 3 (LAG-3) has also been proposed [221-223]. The co-blockade of PD-1 and LAG-3 has been shown to decrease viral load and disease severity more effectively than single molecule blockade [223].

PD-1 in anti-tumour immunity

Tumours use multiple strategies for evading immune responsess. It has been shown that PD-L1 and PD-L2 are expressed on a wide variety of solid tumours and hematologic malignancies [152]. Tumour infiltrating lymphocytes (TILs) display an exhausted phenotype with high PD-1 expression suggesting that tumours create a tolerogenic microenvironment for their growth [224]. A strong correlation was found between the expression of PD-Ls and unfavorable prognosis in oesophageal, gastric, renal, ovarian, bladder, pancreatic cancers and melanoma [152]. It has been demonstrated that PD-Ls on tumour cells prevent tumour destruction by inhibiting T cell activation or inducing apoptosis in TILs. PD-L expressing tumour-associated DCs further suppress T cell responses against the tumour and help adjust the tumour environment [225-226]. The PD-1 pathway has therefore been targeted by several blocking strategies in order to establish more effective anti-tumour therapies. Those strategies include generation of blocking mAbs against PD-1 and ligands, the use of recombinant proteins of the extracellular regions of PD-1 and PD-L1, genetic ablation of PD-1 gene, RNA interference, and DNA vaccination with the extracellular region of PD-1 [225, 227-231]. Extensive investigations have recently led to the development of several blocking mAbs, which are currently being tested in clinical trials [232].

PD-1 in autoimmunity

Blockade of the PD-1 pathway has also been used as a strategy for investigating the role of PD-1 in autoimmunity. In non-obese diabetic (NOD) mice, PD-L1 was found upregulated on pancreatic islet cells and administration of PD-1 or PD-L1 blocking antibodies at the pre-diabetic stage, resulted in a rapid and exacerbated diabetes with severe insulitis and proinflammatory cytokine production by insulin specific T cells [233-234]. A differential role for CTLA-4 and PD-1

has also been attributed to regulating the disease process in NOD mice. Blockade of CTLA-4 by mAbs exaggerated diabetes only in neonates, whereas, blockade of PD-1 led to exaggerated disease in both neonates and in adult mice [234]. This indicates that the regulatory role of CTLA-4 is more limited in NOD mice compared to PD-1, which regulates both initiation and progression of autoimmune diabetes.

PD-1 and its ligands control self-reactive T cells also in EAE. During active EAE, meningial infiltrates express PD-1, PD-L1 and PD-L2 [233]. PD-L1 is expressed on the inflammatory cells accumulating in the CNS, astrocytes and vascular endothelium. It is also inducibly expressed on $CD11b^+$ APCs and on microglial cells in response to IL-12 and IFN-γ respectively [235-237]. Blocking antibodies used in different strains indicated strain specific differences in the utilization of PD-1 and PD-1 ligands. Blockade of PD-1 and PD-L2, not PD-L1, during EAE induction was associated with accelerated disease onset and severity with increased MOG-reactive T cells and autoantibodies in the C57BL/6 background [238]. However, in Balb/c and some SJL/J mice PD-L1, not PD-L2, was found to control the severity of the disease. This strain-specific effect of antibody mediated blockade is probably due to the genetic influence for the differential role of PD-L1 and PD-L2, because it cannot be explained by expression of PD-L1 or PD-L2, since their expression varies little in lymphoid APCs and spinal cord tissues among different strains [239]. Another explanation might be the insufficient blockade of the ligands by the antibodies that were administered for a limited duration since PD-L1 deficient C57BL/6 mice were shown to develop exacerbated EAE [240].

The PD-1-PD-L1 interaction may also regulate autoreactive responses by inducing Treg formation and modulation of Treg function. In EAE studies, pertussis toxin is used for increasing the permeability of the blood brain barrier prior to disease onset [241-242]. However it has also been shown that pertussis toxin administration decreases Treg frequency and function [243-244]. Furthermore, the phenotypic analysis of Tregs revealed that PD-1 was the only Treg

marker that was downregulated after pertussis toxin injection [244-245]. Along with the observation that PD-1 deficient mice given encephalitogenic peptide/CFA without pertussis toxin develop fulminant EAE, it can be suggested that pertussis toxin injection promotes disease also by downregulating PD-1 [245]. However, the role of the pertussis toxin is complicated by the fact that repetitive administration induces Treg formation and may have a disease ameliorating effect [246]. The interaction between neurons and T cells results in the conversion of encephalitogenic T cells to $CD25^{+}TGF\text{-}\beta1^{+}CTLA\text{-}4^{+}FoxP3^{+}$ Tregs that suppress encephalitogenic T cells and inhibit EAE [247]. Along with the evidence for the constitutive expression of PD-1 and inflammation associated expression of its ligands on retinal neurons [248], it is plausible that encephalitogenic effector T cells encounter neurons, stimulate their PD-L1 expression and induce Treg formation during central nervous system inflammation. Experiments in murine models of colitis support a role for the PD-1:PD-L1 pathway in controlling regulatory cells and have identified a subpopulation of regulatory $CD4^{+}CD25^{-}PD\text{-}1^{+}$ T cells that can inhibit the development of colitis [98, 249]. Further studies demonstrated that sequential adoptive transfers of the colitogenic cells from the diseased recipients into new SCID recipients resulted in the loss of the colitogenic phenotype after a number of successive transfers. The colitogenic T cells gradually acquired an exhausted phenotype with high PD-1 expression, which resembles the phenotype of exhausted T cells in chronic viral infections. Further transfer of those exhausted cells, which also express modest levels of Foxp3, suppressed colitis in SCID mice that are co-transferred with freshly isolated colitogenic cells. This data suggests that exhausted $CD4^{+}PD\text{-}1^{+}$ T cells may become iTregs upon stimulation through the PD-1-PD-L1 pathway and suppress the autoreactivity [250]. In the collagen induced arthritis (CIA) model, which resembles human rheumatoid arthritis, pre-treatment of the mice with intraperitoneal administration of PD-L1-Ig inhibited development of arthritis. Possible mechanisms for the tolerogenic effect of PD-L1-Ig are conversion of naïve T cells into iTregs, promoting

maintenance and suppressor function of existing iTregs and induction of the contra-conversion of effector T cells into iTregs [251].

Several PD-1 (*PDCD1*) gene polymorphisms have been reported in association with human autoimmune diseases. A single nucleotide polymorphism (SNP) named PD1.3A (G7146A), which is located in intron 4 has been associated with the development of SLE in Europeans and Mexicans but not in African-Americans. PD1.3A interferes with binding of the runt related transcription factor- 1 (RUNX) which in turn impairs the function of PD-1 probably by destabilizing or reducing the expression of PD-1 mRNA [252]. To date PD1.3A and several other polymorphisms have been linked with the development of various autoimmune diseases including type I diabetes, progressive multiple sclerosis (MS), rheumatoid arthritis and ankylosing spondylitis [253-255]. An association between a SNP in the PD-L2 gene was also identified in SLE patients [256] and a PD-L1 polymorphism was linked with Graves disease in Japanese patients [257]. Altogether, the evidence suggests that PD-1 pathway is critical for maintaining central and peripheral tolerance and limiting autoimmunity. Therefore, modulating PD-1 pathway holds promise for treating autoimmune diseases.

PD-1 in transplantation immunity

Upregulation of PD-1 and PD-L1 on alloreactive T cells and constitutive as well as inducible expression of PD-L1 on somatic tissues may control alloreactive responses [258-260]. PD-L2 may also participate in the regulation of alloreactivity by limiting alloreactive $CD8^+$ T cell proliferation [261]. Studies in cardiac transplant models have demonstrated that PD-L1 is upregulated on both the allograft and the recipient tissues after transplantation. The studies utilizing PD-L1 deficient allografts and recipients suggested that PD-L1 expression on the recipient tissue is mainly responsible for controlling the acute alloreactive responses whereas its

expression on the allograft may control the chronic alloreactive responses and survival of the grafted tissue [262].

Depending on the strength of the allogeneic response, administration of the blocking antibodies against the PD-1 pathway leads to different outcomes. In MHC-I and MHC-II mismatched cardiac allografts, PD-1 is strongly upregulated on alloreactive T cells and blockade of the PD-1 pathway significantly accelerates acute graft rejection [263]. However, in the single mismatched (MHC-I or MHC-II) allografts, chronic rejection in the form of graft vasculopathy with a mild PD-1 and PD-L1 upregulation is observed and blockade of PD-1 pathway does not have any effect on the rejection [259, 264].

The PD-1 pathway may induce transplant tolerance by controlling regulatory and effector T cell balance. In a cardiac allograft model, administration of PD-L1 blocking antibodies led to an accelerated graft rejection with an increase in the number of infiltrating lymphocytes and reduction in the number of Tregs [201]. In the studies on skin allograft and GVHD models, blockade of PD-L1 did not cause any acceleration in the alloresponse after depletion of $CD4^+CD25^+$ T cells [265]. Furthermore, loss of PD-1 and PD-L1 enhanced effector T cell number and cytokine production. These findings suggest that PD-1 pathway may limit the activity of alloreactive T cells by also acting on Tregs [259, 265-266].

PD-L1 may also utilize a PD-1 independent mechanism for regulating alloresponses i.e. through mediating alloreactive T cell apoptosis. In a skin transplant model that was generated using adoptively transferred allospecific TCR transgenic $CD4^+$ T cells, blockade of PD-L1 but not PD-1 inhibited *in vivo* apoptosis of the transferred T cells [258]. Moreover, administration of an antibody which specifically blocked the B7-1-PD-L1 interaction led to more severe chronic allograft vasculopathy with upregulation of proinflammatory cytokines and reduction in the number of splenic Tregs [267]. Therefore the B7-1-PD-L1 interaction has also important

implications in limiting alloreactive responses. In the light of this evidence, it would seem that agonizing the PD-1 pathway could provide a useful therapy option for reducing graft rejection.

1.5 Models of T cell receptor triggering

There are good reasons to want to alter signalling by molecules like PD-1, but we don't really understand how these types of molecules initiate signalling. Metazoan tyrosine phosphorylation dependent receptors either have intrinsic tyrosine kinase activity, as in the case of dimerizing growth factor receptors, or phosphorylation of their tyrosine residues depends on extrinsic tyrosine kinases as in the case of the TCR and likely all the other cell surface receptors that bear tyrosine motifs [175, 268]. To date most discussion of how the receptors that rely on extrinsic tyrosine kinases are triggered focuses on the TCR, for which three types of models have been proposed. The T cell receptor complex is composed of a highly variable TCRα/β heterodimer that interacts with peptide-MHC and a non-variable signal transduction complex of CD3 which contains CD3γ, CD3δ, CD3ε and TCRζ [269].

TCR antigen recognition is distinguished from other cell surface receptor-ligand interactions by some unique features. First of all, the TCR has a remarkable capability of recognizing the agonist peptide-MHC, which is present on the surface of APCs or target cells at a very low density. This recognition is highly sensitive as even a single peptide-MHC can trigger TCR signalling [270]. Secondly, the TCR is able to discriminate the agonist peptide-MHC complex among a large pool of self peptide-MHC complexes that it also recognizes. Although the TCR of a self-tolerant T cell clone recognizes self peptide-MHC with a somewhat lower affinity, it is not that different to the affinity for the foreign peptide-MHC [269]. Therefore, the discrimination between self and foreign peptides depends on a fine sensing mechanism and is probably related to the unique duration of the interactions between the TCR and the ligands [271].

Thirdly, interaction of the TCR with peptide-MHC may lead to different outcomes, such as activation and proliferation upon binding to the agonist peptide or anergy as in the case of binding to a partial agonist peptide, depending on the strength of binding [272]. Additionally, the low-affinity interaction of the TCR with the self-peptide MHC promotes survival of mature T cells probably by delivering low-strength tonic signals [273]. Lastly, the TCR has an enormous structural diversity that is generated by genetic recombination and editing of the germline-encoded segments during T cell development without any contribution of antigenic exposure [274-275]. These features of TCR function don't apply to other receptors such as CD28, which binds low affinity invariant ligands as does PD-1, although multiple-strength interactions resulting form interactions with pairs of ligands may prove to be significant.

The process by which TCR-peptide-MHC interaction leads to molecular changes in the cytoplasmic region of the CD3 complex is known as TCR triggering. Although it has been extensively studied over the years, its mechanism is still unclear. There are three main theories about of TCR triggering: receptor aggregation, conformational change and segregation or redistribution.

1.5.1 Aggregation

Agents such as soluble antibodies or soluble multimeric peptide-MHC complexes which artificially induce aggregation of the TCRs on the T cell surface, lead to TCR triggering [276-277]. This triggering is probably through the accumulation of Lck molecules in the vicinity of the receptors that results in net phosphorylation of the TCRs [278]. Despite being feasible, this observation is unable to explain how a single peptide-MHC can trigger TCR signalling. Several models of aggregation have been proposed to overcome this issue.

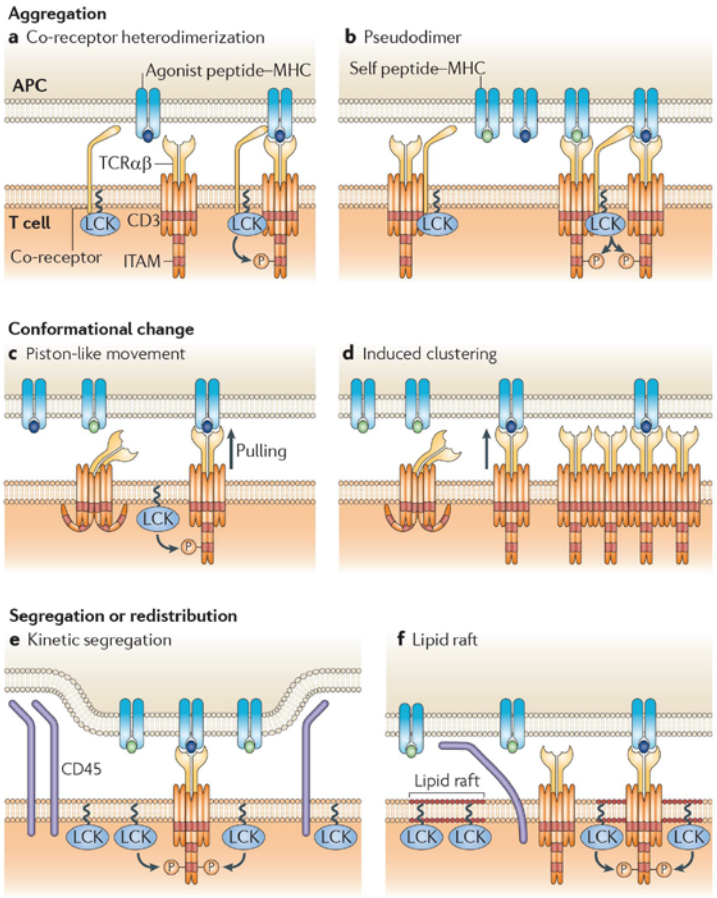


Figure 1.2 Mechanisms of TCR triggering, adapted from [254] Models are grouped according to whether the primary mechanism is aggregation, conformational change or segregation. **a.** In the co-receptor heterodimerization model, co-receptor binding to the same peptide–MHC complex as the T cell receptor (TCR) brings co-receptor-associated LCK into proximity with TCR–CD3 immunoreceptor tyrosine based activation motifs (ITAMs). **b.** The pseudodimer model postulates that two TCRs are brought together by binding low-affinity self (green) or high-affinity agonist (blue) peptide–MHC ligand and that the co-receptor associated with one TCR engages the agonist peptide–MHC complex, thereby forming a dimer. **c.** A piston-like displacement of the TCR–CD3 complex is induced by the mechanical effects (primarily pulling; black arrow) of peptide–MHC binding to the TCR. This leads to a change in the conformation of the CD3 cytoplasmic domains, allowing ITAM phosphorylation. **d.** Clustering is induced by a conformational change in TCR–CD3 complex, possibly enhancing kinase activity. The conformational change in the cytoplasmic domains is depicted as dissociation from the membrane, as proposed in the 'safety-catch' model7. **e.** The kinetic-segregation model proposes that TCR binding to peptide–MHC ligand traps the TCR–CD3 complex in close-contact zones, thereby segregating it from the inhibitory tyrosine phosphatase CD45, leading to stable phosphorylation of TCR–CD3 ITAMs by LCK. **f.** Lipid raft models postulate that peptide–MHC engagement somehow results in partitioning of the TCR–CD3 complex into regions of membrane enriched in LCK and deficient in CD45. APC, antigen-presenting cell.

The co-receptor heterodimerization model proposes that CD4 or CD8 co-receptors bind to the same agonist peptide-MHC and the co-receptor associated Lck phosphorylates the ITAMs of the CD3 complex [279-281]. However, this model is not sufficient to reveal how TCR triggering occurs in co-receptor deficient mice or how most of the studies using soluble agonist MHC monomers fail to show that TCR triggering occurs [269, 282]. Furthermore, molecular analyses have indicated that TCR signals enhance binding of the co-receptors to the MHC molecules and therefore TCR phosphorylation precedes co-receptor recruitment instead of being dependent on it [283-284]. It is also noteworthy that the affinity of the co-receptors for peptide-MHC is extremely low compared to that of the TCR and so co-receptor binding would not be able to stabilize TCR-peptide-MHC complexes [285]. Co-receptor dependent phosphorylation is not sufficient to account for the central TCR triggering mechanism despite its possible contribution to the amplification of the TCR signal by recruting co-receptor associated Lck [286].

The pseudodimer model postulates that the TCR interacting with a self peptide-MHC forms dimers with a second TCR which binds to the agonist peptide. According to this model, one single co-receptor can intracellularly associate with a TCR that is specific for the self peptide-MHC while it also associates with a foreign peptide-MHC through its extracellular domain and the TCR triggering occurs due to phosphorylation of the ITAMs by co-receptor related Lck [269]. Thus, spatial localization of the co-receptor associated Lck in the signalling complexes enables certain self peptide-MHC complexes to trigger many TCRs. CD4 is proposed to play a crucial role in this model. Despite the evidence that soluble peptide-MHC monomers cannot induce TCR triggering, it has been shown that T cells expressing CD4 can respond to a single agonist peptide-MHC that is expressed on the APCs. Interestingly, when CD4 was blocked by antibodies, T cells were capable of detecting only a significant number of ligands (~30). In this study it was also suggested that the angle between the TCR and its associated CD4 is unlikely to allow them to interact with the same peptide-MHC [287]. Further studies demonstrated that T

cells can be stimulated by soluble recombinant agonist/self peptide-MHC heterodimers in a CD4 dependent manner [288]. Although clear evidence has not yet been obtained for CD8+ T cells, pseudodimerization may be a plausible mechanism for how low density agonist peptide-MHC aggregates enhance TCR triggering and T cell activation [269]. However, as in the case of co-receptor heterodimerization, the pseudodimerization model offers no insight for the TCR triggering by co-receptor independent Lck or triggering of the other cell surface receptors such as CD28 which do not have any known co-receptors.

Despite the uncertainty over its valency [289], it is clear that engagement of the TCR with the peptide-MHC either precedes or results in aggregation of the TCRs into microclusters that contain 10-100 TCRs [269]. However, a role for the interaction of the agonist/self peptide-MHC heterodimers with their TCRs in the microclusters may be unlikely since it has been shown that the size of the microclusters varies little with the density of the agonist peptide-MHC and self peptide-MHC is not always required for triggering the TCR [290]. Furthermore, a recent study showed that, upon interaction with the agonist peptide-MHC displayed on a mouse B cell line, TCR triggering can occur in 293T-HEK cells, which are artificially reconstituted with a transgenic TCR and CD3 complex. It seems that this artificial TCR triggering model where there is no role for the TCR/self peptide-MHC interaction, does not support a pseudodimerization based mechanism [291].

1.5.2 Conformational change

There are several studies suggesting that subtle conformational changes occur in the TCR ectodomain upon peptide-MHC binding which lead to TCR triggering [269]. Those studies commonly attribute a role for the membrane proximal AB loop of the TCRα constant domain, which stabilizes TCR-CD3 interactions [269, 292]. Based on the observation that mutations in

the AB loop affect the dimerization of the TCR, the conformational change induced TCR clustering was proposed as a triggering mechanism [293]. However this model does not explain how that change is transduced to the CD3 complex. Moreover, those predictions are limited by the quality of the TCR Cα AB loop resolution in the TCR-peptide-MHC crystals [269].

CD3 ectodomains have also been investigated for possible conformational changes. Since no direct structural evidence has been obtained for how the extracellular domains of TCR and CD3 are organized, most of the models for those conformational changes are incomplete [294-295]. Recent studies demonstrated that only one side of the TCR is occupied by the CD3 heterodimers. Based on this observation Kuhns et al. proposed that conformational changes in the AB loop of TCRα constant domain, which is not in contact with CD3 heterodimers, regulates TCR dimerization and thus binding induced conformational changes may generate signal through TCR clustering [296]. In other studies, in which the short extracellular stalk of CD3ε was mutated, it was demonstrated that signal transmission to the cell interior was impaired while receptor clustering was intact [297-298]. This was interpreted as meaning that receptor clustering is not sufficient to induce receptor phosphorylation, so the absence of the signal is due to abrogation of a conformational change in CD3ε. The possible change was predicted as “stiffening” of CD3ε conveyed to the bottom of its ectodomain [297]. However, it is worth noting that flexibility losses are frequently observed for antibodies interacting with protein antigens [299] and this may not necessarily have any functional consequences [300].

Several studies have suggested that cytoplasmic portions of CD3 undergo conformational changes upon TCR-peptide-MHC binding [301-302]. There is indeed accumulating evidence for the conformational changes in CD3ε. Recently, it was shown that a basic rich sequence (BRS) in CD3ε, and probably in TCRζ, may mediate binding to the negatively charged phospholipids in the membrane [303-304]. Also, results of a nuclear magnetic resonance (NMR) based study indicated that the ITAMs of CD3ε are buried in lipid bilayers [303]. Overall these results imply

that there may be a “safety catch” mechanism which prevents TCR triggering in the resting state [305]. However, the common finding of some old and recent studies, which demonstrated phosphorylation of CD3ε when T cells are exposed to the phosphatase inhibitor pervanadate, provided some counter-evidence to this theory [306-309]. The role of membrane association in CD3ε phosphorylation was also challenged by the comparison of the effect of pervanadate on the phosphorylation of wt CD3ε and membrane non-binding mutants of CD3ε. Similar levels of phosphorylation of both the mutant and wt CD3ε suggested that even if the cytoplasmic domain of wt CD3ε associates with the membrane, it is still accessible to the kinases [309].

1.5.3 Segregation and redistribution based models of TCR triggering

On the T cell surface, the TCR-CD3 complexes are co-expressed with a number of signalling molecules, mainly kinases (such as tyrosine kinase Lck) and phosphatases (such as CD45, CD43 and CD148). On resting T cells, cell surface molecules randomly interact with each other. However, these interactions don’t result in receptor triggering since the amount of phosphatases is sufficient to keep the net phosphorylation of the TCR too low for activation [175]. Treatment of the resting T cells with inhibitors of tyrosine phosphatases leads to increased phosphorylation of TCR-CD3-ITAMs, resulting in T cell signalling and activation even in the complete absence of TCR ligands [306-308]. According to the kinetic segregation model, binding of small adhesion molecules on T-cells and APCs induces formation of multiple close-contact zones which have the right dimensions to allow specific binding of the TCR to its agonist peptide-MHC [175, 310]. The TCRs which bind to their cognate ligands are trapped in those zones from where the bulky surface phosphatases such as CD45 and CD148 are excluded. This leads to a dominance of the small kinases in the close-contact zones, and net phosphorylation of the trapped TCRs in the absence of any counter-effect of phosphatases [175]. Signalling through the TCR is a multi-

step process which starts with the earliest changes in its phosphorylation induced by the binding of agonist peptide and continues with the assembly of a large multi-molecular signalling complex (signalosome). In the case of a sub-optimal TCR-peptide-MHC interaction which has a shorter half-life than the optimal interaction, the TCR is reversed back to its resting state without its signalosome being phosphorylated enough to transmit any activation signal. This “kinetic proofreading” [311-312] mechanism, which allows the T cells to discriminate between agonist peptide-MHC complexes, agrees with how the kinetic-segregation mechanism proposes that specificity is achieved [310].

There are several lines of evidence for the kinetic-segregation model. Initially, it was shown that CD45 and CD148 are excluded from the microclusters where the TCR triggering occurs [290, 313]. CD45 has also been shown to be excluded from the focal sites where TCR triggering was induced by immobilized monoclonal antibodies against the TCR [314]. Truncation of the large extracellular domains of CD45 and CD148 phosphatases inhibits TCR triggering [313, 315]. Since the CD45 ectodomain is required for maintaining the active pool of Lck [315-316], its truncation may result in inhibition of TCR triggering solely due to reduced levels of active Lck. Therefore, despite apparently supporting the model, the truncation of CD45 does not provide definitive evidence. Similarly, the implications of the truncation of CD148 may also be debatable since recent studies attribute a role for CD148 also in the positive regulation of Lck in T cells [317]. Nevertheless, there is still robust evidence for a size dependent segregation mechanism such as the demonstrated inhibition of TCR triggering by elongated peptide-MHC [318-319]. Comparison of the effects of surface associated ligands and soluble ligands have emphasized the link between immobilization and TCR triggering [320-321]. Recent studies demonstrated the effect of the proximity between the membranes of the T cell and APC by engineering the TCRs of tumour specific T cells for directing them to the epitopes which are closer to the target cell membrane. It was found that binding to membrane proximal epitopes enhanced the effector

function of T cells [322-323]. Another recent study which used artificially reconstituted 293T-HEK cells, demonstrated that CD45 exclusion is necessary for the TCR triggering [291]. They also propose that conformational changes in the TCR are unlikely to be critical for the fundamental mechanism of triggering since the TCR-peptide-MHC module can be replaced completely with other similar sized artificial modules, which also leads to ZAP70 phosphorylation. This study suggests that phosphatase segregation is driven by decreased unfavourable membrane bending due to consolidation of the initial high energy TCR-peptide-MHC contacts into an array of interacting complexes with some help of additional molecules such as CD2 and CD58.

The other segregation or redistribution based model builds on the lipid raft concept and proposes that TCR binding to peptide-MHC complexes leads to an association of the TCR-CD3 complex with lipid rafts which are rich in Lck and deficient in CD45 [269]. Although a number of studies have offered evidence for the existence of the lipid rafts and their role in TCR signal transduction [324-328], some findings have challenged that evidence [329-331]. For example, it was shown that raft molecules are not co-localized with the TCR in the microclusters [330]. However, this does not exclude the possibility that lipid rafts associate with the TCR at the early events preceding microcluster formation. The association between the lipid rafts and TCR triggering could be re-addressed by higher-resolution imaging techniques [269]. Overall, the evidence suggests that segregation and redistribution-based mechanisms play important roles in TCR triggering. However, it is still unclear if these processes are enough to induce triggering on their own.

1.5.4 Implications for antibody induced signalling of segregation and redistribution-based models of receptor triggering

An important requirement of the “correct” TCR triggering mechanism is that it should also explain how other similar receptors are triggered and how other types of ligands, such as antibodies, are able to trigger these receptors. One frequently shared characteristic of the receptors that are dependent on extrinsic kinases is that their extracellular portions have similar small sizes to their ligands and to the TCR/MHC complex, therefore the ligand-receptor complexes would span similar distances [175]. Most members of the membrane tyrosine phosphatases share some common structural characteristics as well, such as having large extracellular domains [332]. Those similarities suggest that there may be a common triggering mechanism for all the receptors that are dependent on extrinsic tyrosine kinases. The kinetic-segregation model was initially proposed for TCR triggering. However, there is accumulating evidence for the possible roles of a segregation based mechanism for the antibody mediated receptor triggering and the triggering of co-receptors by their natural ligands.

Most of the antibodies targeting the receptors of T cell surface are “co-mitogenic” if they induce signalling at all, which means they require additional TCR-derived stimulus in order to exert agonistic activity. It has been shown that there are a few antibodies that do not require any additional stimulus and therefore are “mitogenic” alone when they are immobilized. Those antibodies include anti-CD3 and superagonist anti-CD28 antibodies [172, 333-334]. Mapping of the binding motifs of anti-CD28 antibodies has revealed that the conventional (co-mitogenic) anti-CD28 antibodies bind to the membrane distal part of CD28, which is close to the B7 binding site (MYPPPY motif), whereas the superagonists bind to the lateral C”D loop of CD28 [173]. The conventional anti-CD28 mAbs and superagonists are also able to bind CD28 bivalently, and they are also capable of crosslinking the CD28 molecule [174]. However, along with the observation that neither of the antibodies are mitogenic in solution, where crosslinking is likely to

be favored, this indicates that receptors are not triggered by crosslinking alone. One potential mechanism is that superagonist antibodies alter the arrangement of signalling proteins either by physically interfering in the assembly of multicomponent signalling complexes or by affecting the size-dependent segregation of signalling molecules in a way analogous to that proposed for TCR triggering by the agonist peptide-MHC. This suggests that in the physiological setting of membrane bound CD28 molecules, when the TCR stimulus is absent, only CD28 superagonists are capable of mediating size dependent segregation of large phosphatases like CD45 and leading to unfettered phosphorylation of the receptor by extrinsic kinases (Lck) and thus a strong activating signal [174-175] (Figure 1.3). In summary, the antibody superagonists can be defined as the agonist antibodies that target membrane proximal epitopes on the receptors phosphorylated by extrinsic kinases and induce stronger signaling compared to the conventional antibody agonists that bind to membrane-distal epitopes on the same receptors and produce much weaker signalling.

Comment [SD2]: Formatting needs sorting throughout Billur…

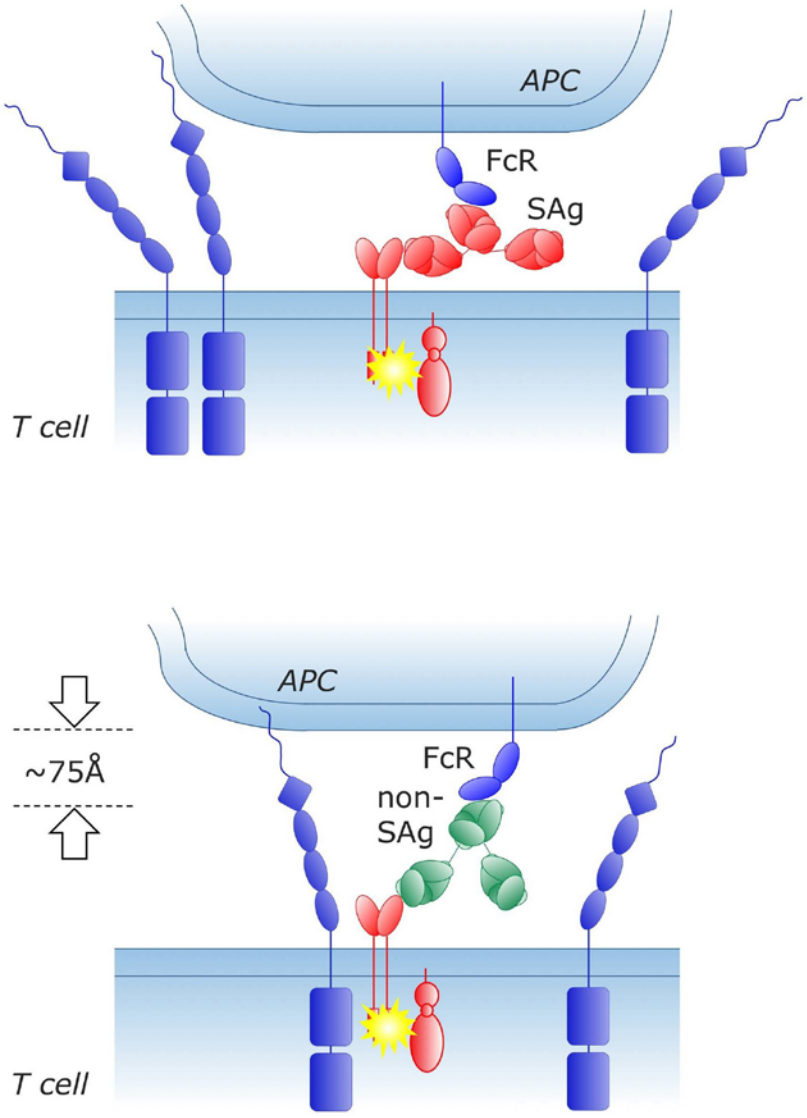


Figure 1.3 Mechanism of superagonistic antibody signalling. Binding of superagonistic antibody (SAg, above) to CD28 and to Fc receptors (FcR) bridges the membranes of two cells, sterically excluding the phosphatase, CD45. The kinase, Lck, retains access to CD28, allowing net phosphorylation of the receptor (yellow flash). The 'conventional' antibody (mAb, below) gives weaker signalling because the ~100Å larger complex it forms less efficiently excludes CD45.

1.6 Work preceding the project

Three anti-human PD-1 antibody clones were produced and initial characterization studies were carried out (by Sara Morgan and Claire Jessup, WIMM, unpublished observations). To identify the epitopes of the antibodies, single residue mutant forms of the extracellular region of human PD-1 were generated (S. Morgan). This revealed that clone 2 and clone 10 bind to membrane distal epitopes whereas clone 19 binds to a membrane proximal epitope on PD-1 (Figure 1.4a-b). Clone 2 and clone 10 antibodies would likely compete with one another for binding to PD-1 based upon the results of this analysis. To characterize the binding kinetics of the anti-human PD-1 antibodies, SPR based S. Morgan carried out surface plasmon resonance-based binding assays. This showed that clone 10 has the fastest off rate (lowest affinity) whereas clone 19 and clone 2 have much slower off rates.

To directly compare the signal-generating activities of the antibodies, a dimeric form of PD-1 was generated by S. Morgan that consisted of the extracellular region of human PD-1 spliced to the transmembrane region of CD3**ζ** (to produce dimers) and the cytoplasmic region of CD28 (in order to have an "active" readout consisting of IL-2 secretion; Figure 1.5a). The IL-2 secretion results indicated that both antibodies are capable of inducing signalling *via* the hPD-1/mCD3ζWT/mCD28 chimera; however Clone 19, which binds PD-1 closest to the membrane induces the largest amount of IL-2 (Figure 1.5b). This supports the notion that the topology of the complex formed by the antibodies is what determines the relative levels of signalling induced by agonists. The data also suggests that the degree of agonistic signalling can be varied with choice of antibody.

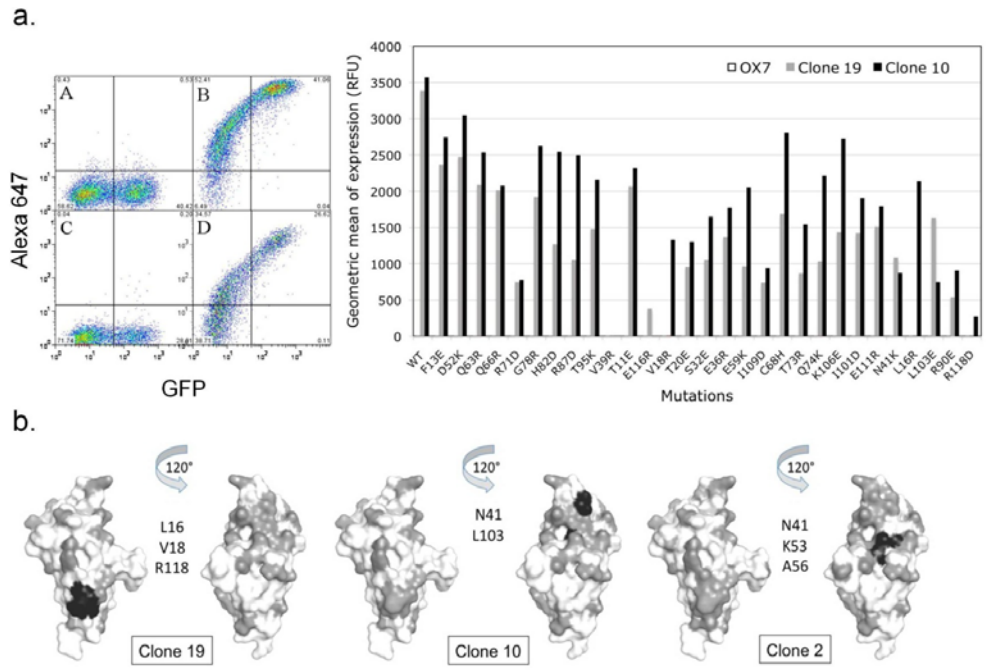


Figure 1.4 Structural characteristics of anti-PD-1 antibodies. a. (Left) Cells were transfected with constructs expressing the extracellular region of human PD-1 (panels A and B) or mutants that affected the binding of Clone 19 (L16R; panel C) or Clone 10 (L103E; panel D) anti-PD-1 antibodies. The cells were labelled with isotype control antibody (panel A) or with Clone 19 (panels B and C) or Clone 10 (panel D) antibody, followed by Alexa647 labelled secondary antibody. Transfected 293T cells are eGFP-positive (x-axis). Antibody binding is shown on the y-axis. (Right) The geometric means of the Alex647 fluorescence levels for the GFP$^+$ cells is given for each of the mutants of PD-1, expressed as full length proteins in HEK 293T cells. **b.** Mouse PD-1 residues equivalent to human PD-1 residues that when mutated partially or fully block the binding of clones 2, 10 and 19 antibody are highlighted in black on the mouse PD-1 crystal structure Mouse-equivalents of human PD-1 residues that have no effect on the binding of the antibodies when mutated are coloured grey. **c.** Dissociation rates for clone 2, 10 and 19 antibodies determined by surface plasmon resonance-based analysis.

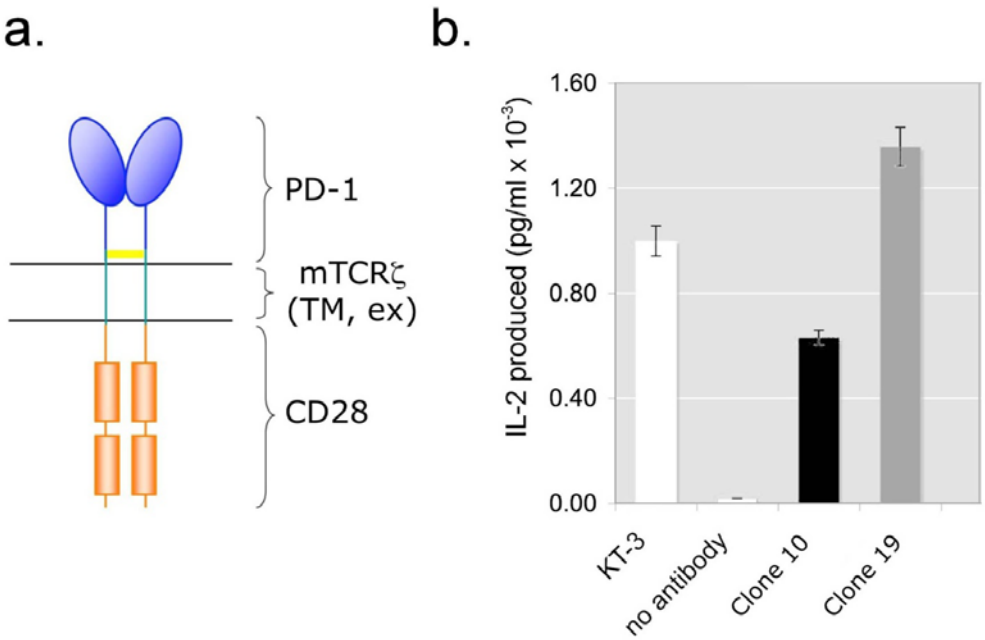


Figure 1.5 IL-2 secretion induced by anti-PD-1 antibodies binding to a hPD-1/mCD3ζWT/mCD28 chimera. a. A chimera consisting of the extracellular region of human PD-1 and the transmembrane and cytoplasmic regions of mouse TCRζ and CD28 was expressed in DO11.10 cells. **b.** The cells were treated with immobilized anti-CD3 (KT3) or anti-PD-1 antibodies and the amount of IL-2 released was measured.

1.7 Objectives of this thesis

This thesis aims to investigate the activities of the putative anti-human PD-1 antibody agonists in the context of signalling by native PD-1 both in vitro and in vivo. It was hoped that this would provide insights into how the binding properties of the antibody agonists may relate to potency, for an inhibitory receptor. The in vivo experiments were performed in a “knock-in” mouse for which the extracellular part of mouse PD-1 was replaced with the equivalent part of human PD-1. The second question that was addressed is whether or not inhibitory agonists/superagonists may be developed as potential immune modulatory agents for controlling normal and dysregulated immune responses, using the PD-1 knock-in mouse as the basis of a therapeutic model.

Chapter 2:

Materials and Methods

2.1 Reagents and solutions

2.1.1 General reagents

.***Phosphate Buffered Saline (PBS):*** PBS was obtained in 500 ml bottles from Hyclone. PBS was used in a range of cellular and biochemical experiments an injections.

PBS/BSA: PBS containing 1% (w/v) bovine serum albumin (BSA) (Sigma Aldrich) was used in ELISA, PBS containing 0.1% (w/v) BSA was used sterile in CFSE labelling, de-gassed PBS containing 0.5% (w/v) BSA was used sterile in magnetic cell separation and flow cytometry associated cell sorting.

PBS/BSA/Azide: PBS containing 2% (w/v) bovine serum albumin (BSA) (Sigma Aldrich),10 mM NaN3 was used in flow cytometry.

HBSS/FCS/Azide: Hanks' Balanced Salt solution (Sigma) containing 2% (v/v) heat inactivated fetal calf serum (Life Technologies), 2% (v/v) HEPES (PAA) 10 mM NaN3 used in the flow cytometry.

RPMI/FCS: Non-sterile RPMI containing 2% (v/v) heat inactivated fetal calf serum, 100 U penicillin (PAA), 100 µg/ml streptomycin (PAA), 10 mM HEPES (PAA) was used as the medium for maintaining the organs and cell suspensions for flow cytometry procedures.

PBS/EDTA: PBS containing 0.4 mM EDTA (Ethylenediaminetetraacetic acid), used sterile in magnetic cell seperation

PBS/Tween: PBS containing 0.05% (v/v) Tween 20 (Sigma) was used in ELISA

Phosphate buffer pH 8: For 0.1 M 100 ml buffer, 47.35 ml 0.2 M Na_2HPO_4*$2H_20$, 2.65 ml 0.2 M NaH_2PO_4*H_20, 50 ml ddH_2O was used for loading Dynalbeads™.

Ear punch buffer: 50mM Tris pH8, 2mM NaCl, 10mM EDTA, 1% SDS

Cell freezing solution: 10% (v/v) dimethyl sulfoxide, 90% (v/v) fetal calf serum

Tris-buffered Ammonium Chloride (TAC): 17 mM Tris base, 144 mM NH4Cl was used for red blood cell lysis.

Ethanol: 70% (v/v) ethanol (Sigma) was used for aseptic removal of mouse organs.

Tris Acetate EDTA (TAE): 40 mM Tris acetate, 2 mM Na2EDTA.2H2O, pH 8.5, used as electrophoresis buffer.

6x DNA Loading Dye (Blue): 2.5 % Ficoll 400, 11 mM EDTA, 3.3 mM Tris-HCl, 0.017 % SDS, 0.015 % Bromophenol Blue

2x SDS PAGE sample buffer (non-reducing): 0.5 M Tris:HCl pH 6.8, 5% (w/v) SDS, 20% (v/v) glycerol, 0.005% (w/v) bromophenol blue, used in protein gel electrophoresis.

2x SDS PAGE sample buffer (reducing): 0.5 M Tris:HCl pH 6.8, 5% (w/v) SDS, 20% (v/v) glycerol, 0.005% (w/v) bromophenol blue, 10% β-mercaptoethanol

20x SDS PAGE running buffer: 50 mM MOPS pH 7.7, 50 mM Tris base, 0.1 % w/v SDS, 1 mM EDTA.

2X 12% acrylamide gel: 35% dH2O, 25% Tris/HCl pH 8.8/ SDS, 40% acrylamide, 0.5% freshly prepared 10% (w/v) ammonium persulphate, 0.2% TEMED

2X Stacking gel: 62% dH2O, 25% Tris/HCl pH 6.8/ SDS, 13% acrylamide, 0.5% freshly prepared 10% (w/v) ammonium persulphate, 0.2% TEMED

Coomassie Blue Stain: 2gr/L Coomassie blue, 10% (v/v) glacial acetic acid, 50% (v/v) methanol.

Coomassie Blue de-stain: 10% (v/v) glacial acetic acid, 50% (v/v) methanol.

2.1.2 Cell culture media

Anti-PD-1 antibody producing hybridoma cells were grown in RPMI-1640 (Sigma) supplemented with 2 mM L-glutamine (Invitrogen) 15% heat inactivated FCS (Gibco), 50 µg/ml penicillin (Gibco), 50 µg/ml streptomycin (Gibco), 100 µg/ml neomycin (Gibco), 100 µM hypoxanthine- 16 µM thymidine supplement (HT supplement- Gibco), 10 mM HEPES (Sigma), 100 µM non-essential amino acids solution (Gibco) and 100 µM sodium pyruvate (Sigma). Heat inactivated FCS was replaced by low-IgG FCS prior to seeding the hybridoma cells into HYPER*Flask* M (Corning) vessels

293 T HEK cell line was grown in DMEM (PAA) supplemented with 10% heat inactivated FCS (Biosera), 100 U penicillin (PAA), 100 µg/ml streptomycin (PAA), 2mM LGlutamine.

Human peripheral blood mononuclear cells, mouse splenocytes and mouse lymphocytes were grown in RPMI-1640 (Sigma) supplemented with 2 mM L-glutamine (Invitrogen) 10% heat inactivated FCS (Biosera), 100 U penicillin (PAA), 100 µg/ml streptomycin (PAA), 10 mM HEPES (PAA), and 50 µM β-mercaptoethanol (Gibco). 100 µM non-essential amino acids solution (Gibco) and 100 µM sodium pyruvate.

2.2 Cellular Methods

2.2.1 Hybridoma culture for large scale antibody production

The recombinant protein PD-1Fc was prepared in Davis Lab using the methods described for the production of CD28Fc (Evans *et al. Nat Immunol.* 6, 271-9 (2005)). It was used as the antigen for the outsourced generation of the anti-PD-1 antibody producing hybridomas. Growth of the final hybridoma clones and antibody production were carried out jointly by Heather Brouwer and Billur Akkaya. Frozen batches of the hybridomas secreting anti-PD-1 clone 19, clone 10 and clone 2 were thawed in 37ºC water bath, washed and supplemented with hybridoma fusion and cloning supplement (HFCS- Roche). When four to six 175cm2 flasks reached confluence, cells were counted, pelleted and reuspended in low IgG heat inactivated FCS containing medium (please refer to 2.1.2) and transferred into HYPER*Flask* M (Corning) vessels with a seeding inoculum of 5.0 x 10^6 to 1.72 x 10^7 cells per flask according to manufacturer's guidelines. The vessels are maintained at 37°C, 5% CO2 incubator for 3-6 weeks prior to antibody purification.

Detection of the antibody secretion

After seeding the hybridomas into HYPER*Flask* M (Corning) vessels, supernatant samples from the flasks that were prepared in parallel with the remainder of the hybridoma cells after seeding into HYPER*Flask* M (Corning) vessels were checked for presence of the antibodies using ELISA. In this experiment seven dilutions of supernatants (neat, 1/5, 1/25, 1/125, 1/625, 1/3125 and 1/15625) were compared with seven dilutions of a standard antibody (20 µg/ml, 4 µg/ml, 0.8 µg/ml, 0.16 µg/ml, 0.032 µg/ml, 0.0064 µg/ml and 0.000128 µg/ml) for their ability to bind plate

bound goat anti-mouse IgG1 and this experiment confirmed the presence of (>10 µg/ml) antibody in each sample. Steps of antibody purification will be discussed in 2.6.

2.2.2 Transfection of HEK-293T cells to analyse antibody binding

The construct encoding the wild type human PD-1 was cloned into the bi-cistronic mammalian expression vector pGFP2-n2 which also encodes GFP. For this purpose, 293T cells were plated onto six well plates the day before transfection (10^6 cells/well in 2ml full growth media). On the day of transfection, 2 µg of the plasmid carrying human PD-1 construct and 6µl Genejuice transfection reagent (Novagen) were mixed in 100µl plain DMEM. This mixture was incubated at room temperature for 30-45 minutes and then applied onto the 293T cells on the plates. Cells were harvested at 24 hours and analysed by flow cytometry.

2.2.3 Human peripheral blood mononuclear cell proliferation assay

Preparation of Dynalbeads™

Tosyl-activated or epoxy 4.5 µm Dynalbeads™ (M450; Invitrogen) were washed in 0.1 M sterile phosphate buffer (pH 8) and loaded with 7.5 µg total antibody per $3x10^7$ beads in 75 µl at 24- 37 ºC for 18-24 hours with continuous mixing. During preparing beads for bead bound stimulation assays, varying amounts (0.8 µg- 2.56 µg) of anti-human CD3 antibody (OKT3, in-house) were loaded along with maximal amounts anti-PD-1 antibodies (4.94 µg- 6.7 µg). For plate bound stimulation assays, beads were coupled with either clone of the anti-PD-1 antibodies at the maximal amount (7.5 µg). OX7 (anti-rat Thy1.1, in-house) was used as the control antibody to equalise the amount of total antibody per bead-loading reaction. Beads were blocked with 1 ml

cell culture media for 2 hours (2.1.2) at room temperature and washed three times in the same medium. Bead-bound antibody was quantified by flow-cytometry.

Preparation of antibody-coated plates

2 mg/ml OKT3 antibody was diluted into 0.5 µg/ml, 1 µg/ml, 5 µg/ml in sterile PBS. Control antibody OX7 was also diluted into 5 µg/ml in sterile PBS. 100 µl antibody solution was added to each well in triplicates. The plates were incubated at 37 ºC for 2 hours and then washed by sterile PBS twice. 100 µl/ well cell culture media was added to the plates and plates were incubated for 10 minutes at room temperature for blocking the non-specific interactions. After a final wash, cells are added into the wells.

Preparation of the human peripheral blood polymorphonuclear cells

Blood samples were taken from healthy individuals with their informed consent. Fresh heparinized blood was diluted 1:1 with PBS (HyClone) and the peripheral blood mononuclear cells (PBMCs) were isolated by density gradient separation (Ficoll Hypaque). In order to minimize the variations between the repeats of experiments, PBMCs were resuspended in freezing solution (2.1.1) and stored at -80ºC. In some experiments, accessory cells were depleted by plastic adherence for 2 h at 37ºC. Cells were washed in sterile, de-gassed PBS + 0.5% BSA and were incubated with anti-human CD3-coated magnetic beads (MACS) for 10 minutes at 4ºC. $CD3^+$ cells were then selected by applying magnetic field (MACS) according to manufacturer's guidelines. Cells were counted and washed with PBS. They were then resuspended in 1 ml PBS + 0.1% BSA if the total cell number was below 10^7 or resuspended in 2 ml PBS + 0.1% BSA if the total cell number was above10^7. Cells were labelled with a final

concentration of 2 µM CFSE (Invitrogen) in PBS + 0.1% BSA for 10 min at 37ºC in dark. CFSE was quenched with an equal volume of FCS at 4ºC. Cells were washed 3-5 times with the relevant cell culture media (2.1.2), using a fresh falcon tube each time. Antibodies (beads) or media was added to the relevant wells in 96-well round-bottomed plates and 10^5 cells/well were distributed and incubated at 37ºC for 3-5 days.

2.2.4 Stimulation assay for upregulating humanized PD-1 protein expression on the T cells of hPD-1KI mice

75 cm² tissue culture flasks were coated with 1 µg/ml anti-mouse CD3ε (Ebioscience) antibody for 2 hours at 37ºC. Spleens were aseptically removed from wild type (WT) C57BL/6, heterozygote hPD-1KI and homozygote hPD-1KI mice. Single cell suspensions were prepared by passing the cells through a 70uM nylon mesh. Splenocytes were seeded into the flasks at a density of $5x10^6$ cells/ml in 10 ml. Cell cultures were incubated at 37ºC with 5%CO_2 for 2 days. Unstimulated cells were kept at 4ºC until flow-cytometric analysis.

2.2.5 iTreg formation assay

Preparation of Dynalbeads™ and antibody coated plates

Anti-mouse CD3ε plus anti-mouse CD28 (Ebioscience) were covalently attached to Epoxy 4.5 µm Dynalbeads™ (M450; Invitrogen) according to manufacturer's instruction. We ensured equal loading of proteins during preparation by keeping the total amount of protein (antibodies and fusion proteins) constant at 5 µg per 10^7 beads. For bead bound iTreg formation assays, 10^7 beads were coated with 1 µg of anti- CD3ε (20% of total protein), 1 µg of anti-CD28, and either

60% control mouse IgG1 (Clone 101.4 , UCB, referred to control Ig beads) or 40% PD-L1-hIgG1 Fc fusion protein (referred to as PD-L1–Ig beads; R& D Systems), anti-PD-1 clone 19 or anti-PD-1 clone 10 (referred to as clone 19 or clone 10 beads) plus 20% control rat IgG1 in 15 µl. For plate bound iTreg formation assays, $3x10^7$ beads were coated with 15 µg of anti-PD-1 antibodies or PD-L1-hIgG1 Fc fusion protein in 75 µl. Covalent attachment of the proteins to the beads was performed in 0.1M phosphate buffer for 24 hours at room temperature with continuous mixing. Beads were then washed three times in PBS over a magnetic column, blocked with the cell culture media for 2 hours at room temperature and resuspended in cell culture media before use. For plate bound iTreg formation assays 24 well plates (Greiner) were coated with 250 µl 0.5 µg/ml anti-mouse CD3ε in duplicates as mentioned in 2.2.3.

Preparation of the cultures

Spleen and lymph nodes (mesenteric, popliteal, and inguinal) of naïve hPD-1KI-Foxp3-GFP double homozygote mice were aseptically removed and single cell suspensions were prepared by mechanical dissociation. Red blood cells were lysed by treating the cells with 10 ml Tris Ammonium Chloride (TAC) buffer for 10 minutes at 37ºC. Cells were then washed with cell culture media and subjected to either flow cytometry based cell sorting for obtaining naive $CD4^+CD62L^+Foxp3.GFP^-$ T cells or magnetic labelling by anti-mouse CD4 antibody coated magnetic beads (MACS) for positively selecting $CD4^+$ T cells according to manufacturer's guidelines. FACS sorted naïve $CD4^+CD62L^+Foxp3^-$ T cells were cultured with beads at a fixed ratio of 2:5 (T cells/beads). Cells were plated at $5x10^5$ cells/well (500 µl/ well) in a 24-well flat-bottom tissue culture plates with beads in complete media supplemented with varying amounts of TGF-β (Peprotech) (0 ng/ml- 0.0625 ng/ml, 0.1255 ng/ml, 0.5 ng/ml) for 3 days at 37°C, 5% CO2. Positively selected $CD4^+$ T cells were cultured with beads at a fixed ratio of 1:3 (T

cells/beads). Cells were plated at $5x10^5$ cells/well (500 µl/ well) in a 24-well flat-bottom tissue culture plates with beads in complete media supplemented with 1 µg/ml soluble anti-mouse CD28 varying amounts of TGF-β (Peprotech) (0 ng/ml- 0.0625 ng/ml, 0.1255 ng/ml, 0.5 ng/ml) for 3 days at 37°C, 5% CO2.

2.2.6 Mouse mixed lymphocyte reaction

For these assays Balb/c mice (MHC haplotype H-2d) were used as stimulators and hPD-1KI mice which are in C57BL/6 background (MHC haplotype H-2b) were used as responders. Spleens of naïve Balb/c and hPD-1KI mice and mesenteric lymph nodes of naïve hPD-1KI mice were aseptically removed and single cell suspensions were prepared by mechanical dissociation. Balb/c splenocytes were washed and resuspended in 1ml cell culture media containing 50 µg/ml Mitomycin-C (Sigma) and incubated for 30 minutes at 37°C in dark. They were then washed 4-5 times with cell culture media changing the tubes each time. For hPD-1KI mice, red blood cells were lysed by TAC buffer as in 2.2.5. Remaining cells were washed with de-gassed sterile PBS+ 0.5% BSA, resuspended in 1ml de-gassed sterile PBS+ 0.5% BSA and incubated with sterile biotinylated anti-mouse B220 (1/100), anti-mouse Ly6G, anti-mouse Gr-1, anti-mouse CD11b, anti-mouse CD11c, anti-mouse NK1.1, anti-mouse CD49 and anti-mouse TER119 for 25 minutes at 4°C. All these antibodies were purchased from Ebioscience and used at 1/200 dilution unless otherwise stated. Cells were then washed once with de-gassed sterile PBS+ 0.5% BSA and incubated with streptavidin coated magnetic beads (MACS) for another 15 minutes on ice. $CD4^+$ and $CD8^+$ T cells were then negatively selected using manufacturer's guidelines. Pure $CD4^+$ and $CD8^+$ T cells were counted and washed in PBS. They were labelled with CFSE as in 2.2.3. Those cells were mixed with Mitomycin-C treated Balb/c cells at a 1:1 ratio and the mixture was seeded into round bottom 96-well plates at $2x10^5$ cells/well (200 µl/

well). Soluble anti-PD-1 antibodies were added to the wells in duplicates at varying concentrations (0 µg/ml, 2 µg/ml, 10 µg/ml, 50 µg/ml, 100 µg/ml). The cultures were incubated for 3-5 days at 37°C, 5% CO2.

2.3 Localizing the targets of anti-PD-1 antibodies in human lymphoid tissue by immunohistochemistry

The human tonsil that was derived from tonsillectomy specimens was a kind gift of Dr. Margaret Jones and Dr. Karen Pulford from LRF Haemato-oncology Group, University of Oxford. Tissue was snap-frozen in liquid nitrogen and embedded in optimum cutting temperature compound (Tissue-Tek). Sections were cut in 8 um thickness and air-dried for 30 minutes and were fixed for 10 minutes in neat acetone. Slides were maintained at room temperature for 18 hours and stored at -20°C. Slides that were retrieved from freezer were allowed to warm up at room temperature prior to staining. For primary staining, 100 µl 10 µg/ml anti-PD-1 antibodies (Clone 19, clone 10, clone 2; in-house) in PBS+ 0.02% Azide were added on the sections and slides were incubated for 40-60 minutes at room temperature. Sections were washed with PBS and 100 µl peroxidase conjugated polyclonal goat anti-mouse IgG (Dako) secondary antibody was added according to manufacturer's instructions. After slides were washed with PBS, Peroxidase was detected with 3,3'-diaminobenzedine (Sigma) substrate according to manufacturer's instructions. Images were obtained with an Olympus IX71 microscope.

2.4 Mice and immunizations

C57BL/6 mice that were humanized for *Pdcd1* exon 2 (hPD-1 knock-in mice) were purchased from Taconic Artemis. Foxp3-GFP reporter mice were a kind gift from Alexander Rudensky

(Sloan-Kettering Institute). Ovalbumin-specific TCR transgenic OT-I mice were a kind gift from Vincenzo Cerundolo, University of Oxford. Eight to twelve weeks old wild type C57BL/6 and Balb/c mice were purchased from Harlan Animal Research Laboratory, congenic C57BL/6SJL and GFP-reporter mice were purchased from University of Oxford Biomedical Services. All the mice were housed and maintained in individual ventilated cages in Wellcome Trust Centre of Human Genetics Functional Genomics Facility.

2.4.1 Humanized PD-1 knock-in mice

Generation of the mice

The out-sourced production of a mouse model that expresses human PD-1 extracellular/ mouse PD-1 transmembrane & intracellular domains was undertaken using a constitutive knock-in strategy (Figure 2.1).

Genotyping strategy for the identification of mouse PD-1 and humanized PD-1 genes

Ear punch samples were incubated with 20 µl ear punch buffer with proteinase K (150ul 20mg/ml proteinase K per 2.85ml of ear punch buffer). for 40 minutes in 55°C water bath, vortexing every 20 minutes. Samples were then incubated at 100°C for 5 minutes to inactivate the proteinase K and cooled to back to 4°C. 2 sets of genotyping primers that were either directed against exon 2 of mouse PD-1 or human PD-1 genes were used for detecting mouse and human alleles together in one PCR. Primers were as follows: hPD1-exon2 forward TCGTGGTGACCGAAGGGGAC, hPD1-exon2 reverse GCAGGCTCTCTTTGATCTGCG, mPD1-exon2 forward CTCACAGTGTCAGAGGGAGCA, mPD1-exon2 reverse CGGGTTGGCTCAAACCATTAC. Components of the PCR mix for one DNA sample were 2.5 µl 10x reaction buffer (Bioline), 1.25 µl MgCl2 (50 mM, Bioline), 0.625 µl dNTPs (12.5 mM,

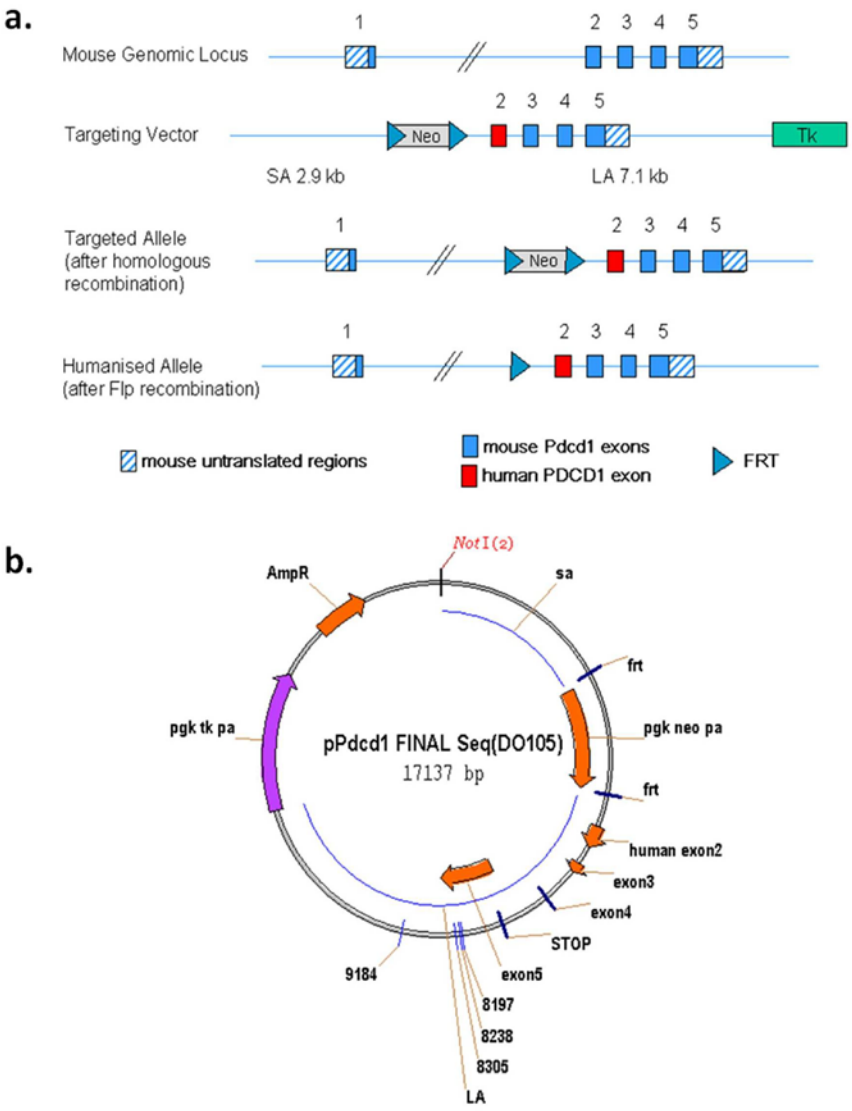


Figure 2.1 Generation of humanised allele. (a) Human PDCD1 exon 2, encoding the extracellular domain of PD-1, has been PCR amplified from human genomic DNA and mouse Pdcd1 exon 2 has been replaced with the human counterpart. In order to make sure that the humanised mRNA will be spliced properly, the mouse sequence at the exon-intron junction around exon 2 and structure of the mouse gene has been left intact. Selection marker has been flanked by frt sites and humanised allele was generated after in vivo Flp-mediated removal of selection marker. **(b)** Map of the targeting vector.

Bioline), 0.75 µl of primers (10 mM, Eurofins), 0.125 µl Taq DNA polymerase (Bioline), 16.5 µl ddH_2O (Sigma) and 1 µl DNA from ear punch extracts. The PCR program that was set on the thermocycler (Biorad) was: 95ºC (5')- 95ºC (10")- 58ºC (30")- 72ºC (30")- 72ºC (10')-16ºC (Forever), 35 cycles. Samples were run in 1% Agarose gel for 30 minutes. The band lengths for mouse PD-1 exon 2 and human PD-1 exon 2 were 150bp and 300bp respectively.

Immunizations for the immune response models

For the stimulation of primary germinal centre (GC) reaction in vivo, sheep red blood cells (SRBCs) were used as the immunogen. Fresh SRBCs were washed once with PBS and resuspended at a density of 10^{10} cells/ml. Mice were injected i.p. with $2x10^9$ SRBCs per mouse. GC reaction in spleen and mesenteric lymph nodes was analysed by flow cytometry on day 7. Antibody responses against SRBCs were analyzed by ELISA.

$CD8^+$ T cell driven immune reponses were induced by Modified Vaccinia Ankara (MVA) immunizations. Mice were infected with 10^6 PFU heat inactivated MVA i.m. (under general anesthesia). On day 9, spleens and reactive lymph nodes were removed and mechanically dissociated into RPMI/FCS. Cells were counted and resuspended at a density of 10^7 cells/ ml. They were then plated at a seeding inoculum of 10^5 cells/well) in two 96 well round bottom plates. One of the plates was allocated for peptide stimulation and the other plate was kept as no-stimulation control. Cells were incubated in the presence of 2 µg/ml MVA specific peptide B8R (Neo-peptide) and FITC conjugated LAMP-I antibody (eBioscience) for 2 hours at 37ºC in dark. After this step, Golgi plug (BD Biosciences) was added to the wells according to manufacturer's instructions and cells were incubated for another 4 hours at 37ºC in dark. Cells

were rested at 4ºC overnight in dark. The next day cytokine producing ability of $CD8^+$ T cells were analyzed by flow cytometry.

For testing the effects of the antibodies on the immune responses, the anti-PD-1 antibodies or isotype control antibody were injected s.c. 24 hours after the immunogen administration. The dose used for the antibodies was 30 mg/kg.

Immunizations for adoptive transfer experiments

For adoptive transfer experiments, OT-I mice were bred with hPD-1KI mice. The double heterozygote litter of the OT-I-hPD-1KI pair was then bred with GFP mice in order to obtain triple heterozygotes. Spleens of naïve OT-I-hPD-1KI-GFP and C57BL/6-OT-I were aseptically removed and single cell suspensions were prepared by mechanical dissociation. Red blood cells were lysed by treating the cells with 10 ml TAC buffer (2.2.5). $CD8^+$ T cells were selected by depleting the $CD4^+$ T cells, B cells, NK cells and macrophages by magnetically separating the cells that bind biotinylated anti-mouse B220, anti-mouse Ly6G, anti-mouse Gr-1, anti-mouse CD11b, anti-mouse CD11c, anti-mouse NK1.1, anti-mouse CD49 (2.2.6). Selected cells of OT-I-hPD-1KI-GFP and C57BL/6-OT-I were counted and mixed at 1:1 ratio at a final density of $5x10^6$ cells/ml in sterile PBS. Congenic C57BL/6SJL recipients were transferred with 10^6 cells i.v. Mice were rested for 24 hours and injected with 10^6 pfu MVA-OVA (Jenner Institute, University of Oxford) i.m. (under general anesthesia) to elicit OVA specific immune response. Lastly, anti-PD-1 antibodies or isotype control antibody were administered s.c. 24 hours after the MVA-OVA injection. The effect of the antibodies on the expansion of adoptively transferred OT-I transgenic T cells was analysed by flow cytometry on the day of the peak response (day 9).

Immunizations for inducing experimental autoimmune encephalomyelitis (EAE)

9 weeks old female hPD-1KI mice were immunized s.c. with myelin oligodendrocyte glycoprotein (MOG) 35-55 peptide which was emulsified in complete freund's adjuvant (CFA). Pertussis toxin was administered in two doses for breaking the blood brain barrier. EAE induction was performed by Kathrine Attfield. Mice were followed up by weight measurements and clinical scoring. The mice that had more than 20% weight loss were culled humanely. The neurological deficits and the corresponding clinical scores were as follows: score 0.5- weak tail, score 1-tail paralysis, score 2a/2b- loss of the righting reflex and/or abnormal gait, score 3: partial hind limb paralysis, score 4: complete hind limb paralysis. The mice that had a score of 4 for the 3 consecutive days, developed side paralysis and were not capable of moving on the forelimbs or developed resistant ulcers which did not show any signs of healing within 7 days were also culled humanely. The weight measurements and cinical scores were plotted on XY graphs and analysed.

Anti-PD-1 antibodies were injected i.p. 24 hours after the EAE induction. For some experiments, two doses were administered on day 4 and day 7.

2.4.2 Foxp3-GFP-hPD-1KI reporter mice

Genotyping strategy for the identification of the reporter allele

The genotyping primers that were directed against Foxp3 gene was used for detecting GFP containing Foxp3 allele. Primers were as follows: forward ATTCCACTGTTATCCCTGCAG, reverse CGGGCCTCACCTGCAGCTG. Components of the PCR mix for one DNA sample were 2.5 µl 10x reaction buffer (Bioline), 1.25 µl MgCl2 (50 mM, Bioline), 0.625 µl dNTPs (12.5 mM, Bioline), 0.75 µl of primers (10 mM, Eurofins), 0.125 µl Taq DNA polymerase (Bioline), 18 µl

ddH_2O (Sigma) and 1 µl DNA from ear punch extracts. The PCR program that was set on the thermocycler (Biorad) was: 95ºC (5')- 95ºC (10")- 60.4ºC (30")- 72ºC (1')- 72ºC (10')-16ºC (Forever), 35 cycles. Samples were run in 1% Agarose gel for 30 minutes. The expected band lengths for native and GFP containing Foxp3 alleles were ~150 bp and ~850 bp respectively.

2.4.3 OT-1-GFP-hPD-1KI mice

Genotyping strategy for the identification of the GFP reporter allele and the TCR transgene

The genotyping primers were either directed against TCRα or TCRβ for detecting the OT-1 allele. Primers were as follows: TCRα forward CAGCAGCAGGTGAGACAAAGT, TCRα reverse GGCTTTATAATTAGCTTGGTCC, TCRβ forward AAGGTGGAGAGAGACAAAGGATTC, TCRβ reverse TTGAGAGCTGTCTCC, internal control forward CAAATGTTGCTTGTCTGGTG, internal control reverse GTCAGTCGAGTGCACAGTTT. Components of the PCR mix for one DNA sample were 2.5 µl 10x reaction buffer (Bioline), 1.25 µl MgCl2 (50 mM, Bioline), 0.625 µl dNTPs (12.5 mM, Bioline), 0.75 µl of primers (10 mM, Eurofins), 0.125 µl Taq DNA polymerase (Bioline), 18 µl ddH_2O (Sigma) and 1 µl DNA from ear punch extracts. The PCR program that was set on the thermocycler (Biorad) was: 95ºC (5')- 95ºC (10")- 54ºC (30")- 72ºC (30")- 72ºC (10')-16ºC (Forever), 35 cycles. Samples were run in 2% Agarose gel for 30 minutes. The band expected band lengths for OT-1 TCRα and TCRβ are ~300 bp,

The genotyping primers that were directed against GFP reporter allele were as follows: forward ACGTAAACGGCCACAAGTTC, reverse AAGTCGTGCTGCTTCATGTG. Components of the PCR mix for one DNA sample were 2.5 µl 10x reaction buffer (Bioline), 1 µl MgCl2 (50 mM, Bioline), 0.625 µl dNTPs (12.5 mM, Bioline), 0.75 µl of primers (10 mM, Eurofins), 0.125 µl Taq DNA polymerase (Bioline), 18.25 µl ddH_2O (Sigma) and 1 µl DNA from ear punch extracts. The

PCR program that was set on the thermocycler (Biorad) was: 95ºC (5')- 95ºC (10")- 64ºC (30")- 72ºC (30")- 72ºC (5')-16ºC (Forever), 30 cycles. Samples were run in 2% Agarose gel for 30 minutes. The expected band length for GFP is ~200 bp.

2.5 Analysis of the cellular assays and immune responses

2.5.1 Flow cytometry and fluorescence-activated cell sorting

All the assays were performed using a BD FACS Canto flow cytometer and results were analyzed using FlowJo software (Tree Star, Ashland, OR). For fluorescence-activated cell sorting, a *Dako CyAn* ADP flow cytometer was used.

Detection of PD-1 expression on 293T cells

Cells were harvested at 24 hours and stained with 100 µl unconjugated anti-PD-1 antibodies or isotype control antibody at 10 µg/ml in PBS/BSA/Azide for 45 minutes at 4°C. Cells were washed with PBS/BSA/Azide, spun at 300 g for 5 minutes and primary antibodies were labelled with Alexa647-conjugated donkey anti-mouse IgG (5 µg/ml) in PBS/BSA/Azide for 30 min at 4°C. Cells were washed as above and resuspended in 200 µl PBS/BSA/Azide before being analyzed..

Quantification of the antibody levels on Dynalbeads™

$1.5x10^5$ beads were stained with saturating amounts of isotype-specific PE-labelled goat antibodies for 30 minutes at 4ºC in dark. Bead bound anti-PD-1 antibodies, anti-human CD3

(OKT3), anti-mouse CD3ε, anti-mouse CD28 and PD-L1-Fc were labelled with anti-mouse IgG1-PE (Serotec), anti-mouse IgG2a-PE (Serotec), anti-golden syrian hamster IgG-Biotin, anti-armenian hamster IgG-PE and anti-human IgG-PE (Southern Biotech) respectively. Anti-golden syrian hamster IgG-Biotin was detected with Streptavidin-PE. The antibodies and Streptavidin-PE were purchased from Ebioscience unless otherwise stated. Bead-bound antibody was compared with the Quantibrite™ prelabelled quantification kit (BD Biosciences Ltd.). The geometric mean fluorescence PE intensities of bead singlets (minus background of unloaded beads as a control) were used to calculate the absolute amount of antibody loaded per bead.

Analysis of human PBMC proliferation assay

PBMCs were stained with anti-CD3-PE.Cy7, anti-CD25-APC, anti-PD-1-PE (in-house) for 30 minutes at 4ºC in dark. Dead cells were labelled Live/Dead Fixable near-IR dead cell stain (Invitrogen) according to manufacturer's guidelines. Anti-PD-1 clone 2 was conjugated with PE using lynx rapid conjugation kit (Serotec). Cells were washed with PBS/BSA/Azide (2.1.1), spun at 300 g for 5 minutes and resuspended in 200 µl PBS/BSA/Azide. Cells were analysed for CFSE dilution and surface staining.

Detection of the upregulation of humanized PD-1 on cultured mouse splenocytes

WT C57BL/6, heterozygous hPD-1KI and homozygous hPD-1KI splenocytes were either stimulated in the presence of plate bound anti-mouse CD3ε or left unstimulated at 4ºC. Cells were harvested after 48 hours of stimulation. After an initial wash, 10^6 cells per group were stained with anti-mouse CD4, anti-mouse CD3, FITC conjugated anti-mouse PD-1, PE conjugated anti-PD-1 clone 2 (in-house) and Live/Dead Fixable near-IR dead cell stain for 30 minutes at 4ºC in dark. All the antibodies were purchased from Ebioscience unless otherwise

stated. Dead cells that were positively stained by Live/Dead Fixable near-IR dead cell stain were excluded from the analysis. Surface expression of human PD-1 and mouse PD-1 on T cells was analyzed.

Fluorescence activated sorting of naïve $CD4^+$ T cells and analysis of iTreg formation

For fluorescence activated cell sorting of naïve $CD4^+$ T cells, lymph nodes of the mice were mechanically dissociated and single cell suspensions of lymphocytes were obtained. Lymphocytes were washed with PBS+ 0.5%BSA and then stained with saturating amounts of anti-mouse CD4-PE.Cy7, anti-mouse B220-PE, anti-mouse CD62L-APC and Live/Dead Fixable near-IR dead cell stain for 30 minutes at 4ºC in dark. For sorting the naïve $CD4^+$ T cell population, dead cells were negatively gated in the first place. For excluding B cells and Tregs, $B220^+$ and GFP^+ cells were gated out. In the remaining population, $CD4^+CD62L^+$ cells were gated and referred to as naïve CD4+ T cells.

For detecting iTreg formation, cells were stained with PE.Cy7 conjugated anti-mouse CD4 and Live/Dead Fixable near-IR dead cell stain for 30 minutes at 4ºC in dark. After excluding dead cells, CD4 expressing GFP^+ cells were gated for analysis. Percentage of $CD4^+GFP^+$ cells were calculated and referred to as percentage of induced Tregs.

Analysis of the mixed lymphocyte reaction assays

For analyzing the proliferation status of the responder cells in the MLR reaction, cells were labelled with CFSE prior to setting up the allogeneic mixtures. The cell mixture was stained with PE.Cy7 conjugated anti-mouse CD4, APC conjugated anti-mouse CD3, PE conjugated anti-

mouse PD-1 clone 2 and Live/Dead Fixable near-IR dead cell stain for 30 minutes at 4ºC. After dead cell exclusion, CFSE dilution of the T cell subsets was analysed. Stimulator and responder cells were distinguished based on the fact that responders are $CFSE^+$ and stimulators are $CFSE^-$. Stimulated and unstimulated Balb/c splenocytes and stimulated C57BL/6 T cells were used as the staining controls.

Initial characterization of the immune system of hPD-1KI mice

In vivo immunophenotyping assays were carried out with age-matched naïve wt C57BL/6 and hPD-1 knock-in mice. Thymus and spleen from the two groups of mice were aseptically removed and mechanically dissociated into non-sterile RPMI/FCS. After initial washing and resuspension steps, single cell suspensions from thymus were stained with anti-mouse CD4, anti-mouse CD8, anti-mouse CD25, anti-mouse CD69, anti-mouse CD44 and Live/Dead Fixable near-IR dead cell stain in different fluorochrome combinations for 30 minutes at 4ºC in dark. Spleen samples were stained with anti-mouse CD4, anti-mouse CD8, anti-mouse CD44, anti-mouse ICOS, anti-mouse CXCR5-Biotin (BD Biosciences), anti-human PD-1 clone 2 (in-house), anti-mouse B220, anti-mouse GL7, anti-mouse CD95, anti-mouse IgG1, anti-mouse CD21, anti-mouse CD23, anti-mouse IgD and Live/Dead Fixable near-IR dead cell stain in different fluorochrome combinations for 30 minutes at 4ºC in dark. CXCR5 staining was either detected by Percp.Cy5.5 conjugated streptavidin (Caltag) or PE conjugated streptavidin.κ specific biotinylated rat IgG2a was used as the isotype control for anti-mouse CXCR5 antibody. All the antibodies were purchased from Ebioscience unless otherwise stated. The cells were then washed, resuspended with HBSS/FCS/Azide and analysed by flow cytometry. Follicular helper T cells were identified as $CD4^+CD44^+CXCR5^+ICOS^+$. Germinal centre B cells were identified as $B220^+GL7^+CD95^+$. Isotype-switched B cells.were identified as $B220^+IgG1^+$.

Characterization of the immune responses in models of immunity

Detection of SRBC induced primary germinal centre reaction

For detecting the effects of the anti-PD-1 antibodies on the primary germinal centre reaction, spleen and mesenteric lymph nodes were taken 7 days after the SRBC challenge. Cells were mechanically dissociated and stained with the combination of the antibodies used for spleen in the initial characterization of hPD-1KI mice.

Detection of the immune response to MVA challenge

The cells that were stimulated with the peptide the day before were washed and initially treated with CD16/32 (Ebioscience) for blocking the unwanted binding of antibodies to the Fc receptor-expressing cells as well as the unstimulated cells. After a washing step, the surface staining was performed by using anti-mouse CD4-PE.Cy5, anti-mouse CD8-PE.Cy7, anti-human PD-1-PE (clone 2 in-house) and Live/Dead Fixable near-IR dead cell stain. Surface staining was washed with HBSS/FCS/Azide and cells were permeabilized by fixation/permeabilization buffer (BD Biosciences). Intracellular cytokine staining (ICS) was performed for APC conjugated IFN-γ according to manufacturer's protocol (eBioscience). After the last washing step, cells were resuspended in HBSS/FCS/Azide and analyzed in the flow cytometer. Dead cells were excluded in the first place and the IFN-γ producing LAMP-I^{+}CD8^{+} T cell population was analysed.

Analysis of the antigen specific responses in adoptive transfer experiments

Spleens of the C57BL/6 congenic recipients were aseptically removed on the day of the peak response. The spleens of untransferred naïve C57BL/6 congenic mice, naïve OT-I-hPD-1KI-

GFP triple heterozygous mice and naïve OT-I mice were also taken as for the staining controls.. Cells were mechanically dissociated into non-sterile RPMI/FCS and stained with anti-mouse B220-PE, anti-mouse CD8-PE.Cy7, anti-mouse Ly5-APC.Cy7 and Live/Dead Fixable Far red dead cell stain for for 30 minutes at 4ºC in dark. After the last washing step cells were analyzed in the flow cytometer. Congenic recipients, OT-I-hPD-1KI donors and OT-I-WT donors were distinguished by $Ly5^{+}GFP^{-}$, $Ly5^{-}GFP^{+}$, $Ly5^{-}GFP^{-}$ staining patterns respectively. The percentages and absolute numbers of the adoptively transferred OT-I-hPD-1KI and OT-I-WT donors were calculated.

EAE induction was performed as mentioned in 2.4.1. Reactive lymph nodes of three mice were removed on day 0, day 4, day 7 and day 10. Cells were mechanically dissociated, washed and stained with anti-mouse CD3, anti-mouse CD4, anti-human PD-1 clone 2-PE, anti-mouse CD69, anti-mouse CD44. The cells were then washed, resuspended with HBSS/FCS/Azide and analysed by flow cytometry.

2.5.2 ELISA

Sheep red blood cell specific ELISA

SRBCs were washed and resuspended with PBS at $5x10^{7}$ cells/ml. ELISA plates were coated by adding 100 µl of this SRBC suspension to each well and incubating the plates overnight at 4ºC. Next day, 20 µl 1.8% glutaraldehyde (Sigma) solution was added to each well to fix the SRBCs and plates were incubated for 30 minutes at room temperature. Plates were washed with PBS for four times and blocked with 1% skimmed milk in PBS for 1.5 hours at 37ºC. Each mouse sample was diluted in PBS. The dilutions were as follows: 1/16-1/64-1/256-1/1024-1/16384. After a washing step, diluted mouse sera was added to the wells and incubated for 1.5

hours at 37ºC. Plates were washed and ALP conjugated goat anti-mouse IgM (1/30000, Sigma) or goat anti-mouse IgG (1/1000, Sigma) was added to the wells and incubated for 1 hour at 37ºC. After the last wash, ALP substrate was dissolved in NPP buffer at 2mg/ml. It was then added to the wells and incubated for 1 hour at room temperature. Plates were readed at Biorad plate reader at 405 nm. A pool of serum from15 mice that were injected with SRBCs was used as the standard. Serum from naïve mice was used as the negative control. All the samples, standard and negative control was serially diluted starting from 1/16.

2.6 Protein Methods for antibody purification

2.6.1 Protein G purification

The hybridoma suspensions were spun at 4000 rpm for 15 minutes at 4 °C. Tissue culture supernatants were collected, after addition of 0.05% sodium azide diluted 1:2 with PBS/azide and either stored at 4°C or subjected to protein G purification. Considering that 1ml bead can bind approximately 20 g of human IgG, for most of the purification procedures 1 ml protein G (GE Healthcare) bead was used. Protein G beads were washed with PBS/Azide twice and applied to the HiTrap Protein G 10 ml columns (GE Healthcare). After 2-4 L of supernatant was applied throµgh, column was washed with 10 column volumes of cold PBS/Azide that contains 0.5 M NaCl. Using 0.1 M glycine/HCl solution at pH 2.7, bound IgG was eluted into tubes containing 2.7M Tris Ph 8.5 that is enough the neutralize the pH. Ten 0.5-1 ml fractions were collected and their optical densities were measured at 280 nm. Immediately after collecting the fractions, column was neutralized using PBS. was. 10-20 µl of each fraction from the elute that contained antibody and samples from the washing steps were run on reducing and non-reducing 12% acrylamide gels. The fractions that contained antibody were pooled and

concentrated in Vivaspin concentration tubes (Sartorius) into approximately 500 µl. The final volume was adjusted in order to keep the final antibody concentration less than 20 mg/ml.

2.6.2 Gel filtration

The pooled and concentrated fractions from protein G purification were further purified by using gel filtration. Gel filtration Superdex 200 H/R column (GE Life Sciences) was prepared as outlined in the manual. Column was washed using at least one column volume (CV) of HBS pH 7.4 prior to use. The 500 µl-1 ml loop was also washed with HBS pH 7.4. The 500 µl pooled antibody solution was then loaded into the loop. At this step, concentration of the antibody should not exceed 10 OD, otherwise selection process is impaired.

The antibody amount of the peak fractions were quantified by OD measurement. 10 µl of each fractions was run on reducing and non-reducing 12% acrylamide gels. Fractions that contained ≥ 0.3-0.5 mg/ml IgG were pooled, sterile filtered and stored at -80 °C for long-term storage.

2.6.3 SDS-PAGE for detecting the purity of the antibody

12% acrylamide gels and stacking gels were prepared as described in 2.1.1. Samples, controls and markers were mixed with 2X reducing and non-reducing sample buffers and heated to 90ºC for 5 minutes. Samples were then loaded onto the gels. Gels were run at 150V until the bromphenol blue band reaches the base if the glass plates. In order to visualize the bands, gels were stained with Coomassie blue for 20 minutes. Excess stain was removed using destaining solution by the help of a piece clean tissue.

Chapter 3:

Analyzing the effects of anti-PD-1 antibody agonists on human PBMCs

3.1 Introduction

Initial work on the PD-1-CD28 chimera suggested that the difference between the activities of anti-human PD-1 antibody agonists might be attributed to their epitope binding properties. In particular, the experiments suggested that the superagonistic potential of the antibody, clone 19, was consistent with its targeting of a membrane proximal epitope on PD-1. However, since inhibitory superagonists have not previously been designed, it was necessary to show that the antibodies induce inhibitory signalling by native PD-1. I therefore addressed how effectively the novel PD-1 agonists inhibit TCR-derived signals and whether the inhibitory activity indeed correlates with epitope position as predicted by the theory of superagonistic action.

PD-1 was described as an important regulator of immune responses more than a decade ago [102-103]. The studies that investigated the mechanism of PD-1-mediated inhibition revealed that PD-1 executes its inhibitory function through interacting with two different ligands, PD-L1 and PD-L2 [177-178]. In this work, Ig fusion proteins of PD-L1 and PD-L2 were generated and either immobilized onto tissue culture plates or polyurethane-coated tosyl-activated beads together with mitogenic anti-CD3 antibodies. T cells from human peripherial blood, PD-1 deficient or WT mice were then exposed to these stimuli and their proliferative responses were quantified in order to see if the ligands are responsible for PD-1 mediated inhibition and if the inhibition is indeed PD-1 specific. In the current study, we used a similar approach to test the functional significance of the interaction between human PD-1 and anti-human PD-1 antibodies.

Bead bound antibodies and fusion proteins are widely used for delineating the functions of positive and negative costimulatory molecules [192, 335-336]. In previous studies using bead-bound stimuli, the equal covalent loading of each single protein to the different groups of beads was assumed on the basis of keeping the total amount of loaded proteins constant. In other words, it was assumed that all the proteins in the loading solution are coupled proportionately to the beads, as long as their amount in the mixture is kept equal within control and treatment groups and the binding surface of the beads are totally occupied by coating them with the same total amount. However, this approach doesn't allow for possible steric hindrance created by the binding of one type of protein and the potential competition between different proteins for binding to the beads. Indeed, in our experience we could not detect any correlation between the "loading" amount and the final level of antibody on the beads (Table 3.1).

To address this problem, I used a titration and quantification-based bead preparation approach in order to provide near-equal positive stimuli to the cells that are treated with different groups of antibodies (Figure 3.1). I was able to do this due to there being isotype differences among the antibodies that allowed the coupling efficiency to be monitored by flow cytometry. This enabled us to rigorously compare the individual inhibitory effects of anti-PD-1 antibody clones.

3.2 The strategy used for the bead preparation

Tosyl-activated Dynalbeads™ were loaded simultaneously with anti-human CD3 antibody OKT3, which is of IgG2a isotype, and either of the following IgG1 class antibodies: anti-PD-1 clone 19, clone 10, clone 2 or mouse IgG1 isotype control antibody (OX7, anti-rat Thy 1.1). A total of 15 μg of antibody was loaded per $3x10^7$ beads in a volume of 75 μl. During loading, the amount of OKT3 was titrated between 0.64 μg and 2.6 μg per $3x10^7$ beads and the amount of the anti-PD-1 antibodies/mIgG1 isotype control was kept between 12.4 μg and14.36 μg in order

OKT3 (ng)	Control		Clone 19		Clone 10		Clone 2	
	Isotype (mIgG1)	OKT3 (mIgG2a)	Anti-PD-1 (mIgG1)	OKT3 (mIgG2a)	Anti-PD-1 (mIgG1)	OKT3 (mIgG2a)	Anti-PD-1 (mIgG1)	OKT3 (mIgG2a)
40	149961	840	169590	1134	146754	143	54050	58
80	166194	850	166975	1537	162263	1098	46158	896
160	161513	2151	164406	2096	159383	1551	55068	1077
320	156907	3771	167786	4446	158150	3030	55107	1141
640	164206	6378	167249	6693	156476	5739	58841	2235
800	118967	12555	133003	14760	107689	9693	65478	2678
900	142168	13679	131199	14094	112634	8340	74536	2593
1000	121993	11176	130413	15035	106974	12441	72345	3076
1200	122584	13712	134534	10437	113613	15230	58667	4871
1280	125164	18868	128507	12268	115218	10739	74462	4364
1400	125164	18868	124634	13447	106681	15297	68123	5467
1600	124322	16777	145786	14451	106265	18050	78992	8649
1800	118451	19121	142992	16481	126414	22296	81002	10979
2000	107790	18765	119783	26781	111435	23567	78466	12460
2200	109987	20784	131299	23590	121298	26876	78690	12860
2400	103459	24879	122431	23454	113741	21235	82327	14141
2560	101074	23654	124089	18957	123888	22034	79986	7056
2600	-	-	-	-	-	-	84570	19870
2800	-	-	-	-	-	-	85847	20991
3000	-	-	-	-	-	-	90283	23170
3400	-	-	-	-	-	-	80177	23130
3800	-	-	-	-	-	-	80478	23789

Table 3.1 The quantity of the OKT3 antibody loaded and the number of antibody molecules coupled per bead. Levels of the antibodies coupled to the beads were quantified using Quantibrite™ prelabelled quantification kit for flow cytometry. Matched sets of Dynalbeads™ are represented with the same colour code: light blue: low OKT3, dark blue: medium-low OKT3, light purple: medium OKT3, dark purple: medium-high OKT3, pink-purple: high OKT3.

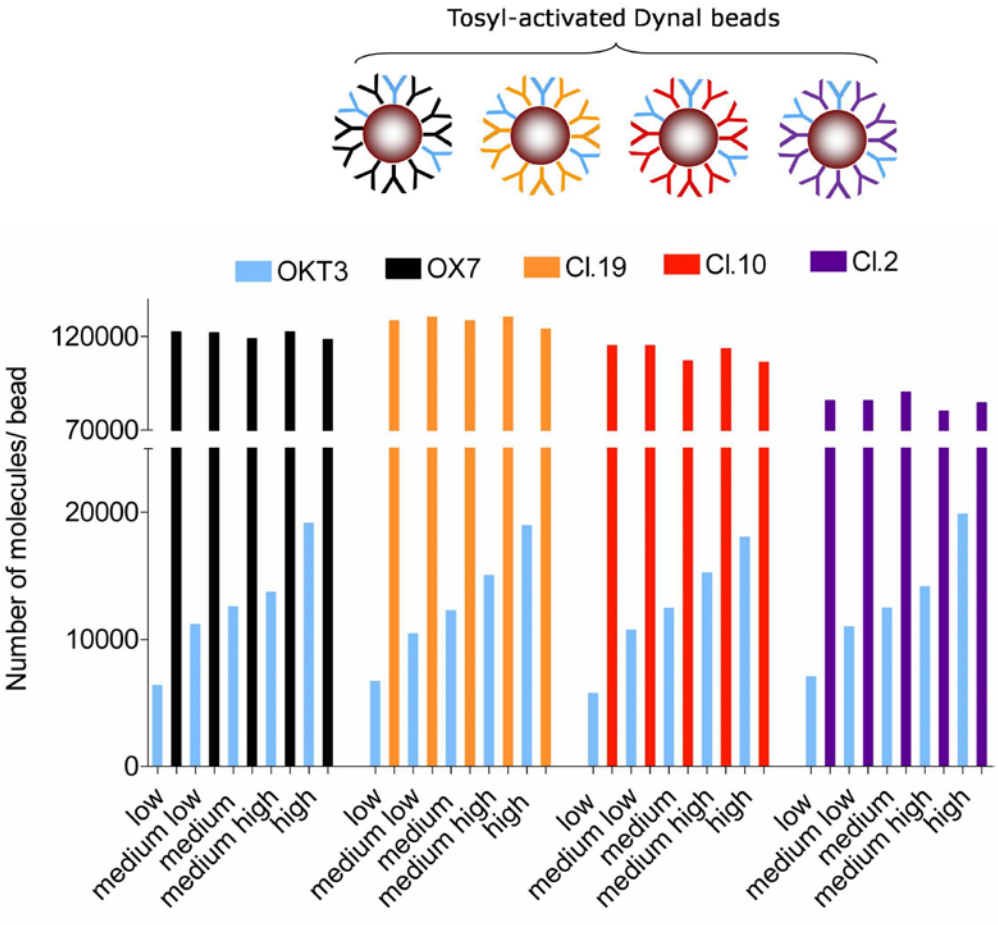


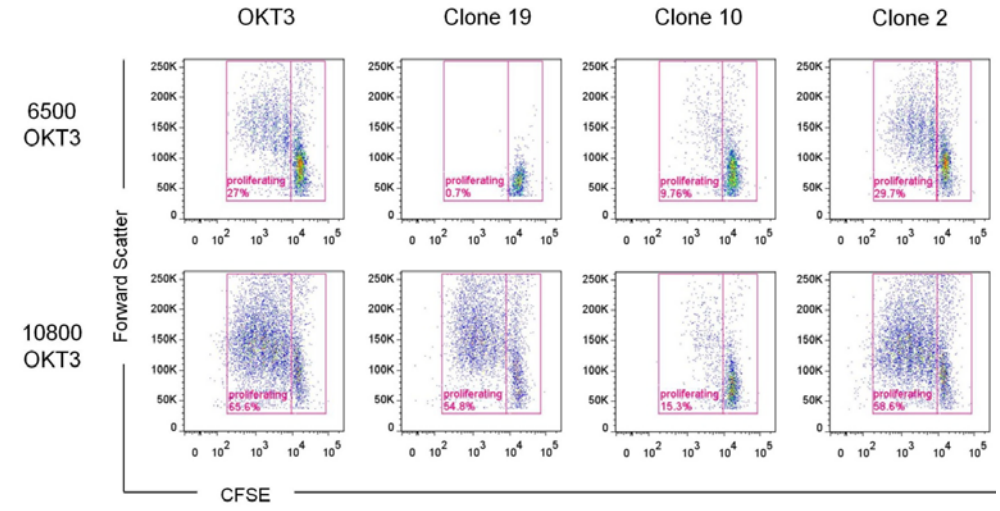
Figure 3.1 The graph showing the titration of OKT3 molecules on Dynalbeads™. Beads were loaded with varying amounts of anti-CD3 antibody (OKT3) along with maximal amounts anti-PD-1 antibodies to inhibit TCR mediated activation of PBMCs. A total of 15ug antibody is loaded per $3x10^7$ beads. OX7 antibody was used as mIgG1 isotype control for anti-PD-1 antibodies. Matched sets with near equivalent levels of OKT3 have been generated in order to keep the positive stimulus constant among different types of beads. Each antibody is represented by the colour next to its name.

to load a total of 15 μg per $3x10^7$ beads. After loading, antibody levels were quantified by flow cytometry using isotype specific secondary antibodies and QuantiBRITE™ beads. For providing similar strength positive stimuli to the cells at the time of the experiment, beads were grouped into the matched sets according to their levels of anti-CD3 antibody. For ease of comparison, the groups of antibody-coupled beads were referred to as: low OKT3 (5739-7055 molecules/ bead), medium-low OKT3 (10437-10979 molecules/bead), medium OKT3 (12268-12440 molecules/ bead), medium-high OKT3 (14141-15230 molecules/ bead) and high OKT3 (18050-19870 molecules/ bead). The types of the beads within the groups are referred to with the name of the antibody (Isotype control beads, Cl.19 beads, Cl.10 beads, Cl.2 beads) that was coupled.

3.3 The effects of the bead-bound anti-PD-1 antibodies on primary human T cells

Fresh human PBMCs were taken from healthy male individuals and T cells were enriched using a positive selection method (see Section 2.2.3). T cells were initially labelled with CFSE and then incubated with either low OKT3, medium-low OKT3, medium-high OKT3 or high OKT3 beads (see Section 3.1) for 4 days. Flow cytometric analysis of CFSE dilution was performed for calculating the percentage proliferation and the degree of inhibition. Proliferation levels (percent proliferation) were measured as the fraction of live T cells with diluted CFSE. The degree of inhibition was calculated as: 1 - (percent proliferation with anti-PD-1 antibodies / percent proliferation with OKT3). The percent proliferation provided by low, medium-low, medium-high and high OKT3 levels was approximately 20%, 61%, 62% and 65%, respectively (Figure 3.2). At the weakest level of TCR stimulation, the degree of inhibition was approximately 80% by clone 10 and 95% by clone 19 (Figure 3.2). At medium-low levels of OKT3 stimulation, although clone 10 still produced more than 65% inhibition, clone 19 did not exhibit any inhibitory effects. Clone 2 did not provide any inhibition at any level of OKT3 (Figure 3.2). At higher levels of OKT3

a.



b.

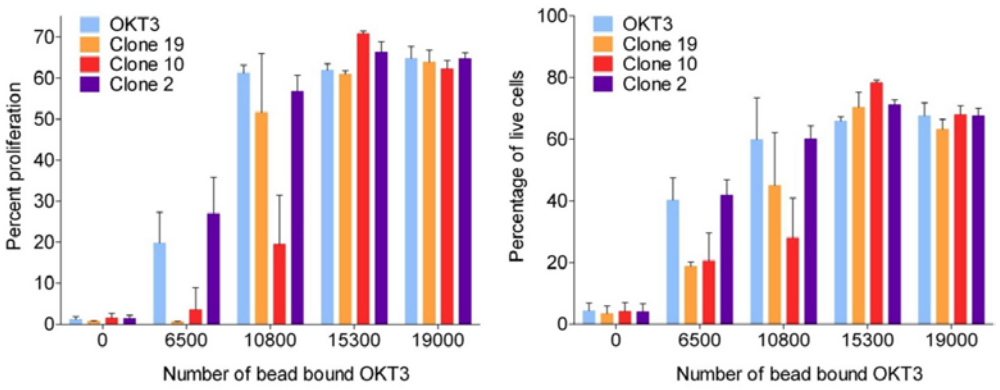


Figure 3.2 Inhibition of T cell proliferation by anti-PD-1 agonists on Dynalbeads™. a. FACS plots showing the proliferation status of T cells after 4 days of culture in the presence of anti-PD-1 antibodies. Inhibition of proliferation was observed with clone 19 and clone 10 treatments. **b.** Graphs showing the percent proliferation (left) and the percentage of live cells (right) when the PBMCs were cultured in the presence of Dynalbeads™ coated with an average of 6397 (low), 10708 (medium-low), 14686 (medium-high), 18960 (high) OKT3 molecules/bead plus maximal levels of anti-PD-1 antibodies ranging between 84570 and 137977 molecules/ bead. Data is representative of three independent experiments. Values are means of triplicates ± SD

(more than ~11200 molecules/ bead) the positive stimulus apparently overcame the inhibitory PD-1 signal and cells kept their activated status. At low and medium-low levels of OKT3 cell death accompanied the reduced proliferation of the live cells with clone 19 and clone 10 treatments (Figure 3.2).

3.4 Analysis of the proliferative responses using an alternative antibody immobilization strategy

In the case of coating beads with two different antibodies, I found that optimization of the final antibody levels on the beads was very difficult. Therefore, I tried uncoupling the positive and negative stimuli by coating the plates with OKT3 and loading the Dynalbeads™ solely with the anti-PD-1 antibodies. Therefore, round bottom 96 well plates were coated with either 0.5 µg/ml, 1 µg/ml, 5 µg/ml OKT3 or 5 µg/ml isotype control antibody for OKT3 (mIgG2a) in triplicate and the Dynalbeads™ were loaded with either clone 19, clone 10, clone 2 or OX7 at the maximal amount (15 µg per $3x10^7$ beads). T cells were positively selected, labelled with CFSE and $2x10^5$ cells were added to the wells coated with OKT3. Dynalbeads™ were then added to the cell culture and incubated for 4 days. At the end of 4 days, the proliferation status of the cells was analysed and the degree of inhibition was calculated. At 0.5 µg/ml of OKT3, clone 19 and clone 10 produced 43% and 51% inhibition respectively whereas, once again, clone 2 did not provide any inhibition (Figure 3.3).

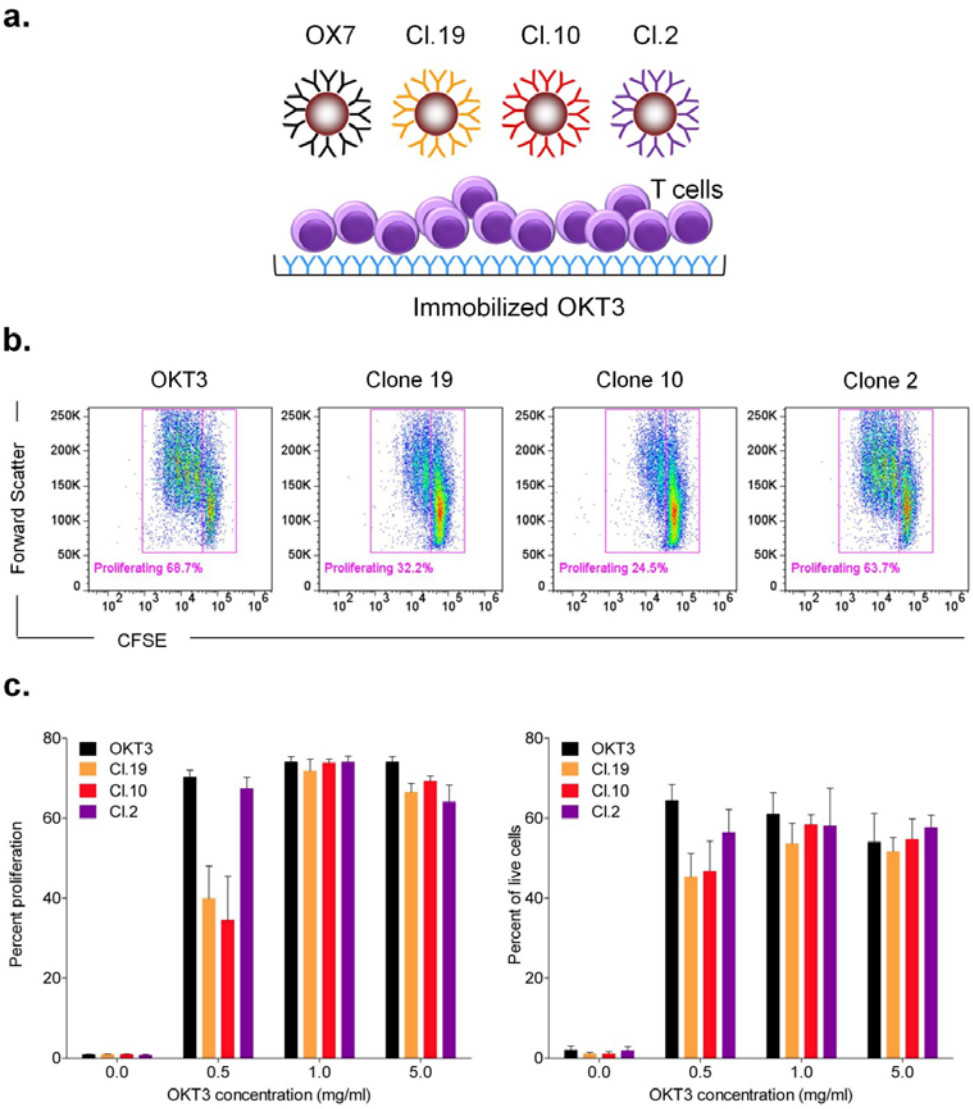


Figure 3.3 Proliferation provided by plate bound OKT3 was inhibited by bead bound Clone 19 and Clone 10. a. OKT3 antibody was immobilized onto plates at 0.5 µg/ml, 1 µg/ml, 5 µg/ml in triplicates and the beads were loaded with either clone 19 (77862 molecules/bead), clone 10 (72112 molecules/bead), clone 2 (34798 molecules/bead) or OX7 (79533). CFSE labelled PBMCs were cultured for 4 days in the presence of the positive and negative stimuli. **b.** Fraction of T cells with diluted CFSE was measured by flow cytometry and represented as the percent proliferation. FACS plots show the proliferation status of cells at 0.5 µg/ml plate bound OKT3. **c.** Graphs show the percent proliferation (left) and the percent of live cells (right). Data is representative of two independent experiments. Values are means of triplicates ± SD

3.5 Discussion

For elucidating the inhibitory potential of anti-PD-1 agonist antibodies a stringent bead preparation approach was undertaken. Characterization of the antibody levels on the beads revealed that there was no correlation between the amount of the antibody added to the "loading" mixture and the final antibody levels that were coupled to the beads. This suggests that steric hindrance and antibody competition may indeed play roles during the simultaneous conjugation of different antibodies to beads.

The PBMCs that were treated with matched sets of Dynalbeads™ had less proliferation upon contact with clone 19 and clone 10 coupled beads at relatively low levels of bead-bound OKT3. This effect was also observed when the PBMCs were stimulated with plate bound OKT3. These data agree with the early experiments on PD-1 and PD-L1 [178] showing that the PD-1 pathway is more effective at low levels of TCR stimulation. Similar to the natural ligands of PD-1, anti-PD-1 agonists only exert their activity while the TCR signal is relatively weak, as is likely the case in vivo. Furthermore, in contrast to the early experiments with hPD-1/mCD3ζWT/mCD28 chimera, clone 10 generally agonizes PD-1 more effectively over a broader range of OKT3 stimulation compared to clone 19. This may be explained by the fast binding kinetics of clone 10, since it may target more PD-1 molecules than clone 19 does in a certain time period and therefore lead to a better overall signal. Of the clone 19 and clone 2 antibodies, which have similar slow off-rates, only clone 19 had any effect in the proliferation assays. Under these circumstances we hypothesize that binding to a more membrane proximal epitope offsets the disadvantage of the slow off-rate.

An interesting observation was that the cells could still integrate the positive and negative signals even when those signals were segregated spatially. In contrast to the studies that propose a model of co-localized TCR and costimulatory receptors forming the immunological synapse [337-338], T cells receiving the TCR signal and the costimulatory signal from different

sites in the cell in the plate/bead assays were able to propagate the overall signal. Recently, Yokosuka et al. demonstrated that PD-1 forms microclusters even in the absence of TCR ligation. However, no PD-1 signalling was observed in those microclusters as indicated by a lack of PD-1 phosphorylation and SHP-2 association [185]. Although this finding contrasts with our observation, the two studies were designed differently and this may be an explanation for the discrepancy. The study of Yokosuka et al. was conducted using a T cell line transfected with an elongated chimeric PD-1 molecule in order to prevent TCR-PD-1 colocalization upon TCR-peptide-MHC engagement whereas ours utilized PBMCs expressing native human PD-1 molecules. Therefore, the findings of the previous study may not represent the physiological situation due to the possibility of a disruption in immune synapse dynamics. Overall, our data suggest that physical interactions between e.g. SHP1/2-loaded native PD-1 and the TCR are not required for generation of the inhibitory effects of PD-1. Given that PD-1 ligands are expressed on many tissues this may mimic the situation in vivo.

Chapter 4:

Characterization of a humanized PD-1 knock-in mouse

4.1 Introduction

Preclinical studies of novel therapies often require in vivo models to predict the effects of the candidate therapeutics on humans, before moving onto clinical trials. Mouse models are also the most commonly used in immunology research because of their short generation times and ease of maintenance. Although mouse and human immune system elements resemble each other, there are significant differences due to ~100 million years of divergent evolution [339]. Non-human primate models, which provide an evolutionarily closer alternative, are accepted as the best models for preclinical trials [340]. However, these models are often limited by their high costs both ethically and financially, and so they are generally used just before new therapeutics are introduced into clinical trials. Furthermore, they are also constrained by the differences between primate proteins and human counterparts [341]. In summary, there is a great need for sensitive, simple and cost-effective animal models.

The generation of transgenic mice offers access to such tools. Based on the conventional "knock-in" approach, which allows the insertion of a transgene in a selected locus, murine genes can be replaced with their human counterparts. This gives the opportunity to study the effects of the candidate human therapeutics directly in mice. Recently, humanized mouse models have been increasingly used for characterizing the effects of antibodies such as blocking anti-human CTLA-4 antibodies or anti-coagulation tissue factor antibodies as well as potentially tolerogenic anti-human CD3ε antibodies [340-342]. To be able to characterize the effects of the anti-human PD-1 superagonist antibodies in vivo, we out-sourced the generation of a humanized PD-1 knock-in (hereafter referred to as hPD-1KI) mouse model that expresses the human PD-1

extracellular region along with the mouse PD-1 transmembrane and intracellular domains (see Figure 2.1). Binding studies suggest that the affinity of human PD-1 for mouse PD-L1 is comparable to its affinity for human PD-L1 [343]. Therefore, we predicted that replacing the extracellular domain of mouse PD-1, while keeping its intracellular signalling portion intact, would not impair endogenous PD-1 signalling and the mice would develop and mount immune responses normally. In order to test this, we carried out initial in vitro and in vivo assays to characterize the hPD-1KI mice.

4.2 Analysis of the expression of humanized PD-1 protein on T cells

To detect the expression of humanized knock-in PD-1 protein, splenocytes from naïve WT C57BL/6, heterozygous hPD-1KI and homozygous hPD-1KI mice were cultured in tissue culture flasks pre-coated with 1 µg/ml anti-CD3ε for comparison with unstimulated cells. Surface expression of human PD-1 and mouse PD-1 were compared after 48 hours of incubation. Expression of the humanized PD-1 protein on the T cells was detected using a PE-conjugated anti-PD-1 clone 2 antibody. PD-1 expression was upregulated on the cells of heterozygous and homozygous hPD-1KI mice (Figure 4.1). No cross-reaction was observed between the anti-human PD-1 clone 2 and mouse PD-1, or the anti-mouse PD-1 antibody and human PD-1.

4.3 Analysis of the upregulation of humanized PD-1 protein upon in vivo stimulation

To demonstrate the normal up-regulation of human PD-1 protein upon stimulation in vivo, WT C57BL/6 and homozygous hPD-1KI mice were immunized i.p. with sheep red blood cells

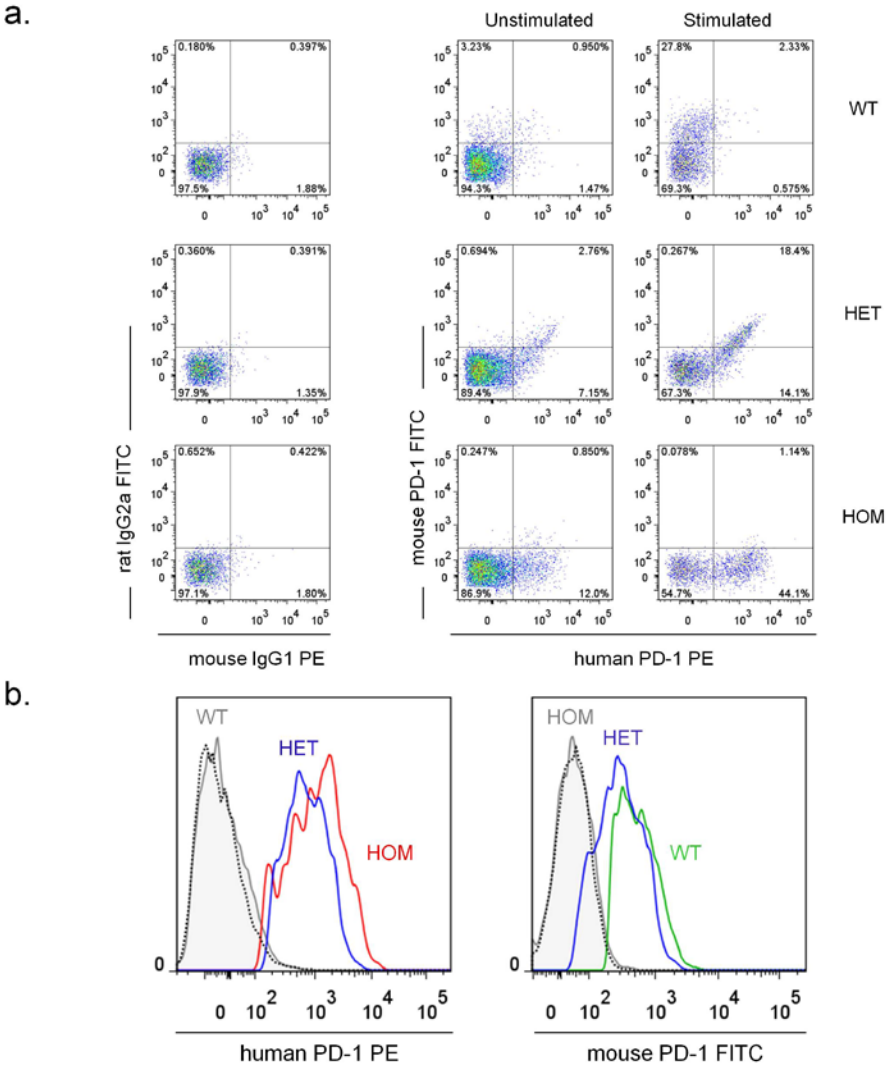


Figure 4.1 Upregulation of the humanized PD-1 protein on T cells upon in vitro stimulation. Splenocytes from naïve WT C57BL/6 (WT), heterozygous hPD-1KI (HET) and homozygous hPD-1KI (HOM) mice were either stimulated using 1 µg/ml anti-CD3ε or left unstimulated. **a.** Flow cytometry plots showing the stimulated T cells that were stained with either isotype controls for mouse and human PD-1 antibodies (left) or FITC conjugated anti-mouse PD-1 and PE conjugated anti-human PD-1 clone 2 (right). Basal expressions of mouse and human PD-1 proteins were also analysed (right). **b.** Histograms for the mean fluorescence intensities of human PD-1 (left), mouse PD-1 (right) and the isotype control (gated on T cells). **Left:** Red: homozygous hPD-1KI; blue: heterozygous hPD-1KI; grey tinted: C57BL/6; dotted line: mIgG1 isotype control. **Right:** green: C57BL/6; blue: heterozygous hPD-1KI; grey tinted: homozygous hPD-1KI; dotted line: rIgG2a isotype control. Data are representative of two independent experiments with one mouse per group.

(SRBCs), which induce a T cell dependent immune response. Seven days after the challenge, the expression of human PD-1 and mouse PD-1 on the T cells of immunized and naïve mice was analysed by flow cytometry. Compared to the T cells of naïve hPD-1KI mice, T cells of the immunized hPD-1 KI mice exhibited increased surface expression of human PD-1 on day 7 (Figure 4.2 a). The T cells of WT C57BL/6 mice, on the other hand, displayed a similar pattern of staining with the PE conjugated anti-human PD-1 antibody and its isotype control. Likewise, T cells of the hPD-1KI mice had comparable isotype control and mouse PD-1 staining patterns (Figure 4.2 b).

4.4 Characterization of the immune system of naïve hPD-1KI mice

Initial immunophenotyping assays were carried out to ensure that the hPD-1KI mice did not have developmental immune system abnormalities that would make the model unusable for studying the immune response to antigen. For this purpose, the thymic and splenic cell subsets of the naïve C57BL/6 and homozygous hPD-1KI mice at 8-12 weeks of age were compared using flow cytometry. The double negative ($CD4^-CD8^-$), double positive ($CD4^+CD8^+$), single positive ($CD4^+$ or $CD8^+$) T cells of the thymus and $CD4^+$ T cells, $CD8^+$ T cells, activated T cells ($CD4^+CD44^{hi}ICOS^{hi}$), follicular helper T (Tfh) cells ($CD4^+CD44^{hi}CXCR5^+$), total B cells ($B220^+$), follicular B cells ($B220^+CD23^{hi}$), marginal zone B cells ($B220^+CD23^{lo\text{-}med}CD21^{hi}$), germinal centre B cells ($B220^+GL7^+CD95^+$) and isotype class switched B cells ($B220^+IgG1^+$) of the spleen were analysed using the gating strategy described in Figure 4.3. No significant difference was observed in the percentage (data not shown) or absolute numbers of any of the cell subsets analysed (Figure 4.4).

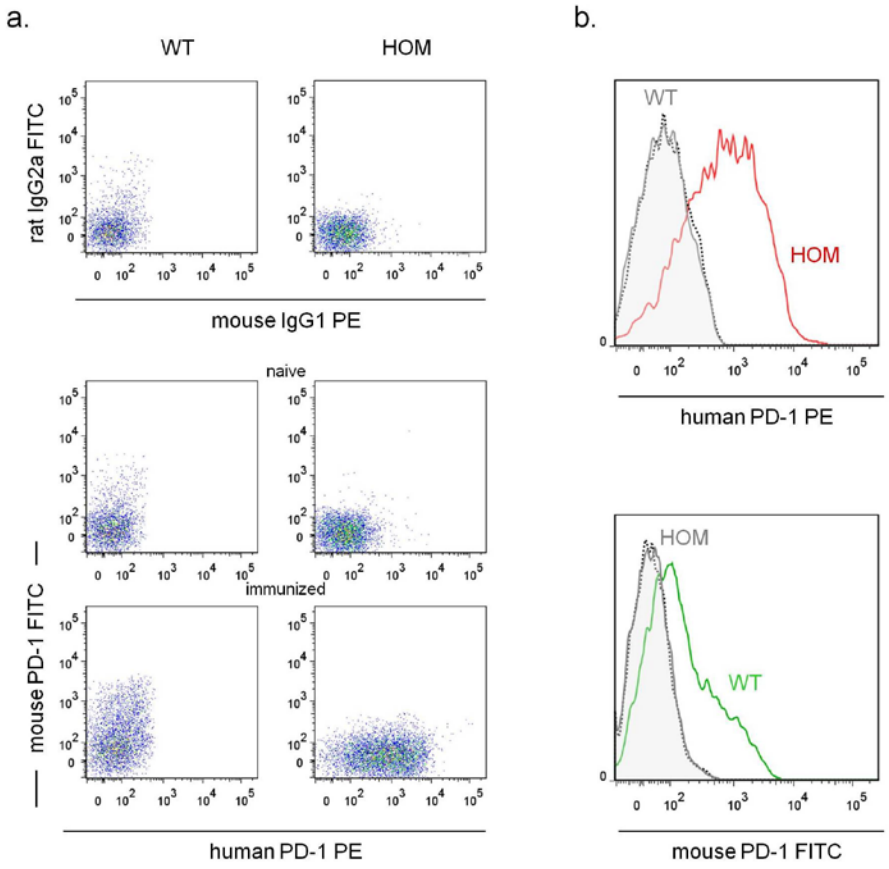


Figure 4.2 Expression of the humanized PD-1 protein on T cells upon in vivo stimulation. Homozygous hPD-1KI (HOM) and C57BL/6 (WT) mice were injected i.p. with $2x10^9$ SRBCs per mouse. 7 days after the injection, the levels of human PD-1 and mouse PD-1 on splenic T cells were analysed. **a.** Flow cytometry plots showing the T cells from immunized WT and hPD-1KI mice that were stained with either isotype controls for mouse and human PD-1 antibodies (above) or FITC conjugated anti-mouse PD-1 and PE conjugated anti-human PD-1 clone 2 (below). Expression of mouse and human PD-1 proteins in the naïve state were also analysed (below) (gated on $CD4^+CD44^{hi}$ T cells). **b.** The mean fluorescence intensities of human PD-1 (above), mouse PD-1 (below) and the isotype control stainings (gated on $CD4^+CD44^{hi}$ activated T cells). **Above:** Red: homozygous hPD-1KI; grey tinted: C57BL/6; dotted line: mIgG1 isotype control. **Below:** Green: C57BL/6; grey tinted: homozygous hPD-1KI; dotted line: rIgG2a isotype control. Data are representative of 3 independent experiments with 2 mice per group.

.

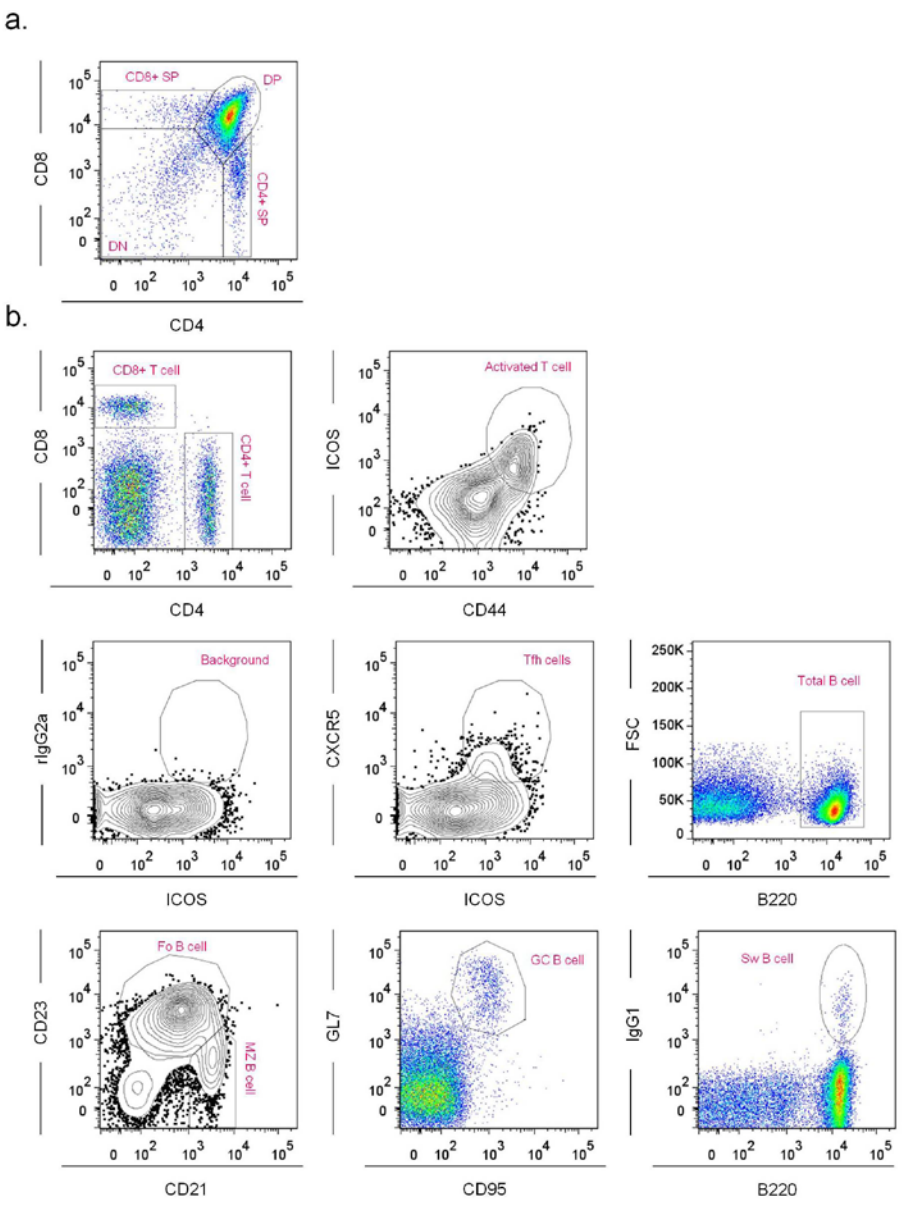
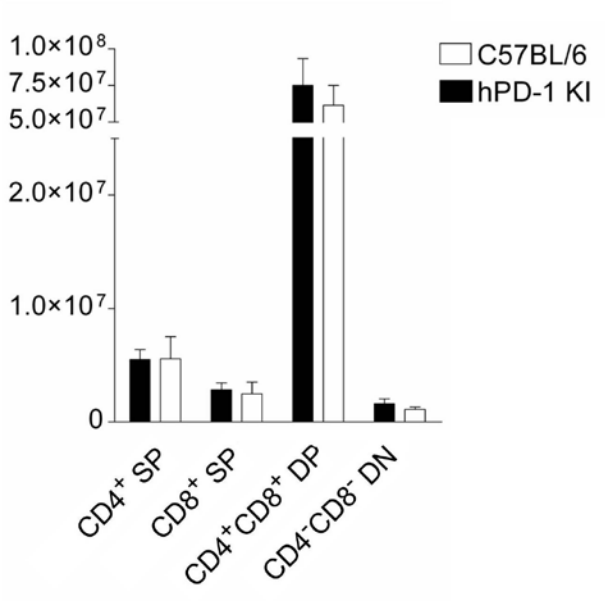


Figure 4.3 Gating strategy for the immunophenotyping assays. a. Thymus staining for $CD4^+$ single positive, $CD8^+$ single positive, $CD4^+CD8^+$ double positive and $CD4^-CD8^-$ double negative thymocytes. **b.** Spleen staining for the T and B cell subsets.

a.



b.

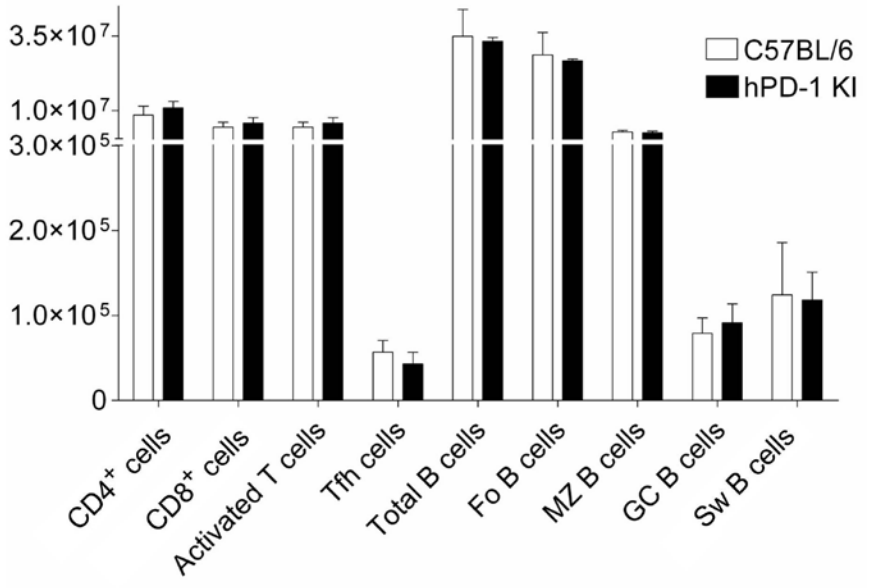


Figure 4.4 Comparison of the naïve status of hPD-1KI and C57BL/6 immune systems. Graphs of the thymic (a) and splenic (b) cell subsets respectively. Data was pooled from 3 independent experiments with 2 mice per group. Graph values are mean ± SD.

4.5 Testing the ability of hPD-1KI mice to mount a normal immune response

Having established that the naïve hPD-1KI mice have a normal resting immune system, I investigated the ability of these mice to mount an immune response. The immune responses generated by the WT C57BL/6, heterozygous hPD-1KI and homozygous hPD-1KI mice were compared after SRBC immunization. As SRBCs are potent stimulators of the germinal centre response, germinal centre components Tfh cells, GC B cells and isotype- switched B cells, as well as activated T cells, were quantitated using flow cytometry. Mice from all groups produced similar strength immune responses against the immunogen (Figure 4.5).

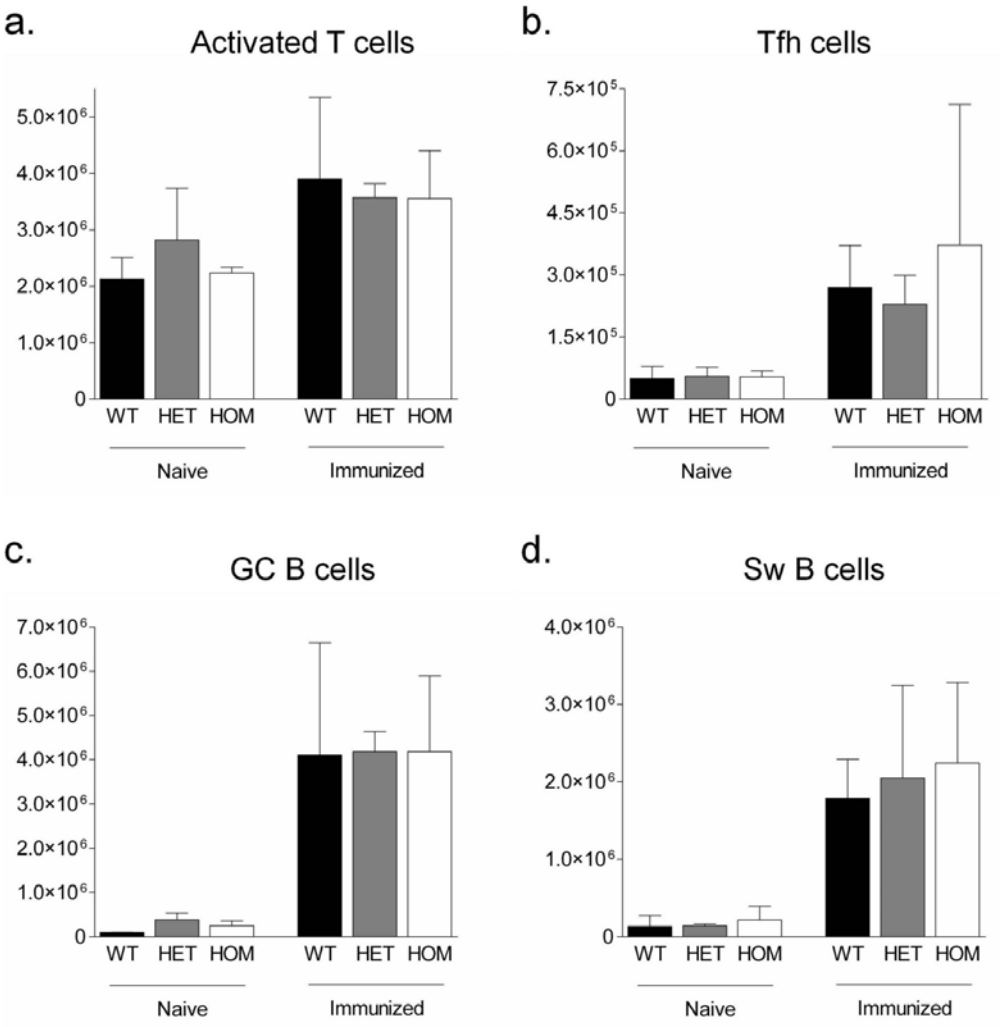


Figure 4.5 Characterization of the immune response in wt C57BL/6, heterozygous and homozygous hPD-1 knock-in mice. The mice were injected i.p. with $2X10^9$ SRBCs. Single cell suspensions from the spleens were stained for the germinal centre parameters, follicular helper T (Tfh) cells, germinal centre (GC) B cells, switched (Sw) B cells as well as for the activated T cells on day 7 (see figure 4.3 for the gating strategy). Absolute numbers of **a.** Activated T cells, **b.** Tfh cells, **c.** GC B cells, **d.** Sw B cells were compared. Data is representative of 2 independent experiments with 3 mice per group. Graph values are mean ± SD.

4.6 Discussion

Analysis of the expression of the humanized PD-1 protein on T cells that were activated in vitro revealed that replacing exon 2 of the intrinsic mouse PD-1 gene with exon 2 of the human PD-1 gene in the hPD-1KI mouse does not disrupt the folding of PD-1 protein, as judged by antibody binding, or its expression on the surface of activated T cells. The normal upregulation of the humanized PD-1 protein on T cells activated in vivo provided further confirmation that the targeted PD-1 gene is expressed normally.

Additionally, the resting immune systems of hPD-KI and WT C57BL/6 mice were dissected to detect any possible abnormalities that may be created by insertion of the humanized PD-1 gene. The lack of a significant difference between the immune parameters of WT and humanized mice suggested that insertion of the humanized PD-1 gene does not cause any overt developmental abnormalities in the adaptive immune system. The ability of the WT C57BL/6 and hPD-KI to respond to an immunogen was also tested using a model T dependent immune response assay. The immunogen induced similar-strength responses in WT C57BL/6 and hPD-KI mice, which further suggested that the effector arm of the adaptive immune system is intact in the humanized mice. From these experiments I concluded that the hPD-1KI mouse is a reasonable and fair model with which to investigate the effects of anti-human PD-1 antibodies in vivo.

Chapter 5:

The effects of PD-1 agonists on humoral and cellular immunity

5.1 Introduction

PD-1 plays important roles in a wide range of immune responses including the germinal centre (GC) reaction and antibody responses, the allogeneic response and responses to acute and chronic infections [201]. The GC reaction results in the formation of memory B cells and either short or long-lived high affinity plasma cells through somatic hypermutation and isotype class switching events. The ongoing proliferation and mutation of GC B cells hold enormous potential for the development of lymphoma or autoimmunity, therefore those processes must also be tightly regulated [344]. PD-1 has been described as a marker of follicular helper T (Tfh) cells which are responsible for controlling the production of high affinity B cell clones in the GCs [345]. However, it is still unclear if PD-1 acts through inhibiting the TCR derived signals in the Tfh cells, limits Tfh cell activity by regulating the development and/or function of the recently described $Foxp3^+$ subset of Tfh cells (follicular helper regulatory T cells) or acts through a totally different mechanism controlling the formation of long-lived plasma cells [200, 344, 346]. I attempted to address these issues, taking advantage of the humanized PD-1 knock-in mouse model, and using the putative PD-1 agonist antibodies to investigate the role of the PD-1 pathway in the germinal centre response to sheep red blood cells.

In chronic viral infections, there is a well demonstrated association between virus specific $CD8^+$ T cell exhaustion, the increased viral load and persistently high PD-1 expression [210]. However, the role of PD-1 in the acute $CD8^+$ T cell driven responses has long remained unclear [347]. Recently, it has been shown that in vitro blockade of PD-1 or in vivo PD-1 deficiency

leads to a higher recall response following the re-stimulation of effector $CD8^+$ T cells from the primary response using virus-specific peptides. This suggests that PD-1 signalling has negative effects on the formation of $CD8^+$ T cell memory [348-349]. Therefore, using a heat inactivated modified vaccinia ankara virus (MVA), I also tested the effects of the PD-1 agonists on the functionality of $CD8^+$ T cells during a primary response.

One valuable tool for predicting the in vivo efficacy of novel biological agents in allogeneic responses is the in vitro mixed lymphocyte reaction (MLR) and a recombinant PD-L1 Fc fusion protein has recently been shown to be effective at increasing graft survival through inducing allograft tolerance in vivo [201, 350], For these reasons, I also investigated the effects of the putative PD-1 agonists on the allogeneic response using an in vitro MLR-based strategy.

5.2 Effects of in vivo administration of PD-1 agonists on primary GC reactions

Before investigating the in vivo effects of the putative PD-1 agonists on the GC reaction, I decided to confirm the reported high expression of PD-1 and the specificity of my antibodies in the germinal centre using immunohistochemistry. For this purpose, tonsil samples were obtained from patients who had undergone tonsillectomy for chronic tonsillitis. Those samples were prepared according to the frozen sample preparation protocol (see Section 2.3) and stained with the anti-PD-1 antibodies (Figure 5.1). The staining was good with the high affinity antibody clone 2 (Figure 5.1a) and the other high affinity antibody, clone 19, produced a similar but less intense surface-staining pattern (Figure 5.1b). In contrast, clone 10 did not stain the tissue at any concentration tested (data not shown), consistent with its high off-rate. Stained cells localized mostly to the light zone of the germinal centre, compatible with the localization of the Tfh cells. Although most of the antibody-stained cells were in the GCs, there were also very

sparse populations of PD-1 expressing cells in the interfollicular T cell zone, which probably represent activated or memory T cells on the background of chronic tonsillitis.

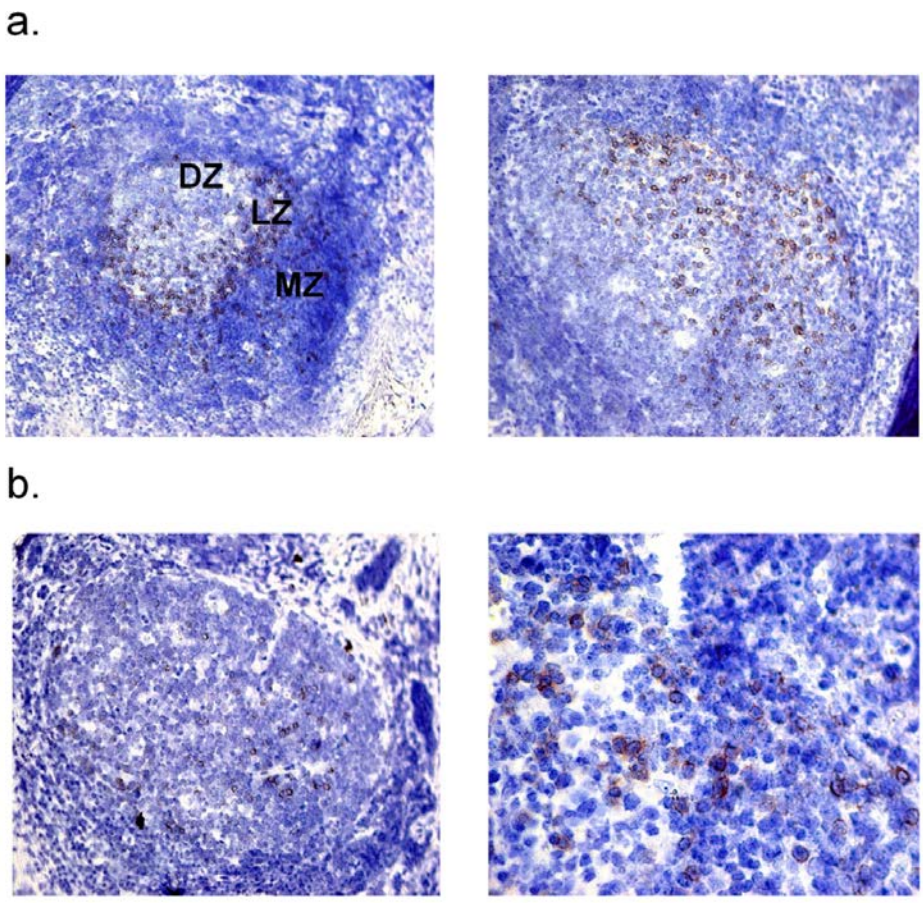


Figure 5.1 Localization of the PD-1 expressing cells (a) Peroxidase staining of frozen human tonsillar sections that were primarily stained with anti-PD-1 Clone 2. Brown colour indicates the cells expressing PD-1 which localize in the apical light zone of germinal centres. Sections were counterstained by hematoxylin. LZ, light zone; DZ, dark zone; MZ, mantle zone (magnification: Right 20x, left 40x). **(b)** Immunostaining with anti-PD-1 Clone 19 (magnification: Right 40x, left 60x).

To observe the consequences of the putative PD-1 superagonist treatment on the primary GC reaction and antibody production, I once again induced a GC reaction in the homozygous hPD-1KI mice using SRBCs. Mice between 8-12 weeks of age were immunized by $2x10^9$ SRBCs intraperitoneally, and 24 hours after the SRBC injection, either clone 19, clone 10 or isotype control antibody was administered subcutaneously at a 30 mg/kg single dose. Clone 2 had not show any inhibitory effects in the in vitro assays and so it was not included in most of these experiments. Instead, clone 10, which binds to a similar membrane-distal epitope on PD-1 and is inhibitory in vitro, was used as the conventional (i.e. non-superagonistic) PD-1 agonist control. Nevertheless, clone 2 was also tested twice for its effects on GCs. 9 days after the SRBC injection, spleens were removed for flow cytometric analysis and blood was collected for determining the antibody responses. Splenocytes were stained for $CD4^+$ T cells, $CD8^+$ T cells, activated T cells ($CD4^+CD44^{hi}ICOS^{hi}$), follicular helper T (Tfh) cells ($CD4^+CD44^{hi}CXCR5^+$), total B cells ($B220^+$), follicular B cells ($B220^+CD23^{hi}$), marginal zone B cells ($B220^+CD23^{lo\text{-}med}CD21^{hi}$), germinal centre B cells ($B220^+GL7^+CD95^+$) and switched B cells ($B220^+IgG1^+$; see Figure 4.3 for the gating strategy) after blocking Fc receptors to eliminate non-specific binding. The percentage and absolute numbers of Tfh cells and activated T cells were significantly lower in the mice that were treated with clone 19 (Figure 5.2). There was a trend towards reduced Tfh and activated T cell numbers after treatment with clone 10 but these effects were not significant. At this stage in the immune response, the percentages and absolute numbers of GC B cells were similar in all groups (Figure 5.2).

The early antibody responses against the SRBCs was also analysed by ELISA (Figure 5.3). SRBC-specific ELISA was performed for the mouse sera that was collected on day 9 post-SRBC immunization using ELISA plates coated with glutaraldehyde fixed whole SRBCs (see Section 2.5.2). Clone 19 treatment suppressed the SRBC-specific primary antibody responses.

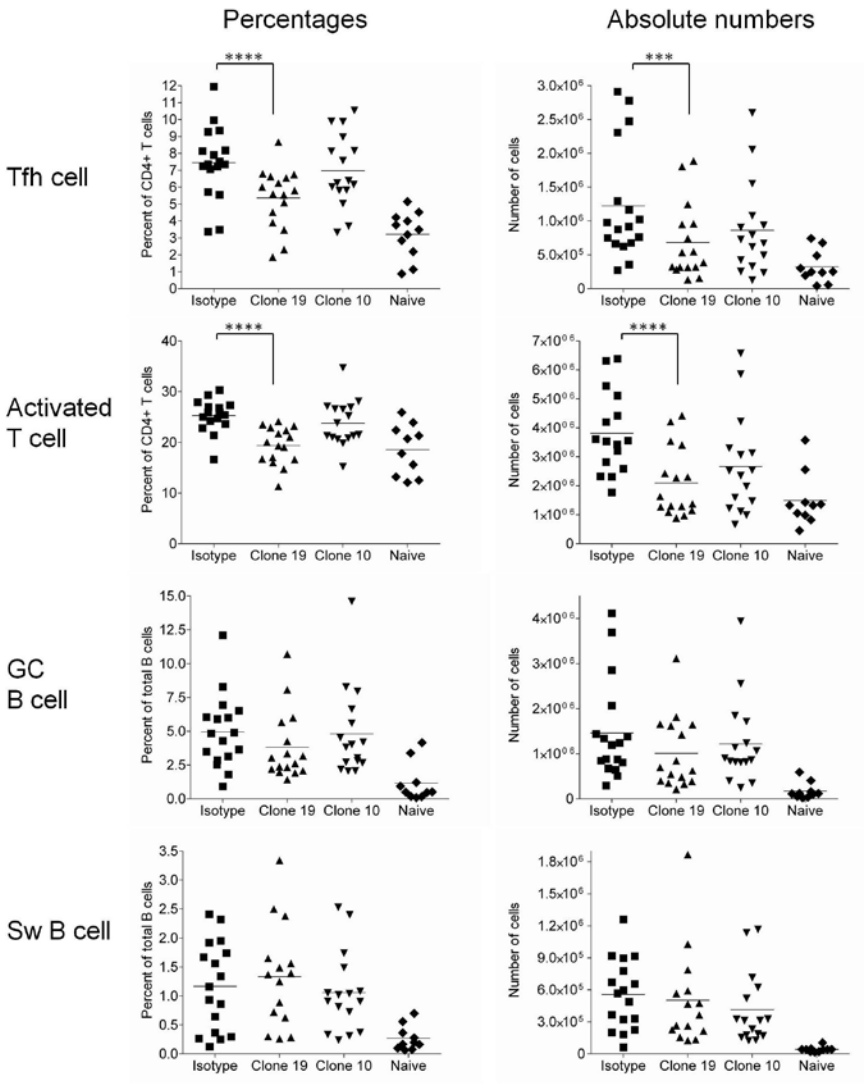


Figure 5.2 Effects of the anti-PD-1 antibodies on the GC reaction. Homozygous hPD-1 KI mice were immunized with SRBCs i.p. and either treated with isotype control, clone 19 or clone 10 s.c. 24 hours after the SRBC administration. The GC reaction was analysed by flow cytometry on day 7 post-SRBC immunization. The graphs show Tfh cells, activated T cells, GC B cells and isotype class-switched B cells as the percentages of $CD4^+$ T or $B220^+$ B cells and the absolute numbers. Naïve group represents the unimmunized control. Data was pooled from four independent experiments. Statistical analysis was performed using two-way ANOVA with Bonferroni correction (***$p< 0.001$, **** $p< 0.0001$).

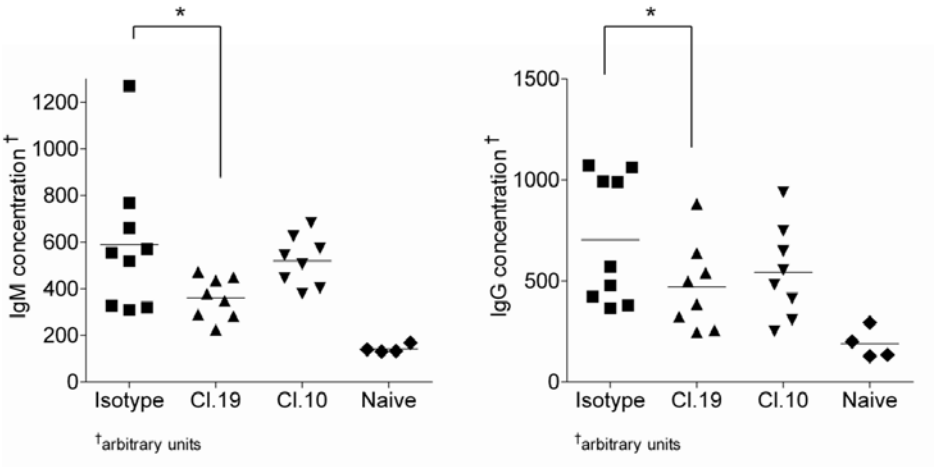


Figure 5.3 The effects of the anti-PD-1 antibodies on the primary antibody responses. SRBC specific ELISA was performed in order to detect the primary antibody responses following SRBC injection . Mouse sera was collected on day 9 post-SRBC immunization. Production of the IgM and IgG class antibodies were detected using the approriate secondary antibodies. Pooled sera from 12 immunized mice was used as the standard and results are displayed in arbitrary units. Data was pooled from two independent experiments. Statistical analysis was performed using two-way ANOVA with Bonferroni correction (*p< 0.05).

(Figure 5.3). This finding correlates with the suppression of the T cell response in the germinal centre response.

Although SRBC-induced Tfh cell expansion was restricted by clone 19 treatment, and thus could be a direct suppressive effect on Tfh cells, PD-1 stimulation has been shown to induce peripheral Treg formation [192]. Therefore, a further possibility was that the formation of $Foxp3^+$ regulatory Tfh cells is enhanced by clone 19 treatment. To test this hypothesis, Foxp3-GFP-hPD-1KI mice were immunized with SRBCs and this was followed by anti-PD-1 antibody administration 24 hours later. The changes in the Tfh cells, GC B cells, isotype-switched B cells and activated T cells were analysed on day 9 post-SRBC immunization. As in the experiment with the hPD-1KI mice, clone 19 treatment caused a reduction in the percentages and absolute numbers of both Tfh cells and activated T cells in the Foxp3-GFP-hPD-1KI mice (data not shown). However, within these subsets the percentages and the absolute numbers of $Foxp3^+$ regulatory cells were not affected (Figure 5.4). This suggests that the negative regulation of the Tfh cells upon clone 19 administration is a general effect rather than one operating specifically through regulatory Tfh cells.

5.3 Effects of the anti-PD-1 antibodies on cellular immunity

To investigate the effects of the anti-PD-1 antibodies on a $CD8^+$ T cell driven response, I used heat inactivated Modified Vaccinia Virus Ankara (MVA) as the immunogen. Mice were infected with 10^6 PFU heat inactivated MVA i.m. and treated with either isotype control, clone 19 or clone 10 antibodies s.c. 24 hours post-MVA administration. On the day approximating to the peak immune response (day 9), spleens were removed, single cell suspensions were prepared and the cells were cultured ex vivo in the presence of MVA specific peptide B8R overnight. The next day, the cells were stained for surface markers and intracellular cytokine staining (ICS) was

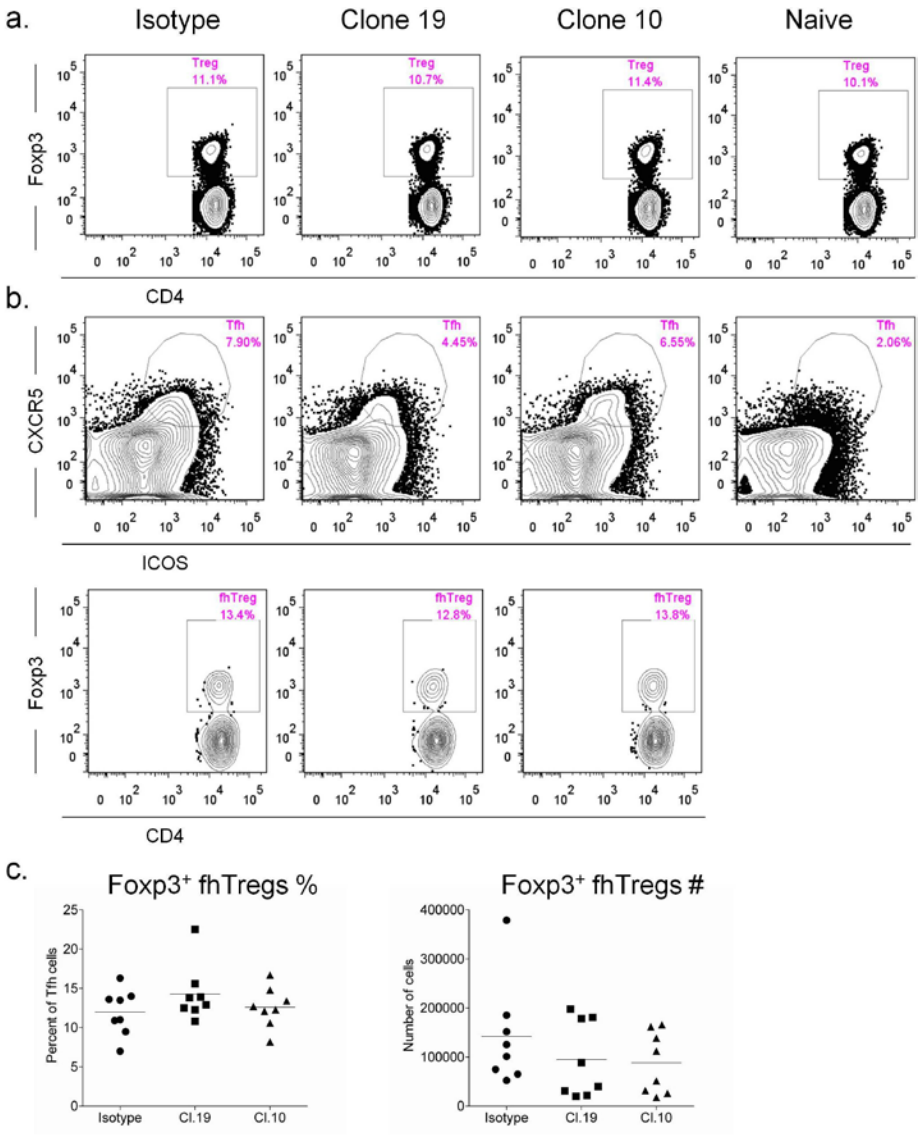


Figure 5.4 The influence of anti-PD-1 antibodies on the Foxp3⁺ regulatory subset of Tfh cells. **a.** Flow cytometry plots showing the percentage of Tregs in the CD4⁺ T cells. **b.** Flow cytometry plots representing the effecs of the isotype control antibody, clone 19 and clone 10 treatments. The lower plots demonstrate the common gating strategy for the Foxp3⁺ subpopulation of the $CD4^+CXCR5^{hi}ICOS^{hi}$ Tfh cells. **c.** The graphs showing the percentages and the absolute numbers of follicular helper (fhTregs). Data was pooled from 2 independent experiments. Each symbol represents one mouse. For the statistical analysis, two-way ANOVA was performed with Bonferroni correction. Compared to the isotype control, the effects of the anti-PD-1 antibodies on the fhTregs were insignificant ($p>0.05$).

performed for IFN-γ (see Section 2.4.1). The cytokine-producing ability of the $CD8^+$ T cells was analysed using flow cytometry, using cells that were cultured ex-vivo in the absence of the peptide and from naïve mice as the negative controls. The percentage of degranulating (LAMP-I^+) IFN- γ^+ $CD8^+$ T cells was determined. Once again clone 19 treatment reduced the percentage and total number of LAMP-I^+IFN-γ^+ cells significantly. No such effect was observed with clone 10 in this experiment (Figure 5.5).

5.4 The effect of anti-PD-1 antibody administration on the antigen specific $CD8^+$ T cell response

The restimulation of T cells with the MVA specific, MHC-I dependent peptide B8R stimulated $CD8^+$ T cells during the recall responses. However, this effect must not be considered entirely $CD4^+$ T cell independent. $CD4^+$ T cell help, which has been inhibited by the anti-PD-1 antibodies following the primary in vivo MVA administration, may also have contributed to the final outcome of the $CD8^+$ T cell responses described in Section 5.3. To be able to observe the changes purely in the antigen specific $CD8^+$ T cell compartment following in vivo immunogen administration I used a transgenic mouse model which produces MHC class I-restricted, ovalbumin (OVA)-specific, $CD8^+$ T cells (OT-I cells). By crossing this mouse sequentially with the hPD-1KI mice and a GFP reporter mouse that expresses enhanced Green Fluorescent Protein (GFP) under the direction of the human ubiqutin C promoter (Jax mice database: 004353, C57BL/6-Tg(UBC-GFP)30Scha/J), I obtained humanized PD-1 expressing OT-I mice carrying a GFP reporter. $CD8^+$ T cells isolated from the spleens of the triple transgenic OT-I-GFP-hPD-1KI (CD45.2) mice by magnetic separation were adoptively transferred into naïve C57BL/6-SJL (CD45.1) congenic recipients together with GFP negative $CD8^+$ T cells from transgenic OT-I-C57BL/6 mice (CD45.2) at a 1:1 OT-I-GFP-hPD-1KI to OT-I-C57BL/6 ratio.

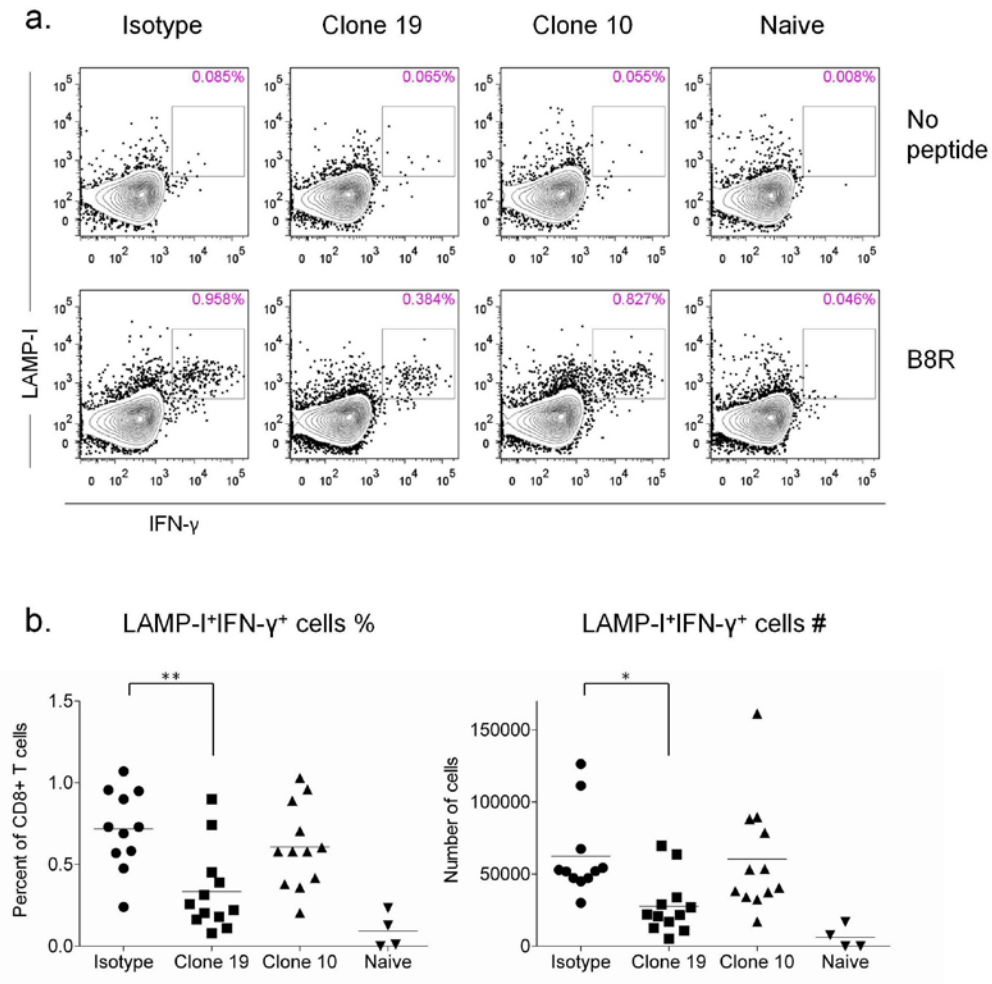


Figure 5.5 Inhibition of the CD8⁺ T cell response with clone 19 treatment. Homozygous hPD-1KI mice were infected with 10^6 PFU heat inactivated MVA and treated with either isotype control, clone 19 or clone 10 antibodies. On day 9 post-immunisation, cells were cultured either in the presence of the B8R peptide or media. **a.** Flow cytometry plots representing the effecs of the isotype control antibody, clone 19 and clone 10 treatments. The CD8⁺ T cells were gated for the LAMP-I⁺IFN-γ⁺ responders. No peptide control and the naïve mice were used as the negative controls. **b**. The graphs showing the percentages and the absolute numbers of LAMP-I⁺IFN-γ⁺ responders. Data was pooled from 2 independent experiments. Each symbol represents one mouse. For the statistical analysis, two-way ANOVA was performed with Bonferroni correction (*p<0.05, **p<0.01).

The recipients were then immunized with 10^6 PFU MVA-OVA i.m. and treated with the anti-PD-1 antibodies s.c. 24 hours after immunization. On the day of the peak response (day 9), spleens from the recipients were removed and prepared for analysis. The final ratio of the OT-I-GFP-hPD-1KI (CD45.2) cells to OT-I-C57BL/6 cells was calculated using flow cytometry. Interestingly, in this experiment, which isolated the CD8 response, the antigen specific response of the transferred OT-I-GFP-hPD-1KI cells was inhibited significantly by all three clones of the anti-PD-1 antibodies to a similar level (Figure 5.6).

5.5 Effects of the anti-PD-1 antibodies on the in vitro allogeneic response

Finally, to detect the potential effects of the anti-PD-1 antibodies on the in vitro allogeneic response, a one-way mixed lymphocyte reaction (MLR) was generated using cells of the two allogeneic mouse strains C57BL/6 (hPD-1KI) and Balb/c as the responders and antigen presenting cells, respectively. Splenocytes from naïve Balb/c mice were treated with 50 µg/ml mitomycin-C to prevent the indirect proliferative effects of cytokines from multiplying Balb/c cells. Cells of hPD-1KI mice were depleted of B cells, macrophages, dendritic cells and NK cells by magnetic separation to enrich the $CD4^+$ and $CD8^+$ T cells. T cells of the hPD-1KI mice were then labelled with CFSE to detect the proliferative responses of the responders using flow cytometry. The mitomycin-C treated and the CFSE labelled live cells were counted manually using trypan blue for excluding dead cells. No toxic effect of mitomycin-C or CFSE was detected. A 1:1 mixture of live mitomycin-C treated Balb/c cells and CFSE labelled hPD-1KI cells was prepared and treated with various concentrations of the soluble anti-PD-1 antibodies or the isotype control antibody. After three days of culture, flow cytometric analysis was performed. Before analysing proliferation, CFSE negative Balb/c cells were gated out and on day 3 the number of these cells was low compared to the hPD-1KI population, indicating that

the they had stopped proliferating or died (Figure 5.7a). The conclusion of the MLR experiments was that clone 19 was inhibitory at an antibody dose of 100 μg/ml, but not at lower concentrations (Figure 5.7b, Figure 5.8). No comparable inhibitory effect was obtained with the other antibody clones.

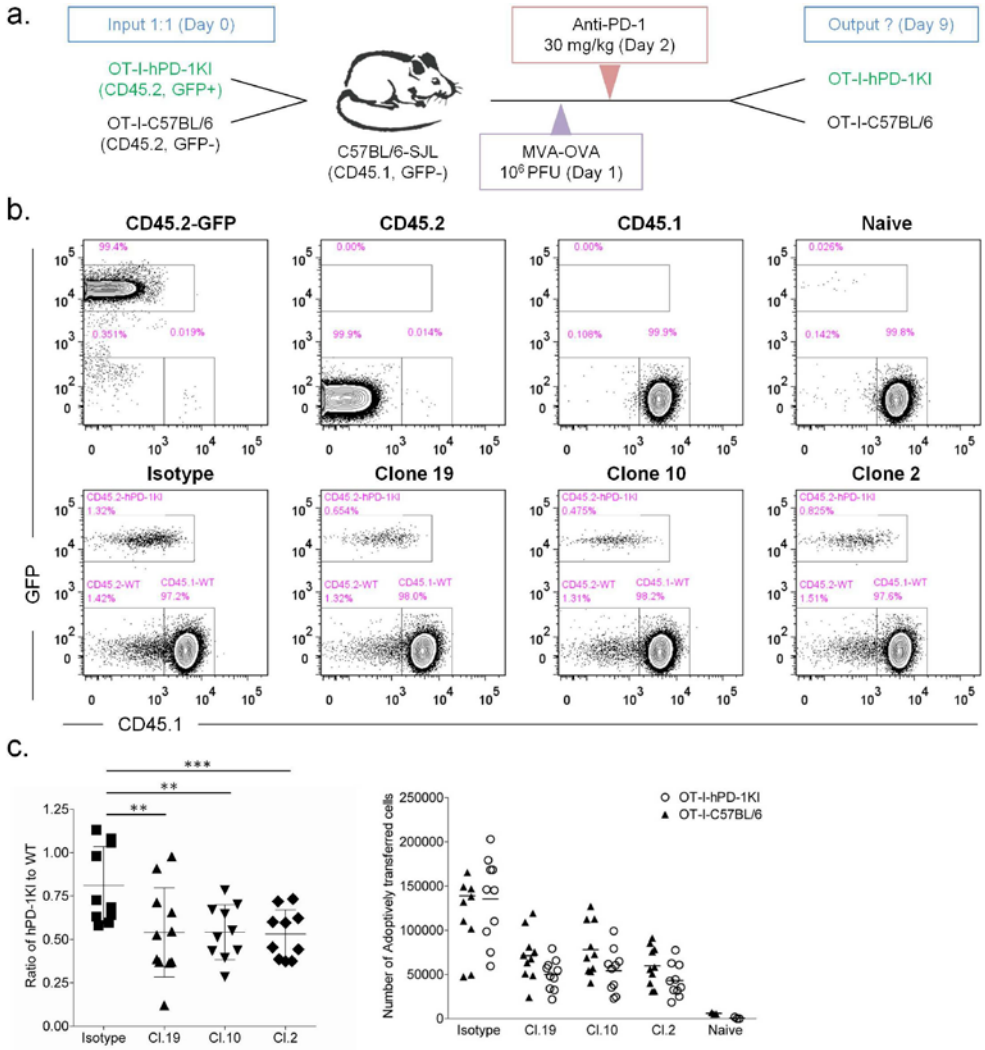


Figure 5.6 Inhibition of the antigen specific CD8⁺ T cell response with anti-PD-1 antibody treatment. OT-I cells from heterozygous OT-I-hPD-1KI-GFP mice and OT-I-C57BL/6 transgenic mice were adoptively transferred into the congenic C57BL/6 mice at approximately 1:1 ratio. Recipients were infected with 10^6 PFU heat inactivated MVA-OVA and treated with either isotype control, clone 19, clone 10 or clone 2 antibodies. **a.** Schematic representation of the experiment. **b.** Flow cytometry plots demonstrate the gating strategy (upper row) for the OT-I-hPD-1KI, OT-I-C57BL/6 and the congenic recipient cells using the naïve CD45.2⁺GFP⁺, CD45.2⁺GFP⁻, untransferred and transferred CD45.1⁺GFP⁻ mice respectively. Lower plots represent the effects of the immunization and the antibody treatment on the cells. **c.** Graphs showing the ratios (left) of the OT-I-hPD-1KI cells to WT OT-I cells and the absolute numbers (right) of the transferred OT-I (hPD-1KI and WT) cells on the day of the peak response. Data was pooled from 2 independent experiments. Symbols on the left represent the ratio of different cell types. On the right, each symbol represents one mouse. For the statistical analysis, two-way ANOVA was performed with Bonferroni correction (**p<0.01, ***p<0.001).

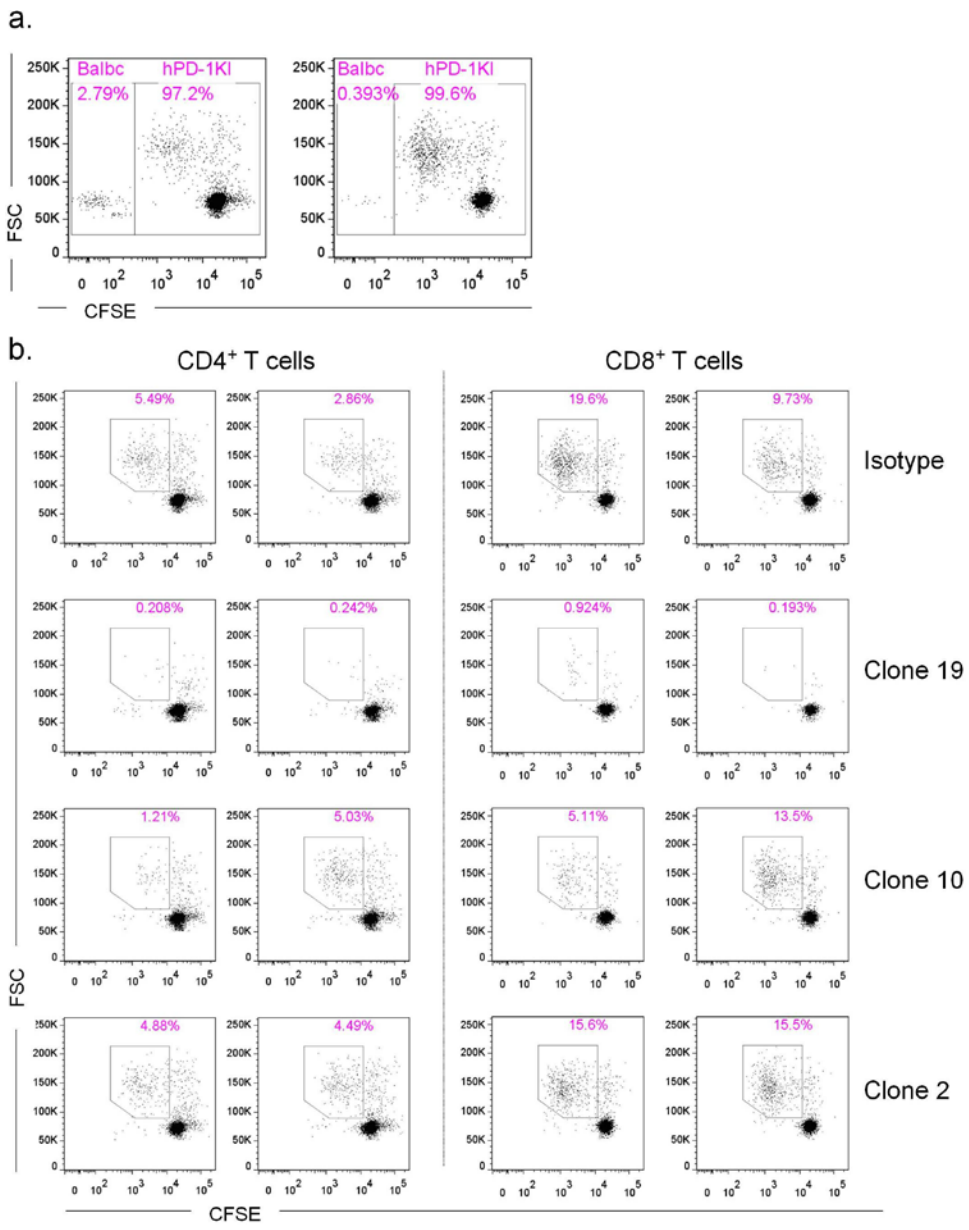


Figure 5.7 Demonstration of the gating strategy used for the analysis of mixed lymphocyte reaction (MLR). a. Flow cytometry plots showing the gating strategy for the nearly undetectable population of CFSE⁻ Balb/c cells and the proliferating CFSE⁺ hPD-1KI cells**. b.** Analysis of the proliferative responses in CD4⁺ and CD8⁺ T cells upon administration of 100 µg/ml isotype control, anti-PD-1 clone 19, clone 10 and clone 2. Each condition is shown in duplicates.

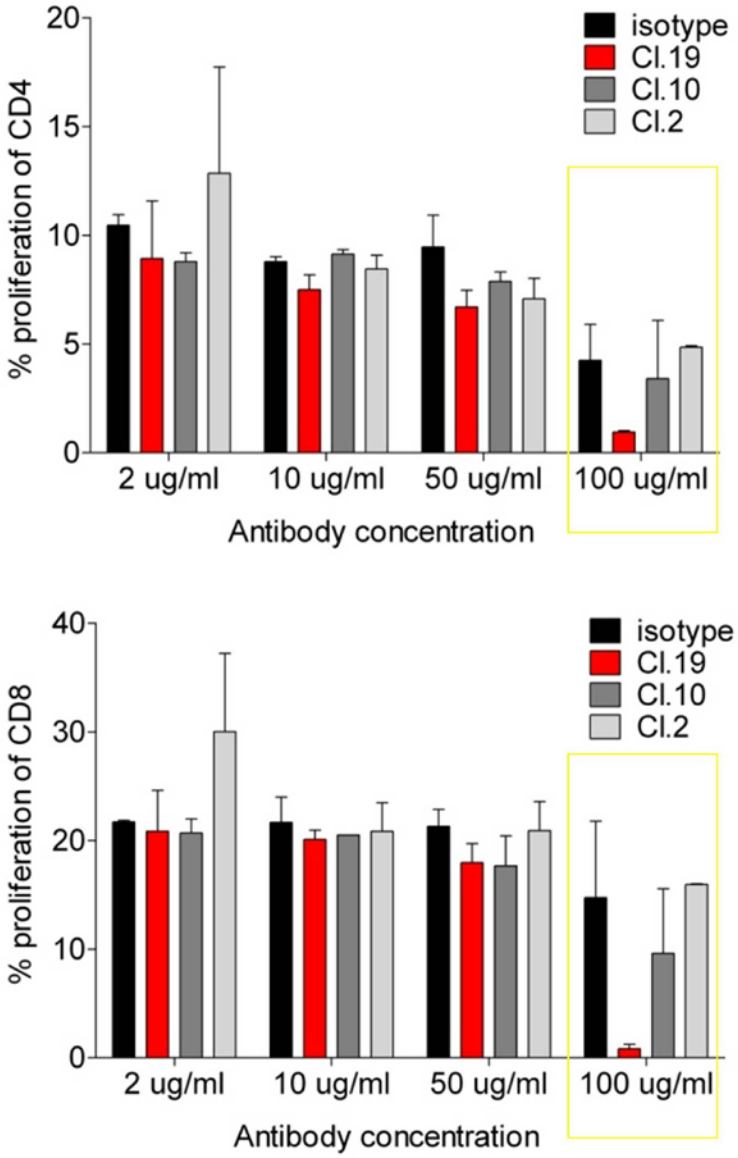


Figure 5.8 Suppressive effect of soluble clone 19 on mouse mixe lymphocyte reaction (MLR). Graphs demonstrating the effects of the different antibody concentrations on the proliferative responses of $CD4^+$ and $CD8^+$ responders in a one-way MLR. Yellow boxes highlight the antibody concentration where a prominent inhibition was obtained with clone 19 treatment. Data is representative of two independent experiments. Values are means of duplicates ± SD.

5.6 Discussion

The data present in this chapter show that agonistic antibodies targeting PD-1 during the development of GC responses reduces the number of activated T cells and Tfh cells, and suppresses the primary antibody responses significantly, but does not affect the total number of Tfr cells, GC B cells or isotype-switched B cells. The failure of the Tfr population to expand upon anti-PD-1 antibody binding suggests that the PD-1 agonists directly act on the Tfh cells during the GC reaction. This needs to be further elucidated by studies addressing the function of Tfr cells and the cell intrinsic changes in Tfh cells upon PD-1 stimulation. The strongest agonistic effect in the GC setting was exerted by clone 19 which we hypothesise is due to its potential superagonistic action. We also found that clone 19, but not clone 10, significantly reduces the $CD8^+$ T cell response following MVA administration which further supports the superagonistic potential of clone 19.

The observation of similar inhibitory effects with clone19, clone 10 and clone 2 in the antigen specific $CD8^+$ T responses, however, is unexplained. This discrepancy might be partially explained by the dependency of clone 19 action on $CD4^+$ T cell help. In the conditions where clone 19 is also capable of inhibiting $CD4^+$ T cell help, such as in the recall response against MVA, superagonistic effect is prominent and the net inhibition on the $CD8^+$ T cells is higher compared to the inhibitory effects of other agonists. This explanation would need to accommodate a general effect of anti-PD-1 antibodies on $CD8^+$ T cell responses and requires further investigation. One approach will be to investigate the net effect of the different antibodies on OTII transgenic CD4 T cells in a similar transfer model. In the MLR experiments, $CD4^+$ and $CD8^+$ T cells were inhibited simultaneously, and strong inhibition of the allogeneic $CD8^+$ T cell response with the clone 19 treatment, albeit at high dose, was also observed. Variation between the PD-1 signalling thresholds of $CD4^+$ and $CD8^+$ T cells or the different dynamics of the primary

and recall $CD8^+$ T cell responses may also account for situations overriding the effects of superagonists. These points are returned to in the General Discussion.

Chapter 6:

Effects of PD-1 agonism on the induction of Treg formation

6.1 Introduction

Regulatory T (Treg) cells are key mediators of peripheral tolerance that actively suppress effector T (Teff) cells and inhibit immune-mediated tissue damage [351-353]. Treg cells can be divided into naturally occurring Treg (nTreg) and induced Treg (iTreg) cells. nTreg cells develop in the thymus, express the cardinal transcription factor forkhead box p3 [354-355], have high levels of CD25, and have a TCR repertoire biased toward self-antigens. In contrast, iTreg cells develop in the periphery. In the presence of TGF-β, naive $CD4^+$ T cells are induced to express Foxp3 and are converted towards an iTreg cell fate [356-359].

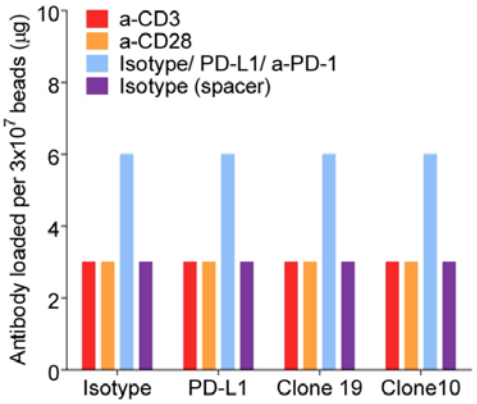
PD-1 and its ligand PD-L1 are highly expressed on Tregs, and it has been revealed that stimulation of the PD-1 pathway by bead bound PD-L1 potentiates TGF-β-induced differentiation of naïve $CD4^+$ T cells into iTregs in vitro [192]. Furthermore, adoptive transfer of naïve $CD4^+$ T cells into PD-L1 and PD-L2 deficient mice was shown to result in a marked reduction in iTreg formation compared to control mice. Therefore, strategies for augmenting PD-1 signalling may be useful in treating autoimmune diseases due to their concomitant effects on the conversion of iTregs and their suppressive effects on effector T cells. To study the effects of the anti-PD-1 antibodies in this context, a Foxp3-GFP reporter mouse model was obtained from the Rudensky Lab (Sloan-Kettering Institute), intercrossed with the hPD-1KI mice and bred to homozygosity. The consequences of the use of PD-1 agonists on the conversion of iTregs were investigated using the hPD-1KI-Foxp3-GFP mouse.

6.2 In vitro induction of Treg formation using bead-bound antibodies against CD3, CD28 and PD-1

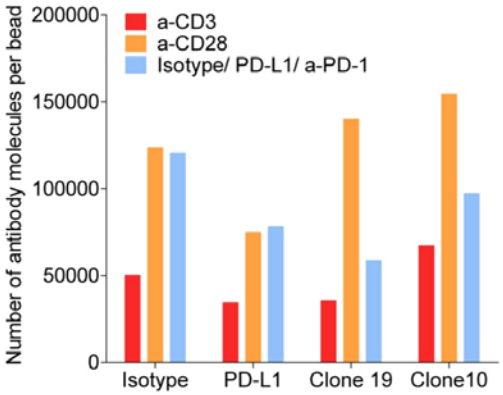
Antigenic stimuli and TGF-β are reported to drive the conversion of naïve $CD4^+$ T cells into Tregs in the periphery [356], and this conversion can be enhanced 2-5 fold through in vitro stimulation of the PD-1 pathway by the native ligand PD-L1 coupled to Dynalbeads™ together with anti-CD3ε and anti-CD28 antibodies [192]. Having replaced PD-L1 by the anti-PD-1 antibodies we wanted to ask if clone 19 or clone 10 would have a similar effect on Treg formation. Dynalbeads™ with active epoxy groups were coated with an anti-CD3ε, an anti-CD28, and either an isotype control antibody, a Fc fusion protein of PD-L1 (PD-L1-Ig), or clone 19 or clone 10 antibody to create artificial APCs (see Section 2.2.5). In this experiment the beads were referred to as isotype, PD-L1, clone 19 or clone 10 beads and, while loading, the individual amounts of the antibodies and the total amount were kept constant. The quantity of the antibody molecules on the beads were calculated by flow cytometric analysis using prelabelled QuantiBRITE™ beads as described in Chapter 3. Whilst the final amount of antibody on each bead type did not correlate directly with the starting amount (1 μg antibody per 10^7 beads), the beads were broadly comparable for different ligands, notably the levels of anti-CD3 and anti-CD28 (Figure 6.1).

Naïve $CD4^+CD62L^{hi}Foxp3^-$ T cells were isolated from the spleen and mesenteric lymph nodes of the hPD-1KI-Foxp3-GFP mice using a flow cytometry based cell sorter. Isolated cells were treated with the isotype, PD-L1, clone 19 or clone 10 beads in the presence of 0.0625 ng/ml, 0.125 ng/ml, 0.25 ng/ml or 0.5 ng/ml TGF-β for three days. Two different seeding densities and bead to cell ratios were tested for the initial optimization of the assay. Interestingly, changes in the culture conditions and seeding conditions had an important effect on the results, something that was not apparent or not noted in the study demonstrating the effects of PD-L1 [192]. When $5x10^5$ cells were plated at a seeding density of 10^6 cells/ ml and treated using a bead to cell ratio

a.



b.



	a-CD3	a-CD28	Isotype/PD-L1/ a-PD-1
Isotype	50172	123531	120567
PD-L1	34248	74660	78249
Clone 19	35451	139884	58484
Clone 10	67075	154296	97244

Figure 6.1 The loading and characterization of the Dynalbeads. a. Graph showing the amounts of the antibodies that were intended to be loaded onto Dynalbeads. **b.** The number of antibody molecules loaded per bead was calculated through the flow cytometric analysis of the beads in comparision to the prelabelled Quantibrite beads. The graph and the table represent the actual quantity of the antibody molecules.

of 5:1, significant cell death was observed with the PD-L1 beads whilst the treatment with the other beads led to increased proliferation (Figure 6.2). Whilst the fraction of Tregs was found to be higher with the PD-L1 treatment compared to the other treatment groups, agreeing with previous data [192], the absolute number of Tregs was not increased due to a high rate of cell death (Figure 6.3).

When $2.5x10^5$ cells were plated at a seeding density of $5x10^5$ cells/ml and treated using a bead to cell ratio of 1.6:1, the size and the granularity of the cells were similar among the treatment groups which were supplemented with the same level of TGF-β (Figure 6.4). Cell viability again decreased with the increasing levels of TGF-β, but to a much lower extent, and stimulation of the PD-1 pathway again decreased the viability further compared to the isotype control (Figure 6.5a). This effect was comparable among the PD-L1, clone 19 and clone 10 treatments. iTreg formation increased with the increasing doses of TGF-β in all the treatment groups (Figure 6.5b). Stimulation of the PD-1 pathway with either PD-L1 or the anti-PD-1 antibodies induced the conversion of naïve $CD4^+$ T cells at a higher level than the isotype control antibody at any concentration of the TGF-β tested.

6.3 The differentiation of naïve $CD4^+$ T cells into Tregs after unlinked activation of the TCR and coreceptors

Since it is difficult to control the final antibody levels on the beads, I separated the physical location of the CD3, CD28 and PD-1 stimuli. In this way I hoped to prevent competition and the potential steric hindrance between the antibodies/ligand and be able to optimize each stimulus individually and in this way make a more accurate comparison of the effects of the isotype control antibody, PD-1 agonist antibodies and PD-L1. I was also very careful to obtain responder cells with similar size, granularity and viability.

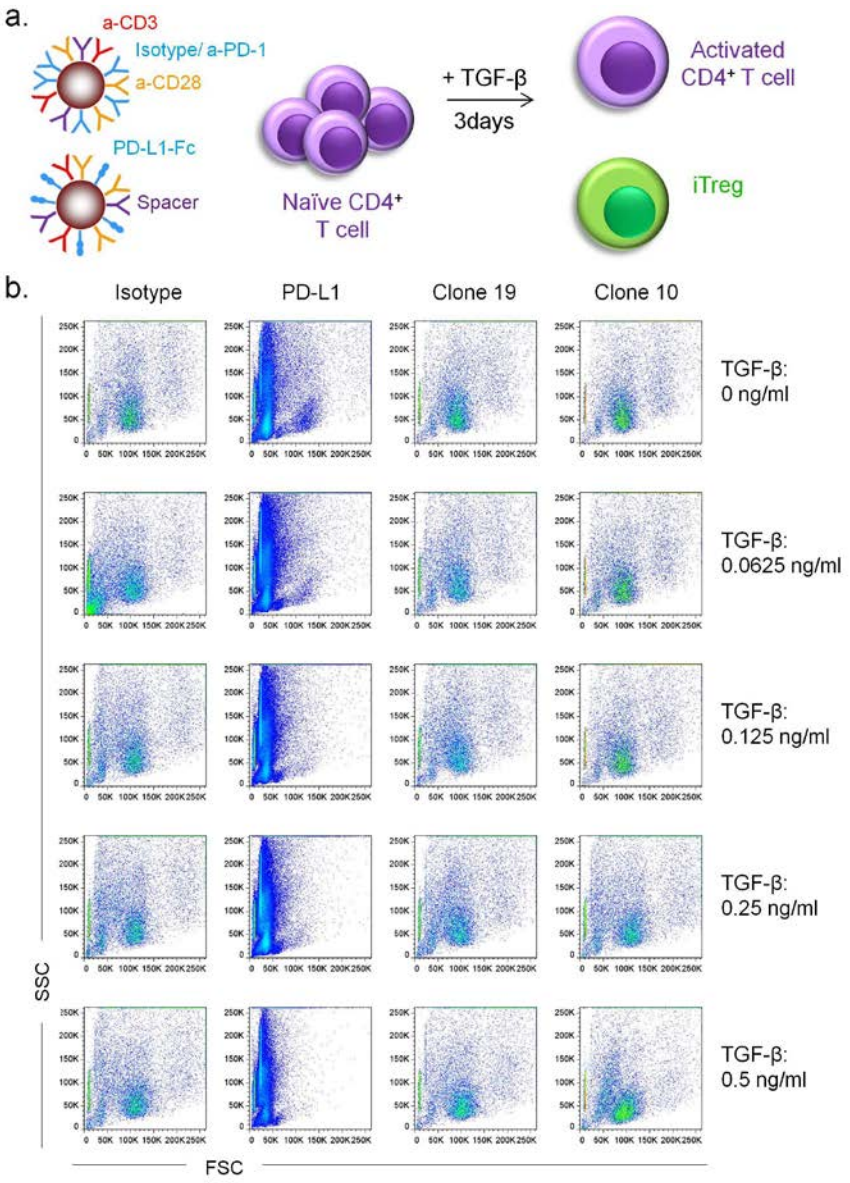


Figure 6.2 The effect of the bead bound stimuli on the cell viability at a high bead to cell ratio. a. Illustration of the experimental design. $5x10^5$ FACS sorted $CD4^+CD62L^{hi}Foxp3^-$ naïve T cells were cultured in the presence of TGF-β and the beads coated with anti-CD3, anti-CD28 and either isotype control, anti-PD-1 antibodies or PD-L1-Fc. Bead to cell ratio was 5:1. **b.** The status of the cells for each treatment condition after three days of culture. FACS plots are representative of two independent experiments that were performed in duplicates.

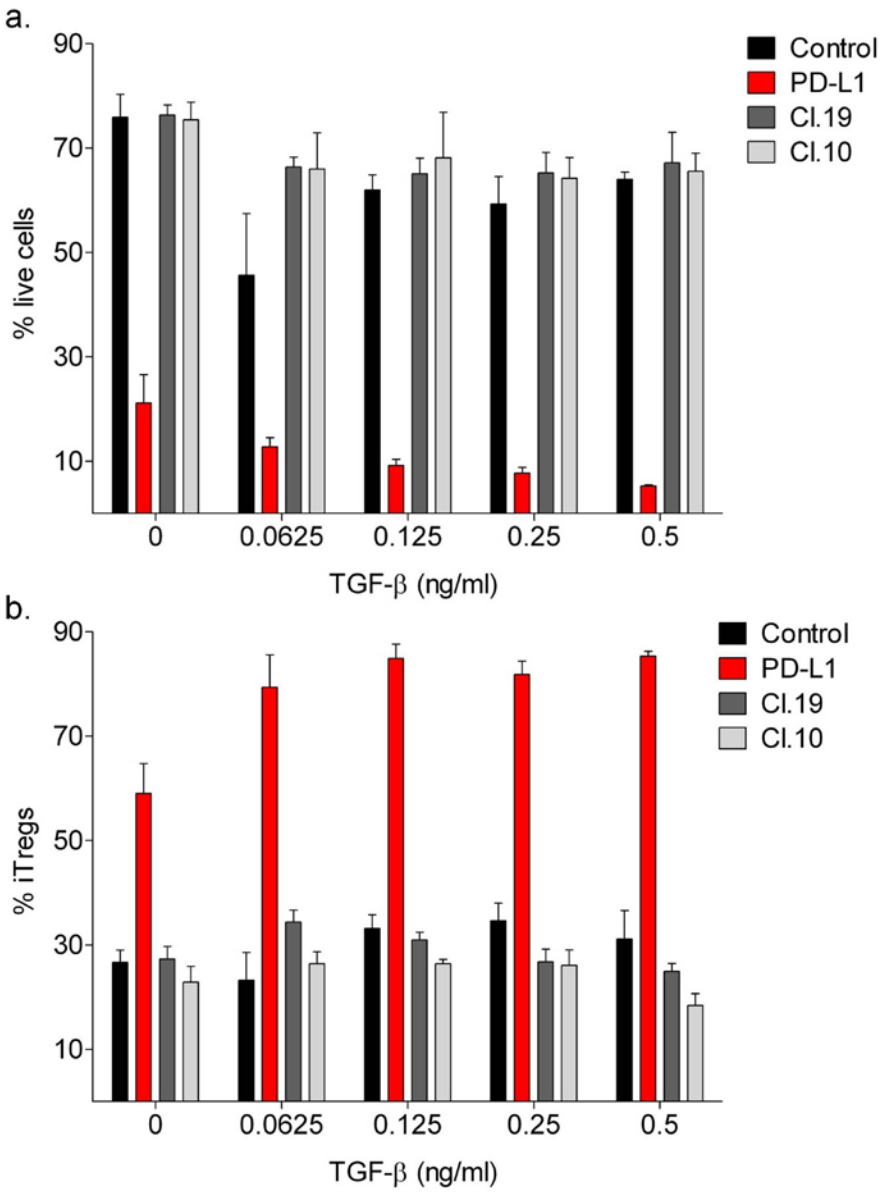


Figure 6.3 The level of iTreg formation at 5:1 bead to cell ratio. a. The graph showing the percentage of live $CD4^+$ T cells following three days of incubation with different types of beads at increasing concentrations of TGF-β. **b.** The level of the iTreg formation in the presence of different stimuli is represented as the percentage of $Foxp3^+$ cells in the $CD4^+$ T cells. Data is representative of two independent experiments. Values are means of duplicates ± SD.

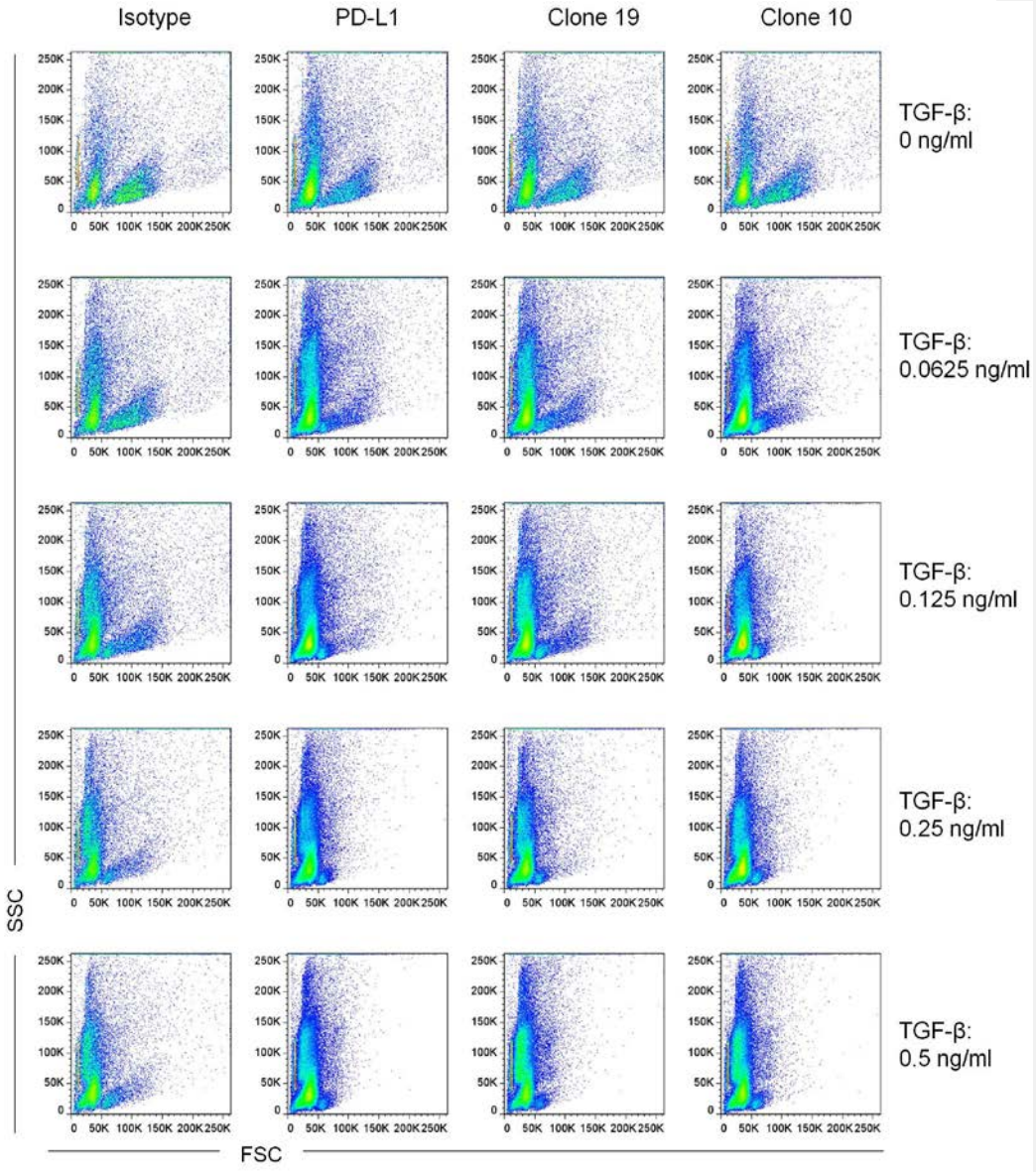


Figure 6.4 The effect of the bead bound stimuli on the cell viability at a low bead to cell ratio. 2.5x10^5 FACS sorted $CD4^+CD62L^+Foxp3^-$ naïve T cells were cultured in the presence of TGF-β and the beads coated with anti-CD3, anti-CD28 and either isotype control, anti-PD-1 antibodies or PD-L1-Fc. Bead to cell ratio was 1.6:1. FACS plots represent the status of cells for each treatment condition after three days of culture. FACS plots are representative of two independent experiments that were performed in duplicates.

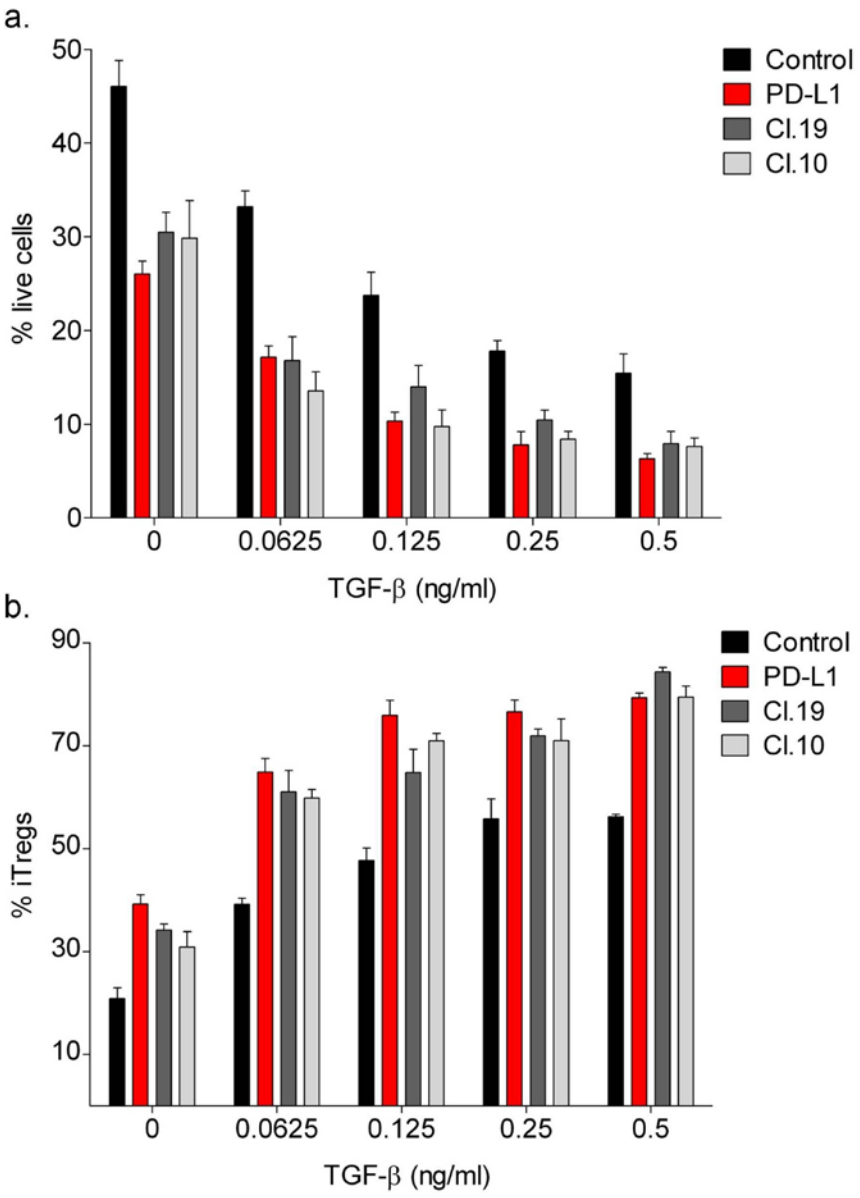


Figure 6.5 The level of iTreg formation at 1.6:1 bead to cell ratio. a. The graph showing the percentage of live CD4⁺ T cells following three days of incubation with different types of beads at increasing concentrations of TGF-β. **b.** The level of the iTreg formation in the presence of different stimuli is represented as the percentage of Foxp3⁺ cells in the CD4⁺ T cells. Data is representative of two independent experiments. Values are means of duplicates ± SD.

Initially, the effects of culture type and the amount of anti-CD3 antibody were tested. For this purpose, standard round bottom 96 well plates and 24 well plates were coated with 0.1 µg/ml, 0.5 µg/ml, 2.5 µg/ml and 12.5 µg/ml anti-CD3ε antibody (see Section 2.2.5). $2.5x10^5$ $CD4^+$ T cells were isolated from the spleens and the mesenteric lymph nodes of the naïve hPD-1KI-Foxp3-GFP mice by magnetic separation and added to the wells. 1 µg/ml soluble anti-CD28 antibody was added to all the wells either with or without 10000 IU IL-2 at a final volume of 0.5 ml. After three days of culture in the absence of TGF-β, the size, granularity and the percentage of the Tregs were again analysed by flow cytometry (Figure 6.6). The percentage of Tregs present in the live cell gate decreased with increased anti-CD3/anti-CD28 induced cell proliferation, particularly when IL-2 was present (Figure 6.6). Treg cell numbers were higher in the cultures from 24 well plates and so I decided to perform all cultures on this scale and to omit IL-2 in further experiments in order to increase sensitivity.

To determine the best plate bound anti-CD3 concentration, the viability and the level of Treg formation was analysed in the presence of different doses of TGF-β. $2.5x10^5$ $CD4^+$ T cells were isolated from the spleens and the mesenteric lymph nodes of the naïve hPD-1KI-Foxp3-GFP mice and seeded into the 24 well plates that were precoated with either 0.1 µg/ml or 0.5 µg/ml anti-CD3. 1 µg/ml soluble anti-CD28 antibody was added to all the wells together with 0.0625 ng/ml or 0.5 ng/ml soluble TGF-β in a final volume of 0.5 ml. The percentage of the viable cells was found to be higher in the cells that were treated with 0.5 µg/ml plate bound anti-CD3 at any concentration of the TGF-β (Figure 6.7a). Under these conditions there was also an induction of the formation of Tregs with 0.5 µg/ml anti-CD3 in combination with the increasing doses of TGF-β (Figure 6.7b). In contrast, the Treg inducing effect of TGF-β was not observed in wells that were treated with 0.1 µg/ml anti-CD3. In the light of these observations, 0.5 µg/ml plate bound anti-CD3 and 1 µg/ml soluble anti-CD28 were selected by me as the default stimuli for testing the effects of the PD-1 agonist antibodies.

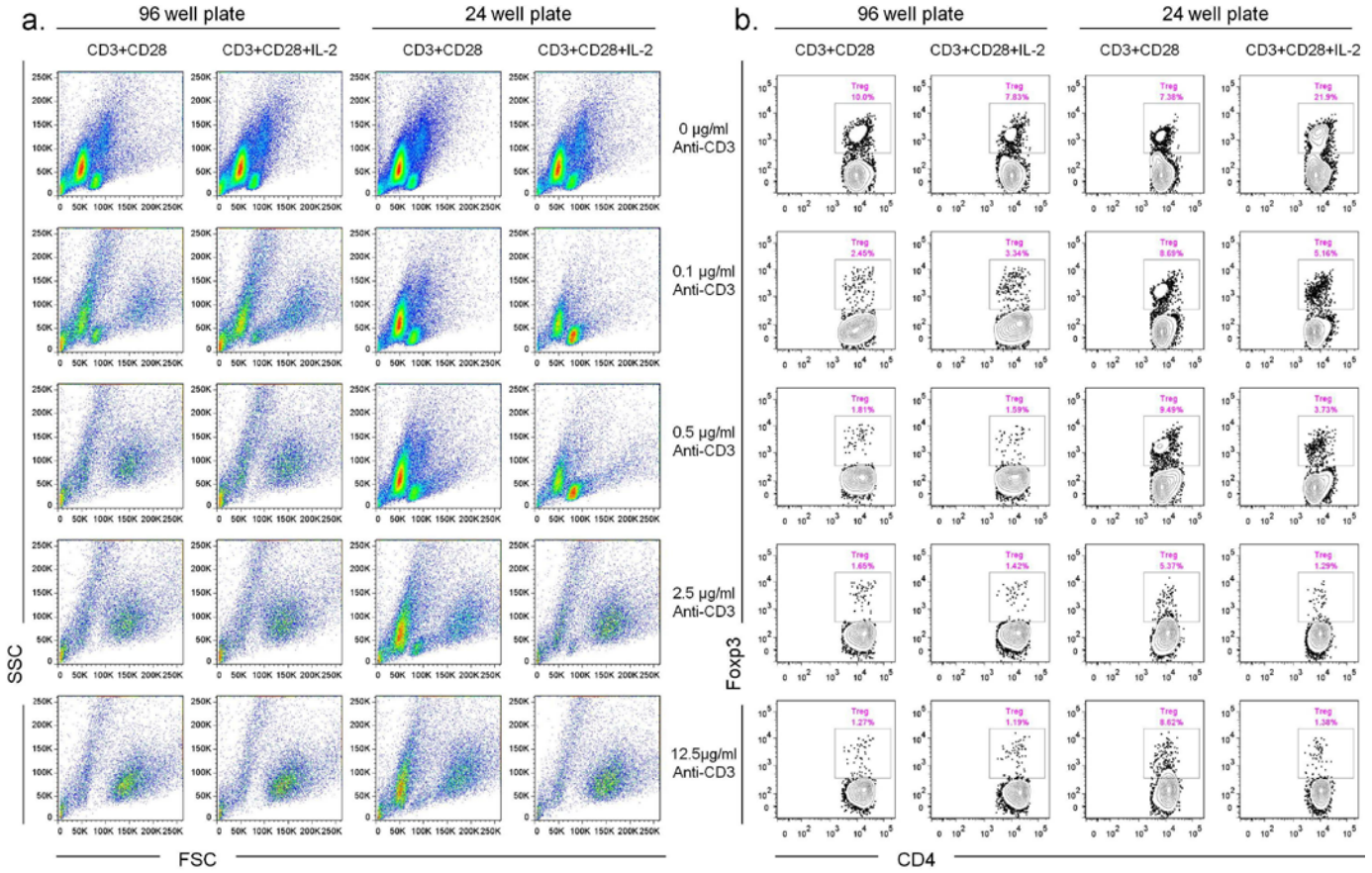


Figure 6.6 Optimization of the plate bound anti-CD3 stimulus for investigating the effects of the anti-PD-1 antibodies on Treg formation. 2.5x10^5 $CD4^+$ T cells isolated from naïve hPD-1KI-Foxp3-GFP mice and seeded either into round bottom 96 well plates or flat bottom 24 well plates that were precoated with varying amounts of anti-CD3.1 µg/ml soluble anti-CD28 was added into the culture with or without 10000 IU IL-2. **a.** FACS plots representing the status of cells after three days of culture with the indicated stimuli. **b.** FACS plots showing the level of Treg formation under the effect of the indicated stimuli. Data is representative of two independent experiments that were performed in duplicates.

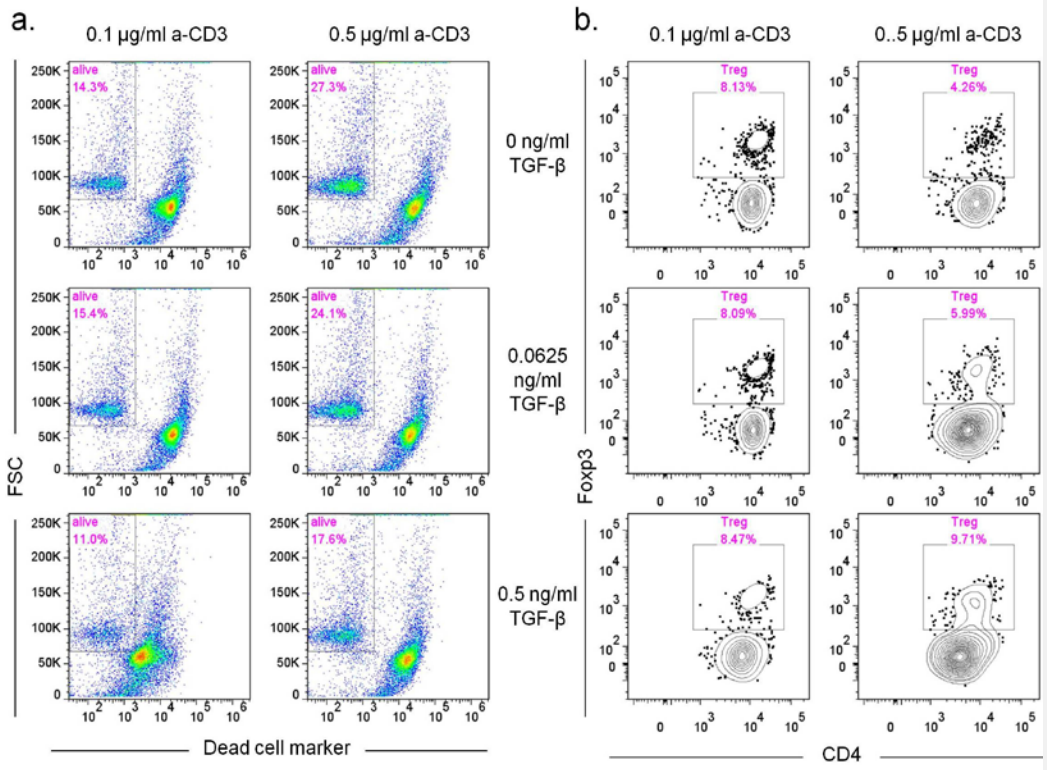


Figure 6.7 The effect of TGF-β on theTreg formation and the viability in the presence of plate bound anti-CD3 and soluble anti-CD28. 2.5x10^5 $CD4^+$ T cells that were isolated from naïve hPD-1KI-Foxp3-GFP mice were seeded into flat bottom 24 well plates that were precoated with anti-CD3. **a.** FACS plots representing the percentage of the viable cells that are identified by the exclusion of dead cells using Live/Dead near IR dead cell stain (see 2.5.1). **b.** The effects of different concentrations of TGF- β on the Treg formation in the presence of 0.1 µg/ml and 0.5 µg/ml plate bound anti-CD3.1 µg/ml soluble anti-CD28 is added in all the conditions. Data is representative of two independent experiments that were performed in duplicates.

To investigate the effects of the PD-1 agonists on the conversion of naïve $CD4^+$ T cells into Tregs, the surface of the Dynalbeads™ that containing active epoxy groups were coated with either isotype control, PD-L1, clone 19 or clone 10 antibodies. $2.5x10^5$ $CD4^+$ T cells were isolated from the spleens and the mesenteric lymph nodes of the naïve hPD-1KI-Foxp3-GFP mice and seeded into the 24 well plates precoated with 0.5 µg/ml anti-CD3. Cells were supplemented with 1 µg/ml soluble anti-CD28 antibody together with 0.0625 ng/ml, 0.125 ng/ml or 0.5 ng/ml soluble TGF-β in a final volume of 0.5 ml. Beads were then added to the culture and incubated for three days. This analysis showed that both native ligand PD-L1 and the PD-1 agonist antibodies potentiated the positive effect of TGF-β on Treg formation (Figure 6.8). To be able to make a comparison between the agonistic effects of the antibodies, the assay was repeated with all three clones of the anti-PD-1 antibodies. Clone 2 also displayed agonistic activity, which was comparable to that of PD-L1. Of the antibodies, clone 19 had the greatest effect on Treg induction, equivalent to PD-L1 ligand, both at the lower end of the TGF-β concentration (0.0625 ng/ml) and also in the absence of TGF-β (Figure 6.9). Interestingly, clone 10 and clone 2 also had inducing effects.

.

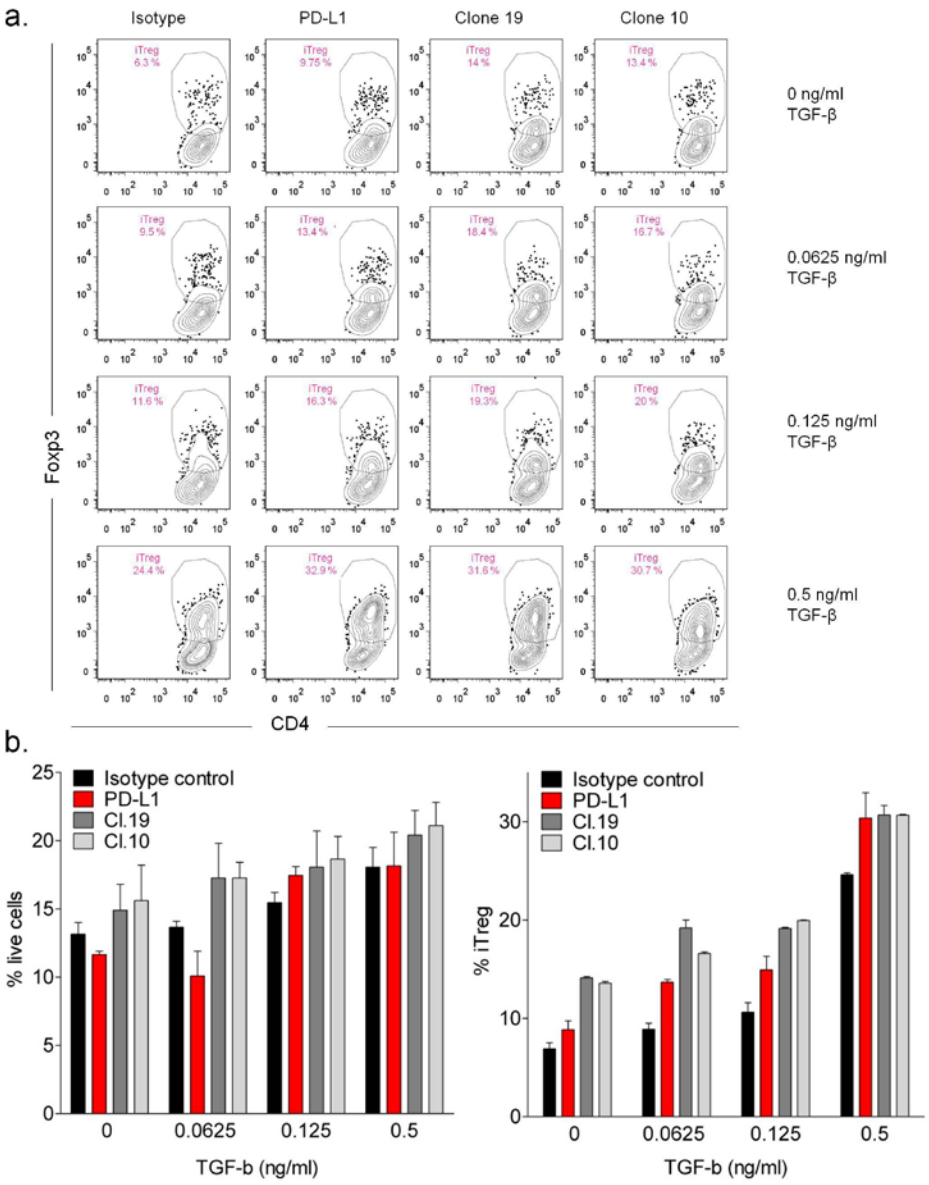


Figure 6.8 Treg formation in the presence of plate bound anti-CD3. 2.5x10^5 CD4$^+$ T cells isolated from naïve hPD-1KI-Foxp3-GFP mice were seeded into flat bottom 24 well plates that were precoated with anti-CD3. Dynalbeads™ that are coated with isotype control, PD-L1, clone 19 or clone 10 were added to the culture together with 1 µg/ml soluble anti-CD28. **a.** FACS plots representing the effects of clone 19 and clone 10 at increasing concentrations of TGF- β. **b.** Graphs showing the viability and the level of the Treg formation. Data is representative of two independent experiments. Values are means of duplicates ± SD

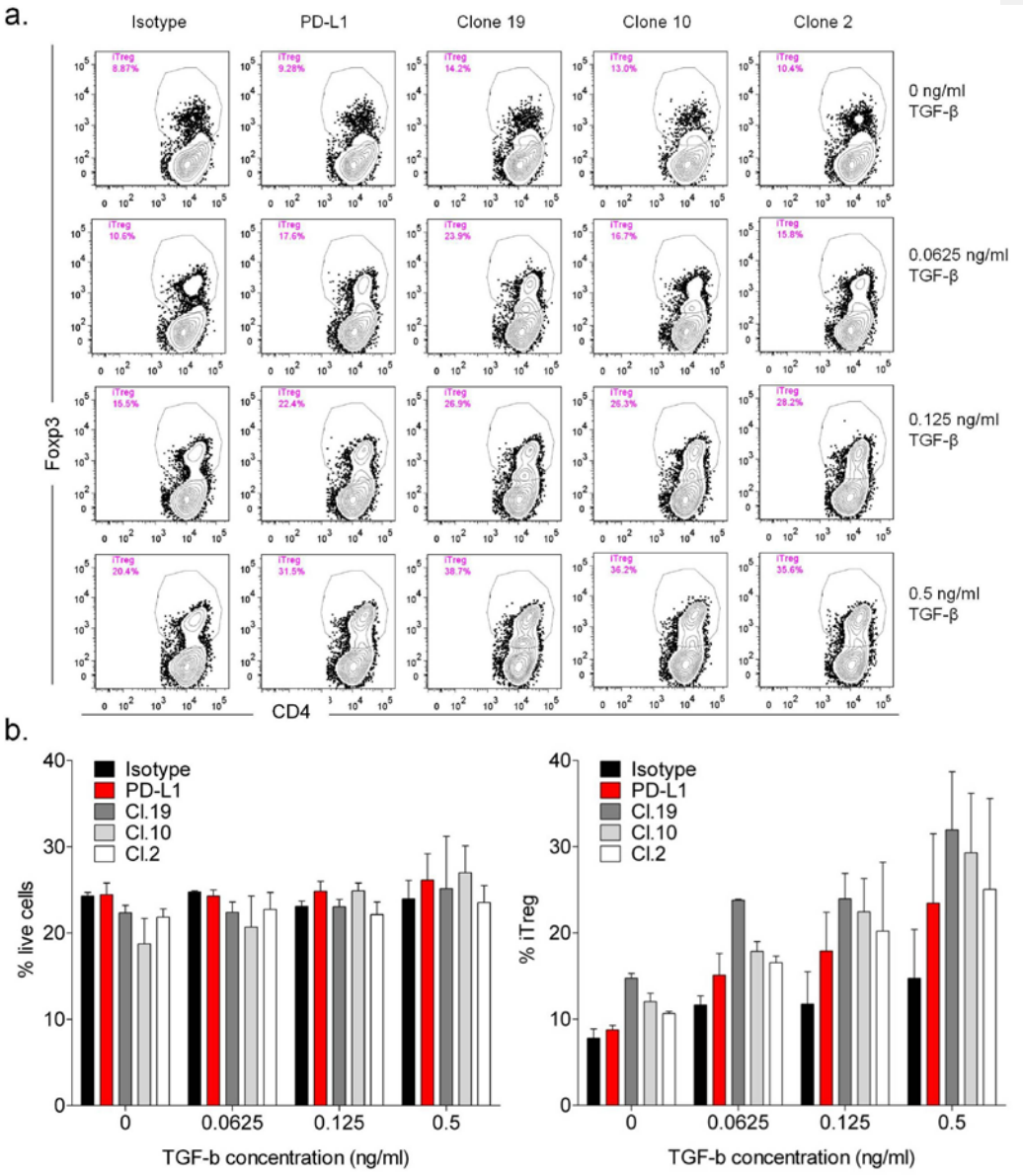


Figure 6.9 The effect of PD-1 agonists on Treg formation in the presence of plate bound anti-CD3. $2.5x10^5$ $CD4^+$ T cells isolated from naïve hPD-1KI-Foxp3-GFP mice were seeded into flat bottom 24 well plates that were precoated with anti-CD3. Dynalbeads™ that are coated with isotype control, PD-L1 or anti-PD-1 antibodies were added to the culture together with 1 µg/ml soluble anti-CD28. **a.** FACS plots representing the effects of anti-PD-1 antibodies at increasing concentrations of TGF- β. **b.** Graphs showing the viability and the level of the Treg formation. Data is representative of two independent experiments. Values are means of duplicates ± SD

6.4 Discussion

Our data show that PD-1 agonist antibodies may have a positive effect on Treg formation in vitro. The analysis of these experiments was complicated by several practical variables, including the co-presentation of antibodies on beads, the cell to bead ratio and seeding density. Rather than try to overcome these practical difficulties by optimizing the antibody levels on the beads, a much simpler way was to optimize the positive stimuli individually. Therefore, I separated the surfaces on which the antibodies were bound in an approach similar to that used earlier (see Section 3.4). In the newly defined assay, PD-L1 and anti-PD-1 agonistic antibodies could regulate the peripheral conversion of naïve $CD4^+$ T cells into Tregs; and, when all the three anti-PD-1 antibodies were tested, clone 19 provided the strongest induction compared to the other clones and the native ligand PD-L1. Further investigation needs to be carried out on systems using real APCs and soluble anti-PD-1 antibodies or in vivo Treg induction models before confidently suggesting a superagonistic role for clone 19 in the regulation of Treg formation.

Chapter 7:

The use of PD-1 agonist antibodies in experimental autoimmune encephalomyelitis

7.1 Introduction

Experimental autoimmune encephalomyelitis (EAE) is a model of human multiple sclerosis (MS) which is extensively used for illuminating the mechanisms of immune regulatory pathways and testing the therapeutic potential of novel biological agents. EAE can be induced by the administration of neural antigens such as myelin oligodendrocyte glycoprotein and is characterized by mononuclear cell infiltration and demyelination of the central nervous system (CNS) [360-361]. Upon antigen contact in the periphery, naïve $CD4^+$ T cells differentiate into effector Th1 and Th17 cell subsets and shortly after these cells cross the blood-brain barrier, the disease becomes symptomatic due to an uncontrolled release of proinflammatory cytokines from stimulated astrocytes and microglia [362]. Symptoms usually start with tail weakness and progress to complete hind limb paralysis, followed by a limited recovery in a majority of cases.

It has been shown that PD-1 and PD-L1 expression increase progressively in the central nervous system of C57BL/6 mice during the course of EAE [238]. Expression of PD-L2 has also been demonstrated in the cellular infiltrates within the meninges during active EAE [233]. Blockade of PD-1 leads to an exacerbated disease with increased frequency of IFN-γ-producing myelin oligodendrocyte glycoprotein (MOG)-reactive T cells and more MOG-specific antibodies in serum [238]. Furthermore, an early blockade during the disease onset was shown to be critical for observing such an exacerbation, which suggests that the PD-1 pathway plays an important role especially during the asymptomatic period of the disease. The studies using PD-1

deficient mice also revealed the importance of the PD-1 pathway in the regulation of the encephalitogenic T cell responses [363-364]. Therefore, EAE might be a good disease model for testing the efficacy of the biological agents that target PD-1 pathway. In the light of the inhibitory effects of the PD-1 agonist antibodies that were demonstrated in the models of immunity described in the previous chapters, I next tested their effectiveness in a monophasic EAE model.

7.2 Investigating a possible regulatory role for clone 19 in EAE

I selected clone 19 for initial EAE trials because it had been shown to exert the best inhibitory effect on $CD4^+$ T cell driven immune responses generated against SRBCs. In the first trial, EAE was induced in 8-9 weeks old female hPD-1KI and WT C57BL/6 mice by administration of myelin oligodendrocyte glycoprotein (MOG) 35-55 peptide in complete Freund's adjuvant (CFA) subcutaneously. As a part of the protocol, pertussis toxin was administered during disease induction and on day 2 post-injection to increase the permeability of the blood-brain barrier. Isotype control antibody or clone 19 was given i.p. 24 hours before the disease induction. WT C57BL/6 control mice received PBS prior to disease induction. Animals were followed up by daily weight measurements and neurological examination. The clinical scores were as follows: score 0.5 - weak tail, score 1 - tail paralysis, score 2a/2b - loss of the righting reflex and/or abnormal gait, score 3 - partial hind limb paralysis, score 4 - complete hind limb paralysis. Mice that lost more than 20% of their initial weight, had a score of 4 for four consecutive days or had resistant ulcers showing no signs of healing for seven days were culled and excluded from the rest of the study (though importantly, the data was included up to this point). Five mice were used per treatment group and all were fed with mash and jelly starting from the day when the first symptoms appeared. During the course of the disease, one mouse from WT C57BL/6 and

one mouse from the isotype control antibody treated group were culled due to excess weight loss. Another mouse from the isotype control antibody treated group was also culled due to a resistant ulcer. The result of this first experiment was that there was no evidence that clone 19 would ameliorate disease (Figure 7.1).

A second trial was performed using 7 weeks old female hPD-1KI mice. In this case the disease was induced the same way but the antibodies were given i.p. 24 hours before the disease induction. WT C57BL/6 mice received PBS prior to disease induction. Eight, seven and six mice were used for the C57BL/6, isotype control treated and clone 19 treated groups, respectively. As a measure to prevent the excess weight loss, the mice were fed with mash and jelly starting from disease induction. In this case, severe disease was present in all the groups. Four mice from the C57BL/6 group, three mice from the isotype control treated group and four mice from the clone 19 treated group had excess weight loss and were culled; and one mouse from the isotype control treated group was also culled due to resistant ulcers. Once again, mice that were treated with clone 19 displayed a more severe disease compared to the isotype control treated mice (Figure 7.2). Having considered the down-modulatory effect of clone 19 treatment on the PD-1 expression of $CD4^+$ T cells, which was observed following the SRBC challenge (Figure 7.3), I wondered if early treatment with clone 19 might strip the PD-1 off the surface of $CD4^+$ T cells and lead to exacerbated EAE. If such a modulatory effect of the clone 19 is attributed to its high affinity, a low affinity agonist might not produce prominent modulation.

7.3 Time course of the PD-1 expression during the disease onset

To be able to circumvent the modulatory effect of clone 19 and be able to target PD-1 when its expression has already been upregulated, I investigated the expression profile of PD-1 during the asymptomatic period of the disease. For this purpose, EAE was induced in twelve 9 weeks-

old female hPD-1KI mice. The mice were divided into four groups and the reactive inguinal lymph nodes of each group were analysed for PD-1 expression on either day 0, day 4, day 7 or day 10 post-disease induction. The activation status of $CD4^+$ T cells was also analysed for the confirmation of the immune process. The percentage of PD-1 expressing $CD4^+$ T cells and surface PD-1 expression per $CD4^+$ T cell were higher than the day 0 levels as early as on day 4 post-disease induction (Figure 7.4). These parameters continued to increase until day 7. The percentage of the activated $CD4^+$ T cells, especially the late activation marker $CD44^+$ cells, continuously increased up to day 10 confirming that immune activation was occurring.

7.4 The disease profile following the late injection of PD-1 agonists

Having established that PD-1 expression has already been upregulated on day 4, we studied the consequences of antibody administration on day 4 and day 7 to see if the disease exacerbating effect of clone 19 could be removed via late injection. This would also model more accurately the likely use of such an agent in therapy for human disease.

EAE was again induced in 9 weeks old female hPD-1KI mice. A total of 36 mice were divided into six groups and each group received PBS, isotype control, clone 19 or clone 10 injections. PBS and isotype control were administered on day 4, clone 19 and clone 10 were administered either on day 4 or day 7 post-disease induction. Mice were fed with baby formula supplemented powder and flavoured jelly starting from the disease induction to minimize deaths due to excess weight loss.

This time disease onset was longer (approx. 12 days) compared to the other trials (approx. 8 days). One mouse from the PBS treated group, one mouse from the group that was treated with clone 19 on day 7, and one mouse from the group that was treated with clone 10 on day 7 were

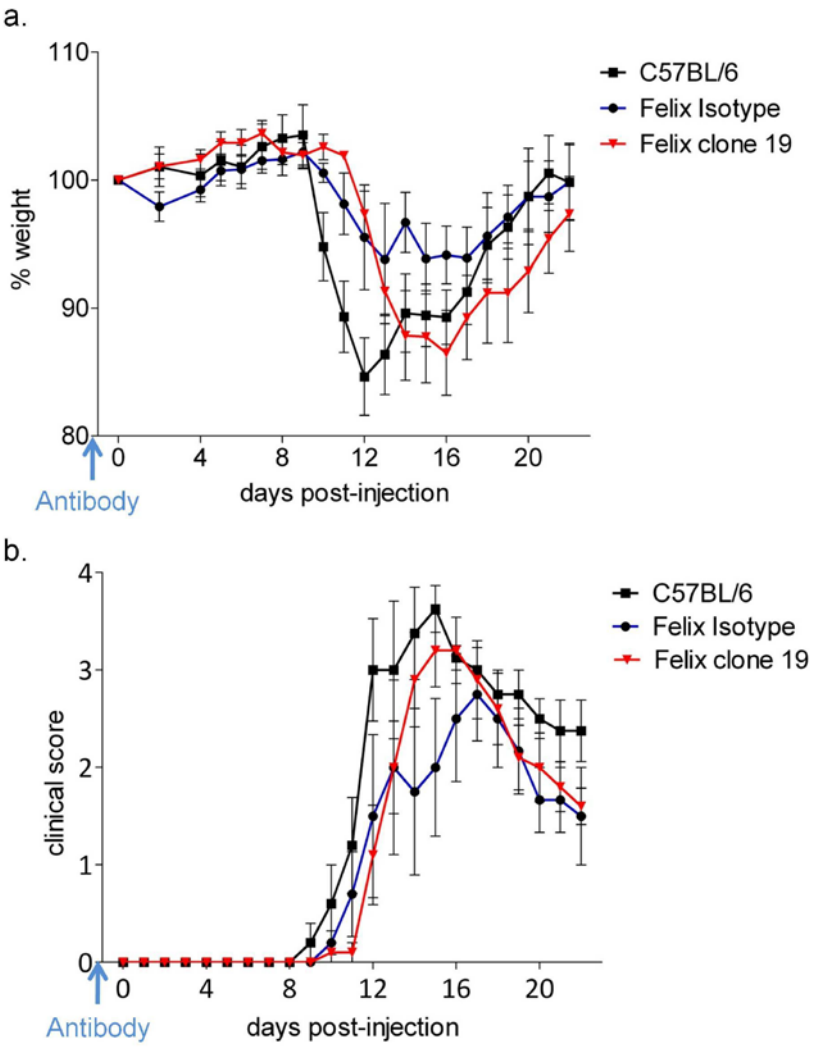


Figure 7.1 First trial for the effect of clone 19 in an EAE model. 8-9 weeks old female hPD-1KI mice per group were immunized s.c. with myelin oligodendrocyte glycoprotein (MOG) 35-55 peptide in complete freund's adjuvant (CFA). Pertussis toxin was administered during the disease induction and 2 days post-injection. Antibodies were administered i.p. 24 hours before the disease induction. **a.** Changes in the weights were represented as the percentage of the initial weights of the mice that were measured prior to disease induction. **b.** The graph showing the trace of the clinical scores that were determined through neurological examination. Score 0.5- weak tail, score 1-tail paralysis, score 2a/2b- loss of the righting reflex and/or abnormal gait, score 3: partial hind limb paralysis, score 4: complete hind limb paralysis. Data is derived from one experiment with five mice per group. Values are means of the measurements for treatment groups calculated for each day ±SEM.

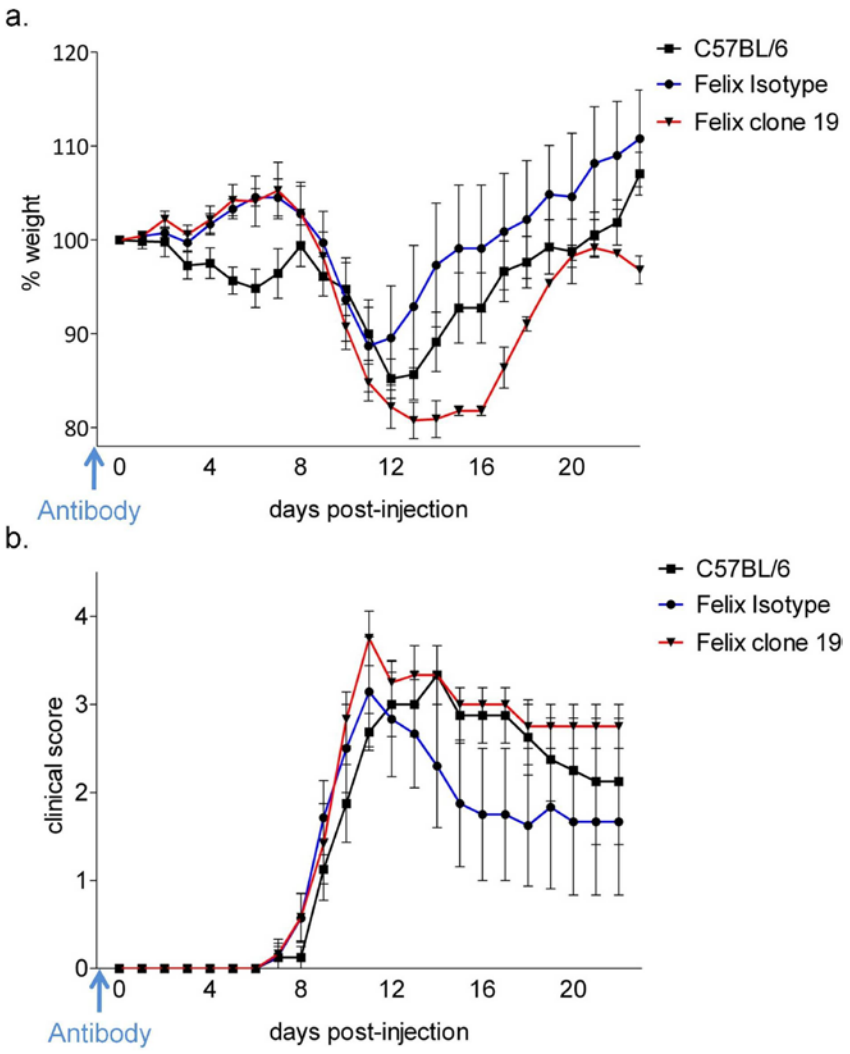


Figure 7.2 Second trial for the effect of clone 19 in an EAE model. 7 weeks old female hPD-1KI mice per group were immunized s.c. with myelin oligodendrocyte glycoprotein (MOG) 35-55 peptide in complete freund's adjuvant (CFA). Pertussis toxin was administered during the disease induction and 2 days post-injection. Antibodies were administered i.p. 24 hours before the disease induction. **a.** Changes in the weights were represented as the percentage of the initial weights of the mice that were measured prior to disease induction. **b.** The graph showing the trace of the clinical scores that were determined through neurological examination. Score 0.5- weak tail, score 1-tail paralysis, score 2a/2b- loss of the righting reflex and/or abnormal gait, score 3: partial hind limb paralysis, score 4: complete hind limb paralysis. Data is derived from one experiment with at least six mice per group. Values are means of the measurements for treatment groups calculated for each day ±SEM.

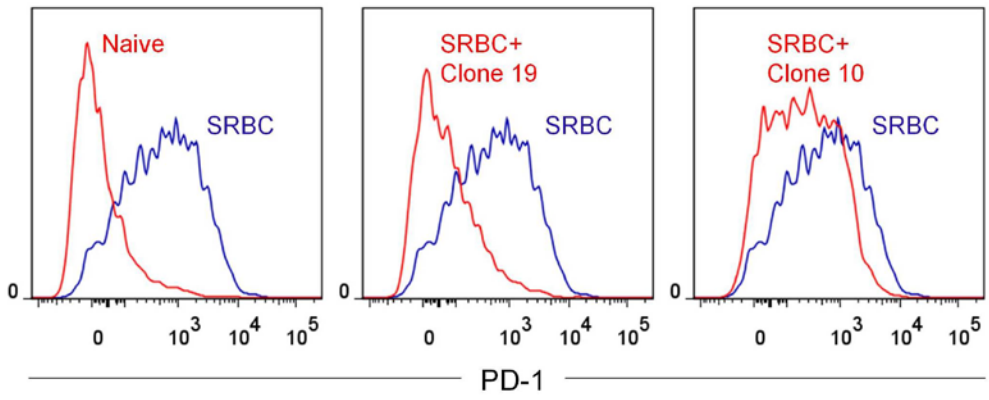


Figure 7.3 Modulation of PD-1 expression by the anti-PD-1 antibody treatment. Homozygous hPD-1 KI mice were immunized with SRBCs i.p. and either treated with isotype control, clone 19 or clone 10 s.c. the day before the SRBC administration. The PD-1 expression on $CD4^+$ T cells was analysed by flow cytometry on day 7 post-SRBC immunization. Red: naïve (left), clone 19 treatment (middle), clone 10 treatment (right), blue: SRBC treatment. Data is representative of four independent experiments with 4-5 mice per group.

culled due to excess weight loss. Another two mice that were treated with clone 10 on day 7 were culled due to resistant ulcers. As in the previous trials, the isotype control antibody showed a disease ameliorating effect compared to the PBS (Figure 7.5b). However, this time clone 19 and clone 10 injections on day 7 showed ameliorating effects greater than the isotype control which were prominent late in the disease process. Disease profiles were compared with the isotype control starting from day 13 when the first disease symptoms were displayed, using a Kruskal-Wallis test. The only significant difference found was between the PBS and isotype control treated mice. However, when a second analysis was performed starting from the time (day 14) when most of the mice had a disease score of 1 or above, both groups of mice that were treated with anti-PD-1 antibodies on day 7 showed a significant difference compared to the isotype control treated mice. So, it remains possible that the severity of the disease might be reduced by PD-1 agonists late in the disease and that positive and negative regulatory effects of clone 19 arise due to timing, its high affinity and the combination of agonism and receptor modulation. Since our data are only from one experiment, it has to be repeated in order to reach a firm conclusion.

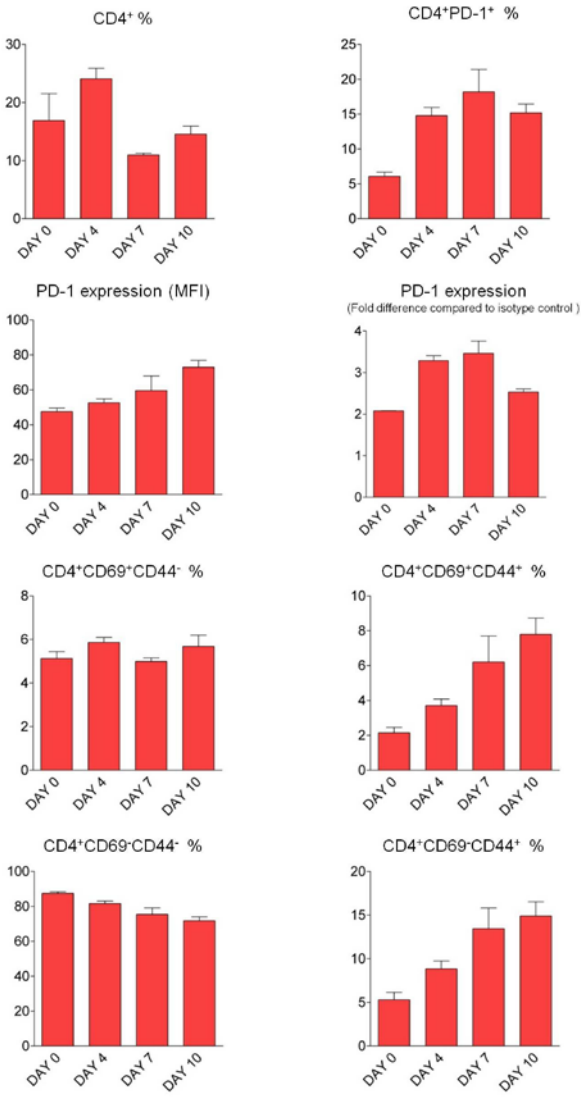


Figure 7.4 Time course for the expression of PD-1 on CD4+ T cells during the disease onset. EAE was induced in 9 weeks old homozygous hPD-1 KI mice with MOG(35-55)/CFA and pertussis toxin administration. During the disease onset, mice were sacrifised on day 0, day 4, day 7, day10 and the draining (inguinal) lymph nodes were removed for flow cytometric analysis of PD-1 expression. For each time point 3 mice were used. CD69 and CD44 expressions were also analysed as the indicators of T cell activation. All the cell subsets are represented as the percentage of CD4+ T cells. The background for PD-1 staining was determined for each time point using a PE conjugated mouse IgG1 isotype control antibody. Data is derived from one experiment. Values are means of three mice ± SD

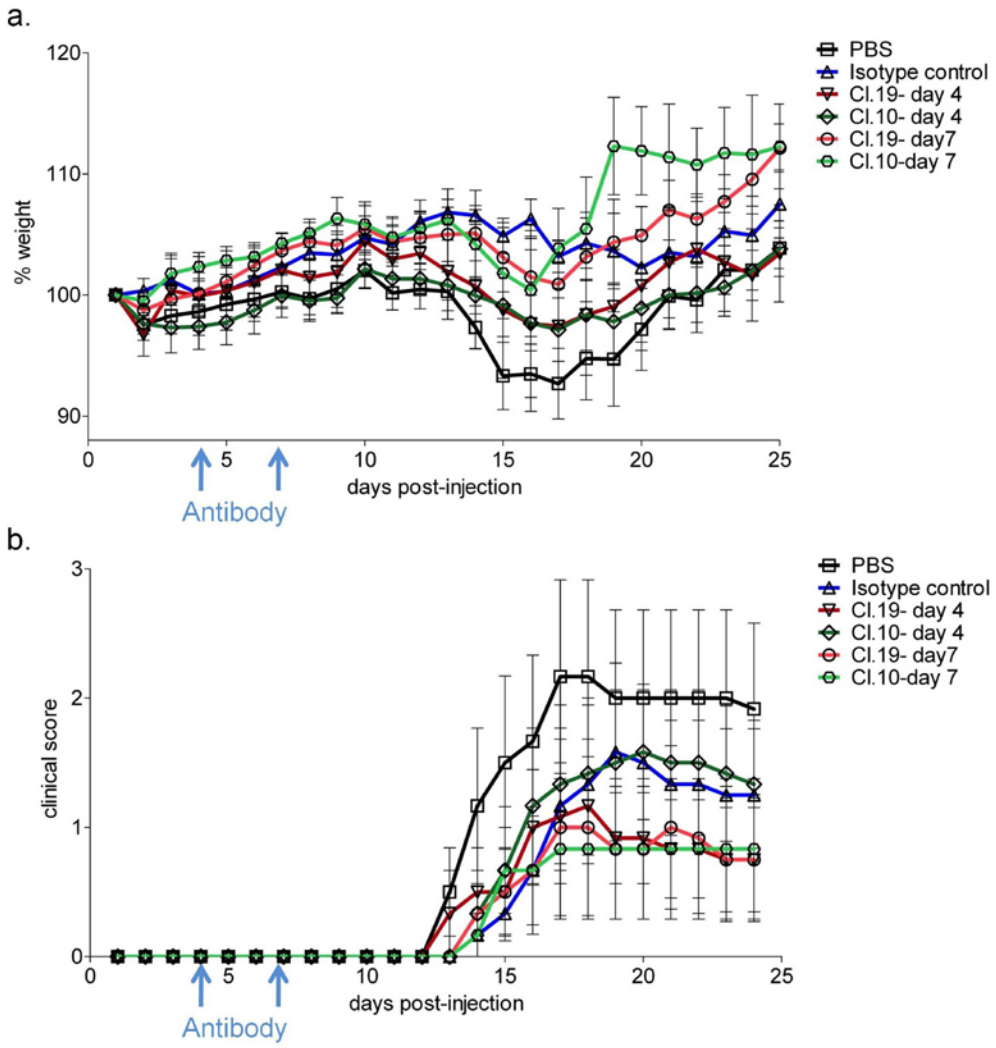


Figure 7.5 The effect of late antibody administration on the progression of EAE. 9 weeks old female hPD-1KI mice per group were immunized s.c. with myelin oligodendrocyte glycoprotein (MOG) 35-55 peptide in complete freund's adjuvant (CFA). Pertussis toxin was administered during the disease induction and 2 days post-injection. Antibodies were administered i.p. 4 days or 7 days after the disease induction. **a.** Changes in the weights were represented as the percentage of the initial weights of the mice that were measured prior to disease induction. **b.** The graph showing the trace of the clinical scores that were determined through neurological examination. Score 0.5- weak tail, score 1-tail paralysis, score 2a/2b- loss of the righting reflex and/or abnormal gait, score 3: partial hind limb paralysis, score 4: complete hind limb paralysis. Data is derived from one experiment with six mice per group. Values are means of the measurements for treatment groups calculated for each day ±SEM.

7.5 Discussion

Arguably the most notable feature of the EAE experiments described in this chapter is the ameliorating effect of mouse IgG1 isotype control antibodies on disease, and since I observed similar outcomes with different mIgG1 isotype control antibodies, the inhibitory effect may well be attributed to a common property of this isotype class linked to the Fc receptor. IgG1 antibodies have the highest affinity for FcRγII which is itself known as an inhibitory Fc receptor [365]. There is a direct link between the FcRγII and EAE since it has been shown that FcRγII deficient mice develop exacerbated EAE [366]. The real question of my experimental approach, therefore, was whether PD-1 agonist antibodies could have an inhibitory in addition to the inhibitory effect of their isotype class.

As already highlighted, initial experiments with clone 19 showed an exacerbation in EAE, showing that this antibody has a similar effect to a blocking antibody against PD-1. I reasoned this could occur if clone 19 induced down-modulation of PD-1 expression, as observed when clone 19 was administered 24 hours before the SRBC challenge. Since PD-1 is up regulated upon activation, I speculated that early treatment with clone 19 might result in modulation of the surface PD-1 before the effects of the PD-1 triggering could be seen. In other words, if clone 19 stripped the PD-1 off the surface, there will be a lack of target for that antibody to signal through. Therefore, I considered allowing some time for PD-1 up regulation and then targeting it when the surface expression is high. Having shown that PD-1 starts increasing early on during the asymptomatic period of EAE and continues to increase gradually, I designed an EAE trial with late antibody treatment. Preliminary evidence suggests that this may ameliorate disease but this observation would need to be repeated.

Since EAE induction requires harsh manipulations such as administration of the neural antigen with a strong adjuvant and breaking the blood-brain barrier by pertussis toxin, it may be very

hard to reverse that condition with any kind of T cell-inhibitory agents. Furthermore, although PD-1 deficiency creates susceptibility to exacerbated EAE, this does not mean that stimulating PD-1 pathway will reverse the condition. This highlights the complexities and uncertainities that remain in trying to modulate disease in vivo. Even if the PD-1 agonist antibodies were proven to be ineffective in the EAE models, the regulatory effects of PD-1 agonists would be uncertain in other disease situations without further careful investigation.

Chapter 8:

General Discussion

PD-1 is an inhibitory member of the CD28 family of co-receptors that has major role in autoimmunity, chronic viral infections, cancer and transplant immunology. Although the blocking effects of an Fc fusion form of its ligand PD-L1 have been tested in many studies, the consequences of in vivo stimulation of the PD-1 pathway by agonistic agents is largely unexplored. This thesis has focused on the in vitro and in vivo effects of a novel class of PD-1 agonist antibodies, namely inhibitory superagonists, for delineating the function of the PD-1 pathway in several models of immunity and investigating the potential of these novel superagonists for treating autoimmunity.

8.1 Inhibitory effects of anti-PD-1 antibodies on human PBMCs

The inhibitory effects of clone 19 and clone 10 on the proliferation of human PBMCs revealed that the off-rates of the antibodies may be relevant to observing immune modulatory effects of PD-1 agonists. Since no inhibition was observed with the slow off-rate anti-PD-1 antibody clone 2, which has an epitope similar to that of the fast off-rate antibody clone 10, the fast off-rate can be considered advantageous in providing inhibition via PD-1. Similar to the physiological ligand PD-L1, which has very fast binding kinetics [367], clone 10 may target more PD-1 molecules within a certain time period and therefore induce a greater amount of overall signalling [368]. As proposed previously for the antibody agonists developed against TNFR superfamily member Fas, our findings also suggest that an inverse correlation between the affinity and the potency of agonistic antibodies may exist [369]. Since PD-1 and Fas belong to different receptor families and are probably triggered in different ways, this inverse correlation may apply to agonistic

antibody signalling in general. Despite their similar slow off-rates, the difference observed between the activities of clone 2 and clone 19 indicates that binding location for the antibodies may be another crucial parameter for the agonistic performance of the antibodies. Clone 2 binds to a membrane-distal epitope on PD-1 which is close to the ligand binding site whereas clone 19 binds to a membrane-proximal epitope. The epitope location may explain the higher inhibitory potential of clone19 since a similar phenomenon was demonstrated for superagonist antibodies that bind to membrane proximal epitopes on the C”D loop of CD28 [173]. Since the effects of these antibodies can only be observed when they are immobilized, their mechanism of action may be attributed to the relatively compact signalling complexes they form and thus their contribution to the size dependent reorganization of immune synapse elements [175]. Indeed, the activity of bead-immobilized, membrane-proximally binding clone 19 is superior to bead-immobilized top-binding clone 2, which suggests an analogy between the CD28 superagonists and clone 19. In our in vitro setting, however, the membrane-proximal binding location did not offer a large advantage over fast off-rate since clone 10 was in fact active at a broader range of OKT3 levels. Hence, an effective approach for developing potent agonists against PD-1, or any other surface protein that signals through tyrosine based motifs (see Table 1.1), may be in combining the two important properties together and generating fast off rate antibodies targeting membrane proximal epitopes. For the existing high affinity antibody clones such as clone 19, improving the activity may be possible by simply obtaining higher off-rate variants.

Another important finding was that the cells were capable of integrating the positive and negative stimuli provided from separate sites. Although this finding is against the proposed dynamics of the immune synapses where the co-localization of TCR and costimulatory receptors is required [290], an explanation might be the rapid re-localization of the stimulated PD-1 molecules to the vicinity of the TCR. This possibility is supported by the observation that clone 10 gave stronger inhibition in these assays, perhaps due to the faster dissociation of PD-1

from this antibody. Another possibility for the cells' ability to integrate the physically separated signals is that co-localization with the TCR is not strictly required. Recently, Yokosuka et al. demonstrated that PD-1 can form microclusters even in the absence of TCR ligation. However, they did not observe any signalling in the PD-1 microclusters insofar as there was a lack of PD-1 phosphorylation and SHP-2 association [185]. However, that study was conducted using a T cell line transfected with an elongated chimeric PD-1 molecule in order to prevent TCR and PD-1 co-localization upon TCR/peptide/MHC engagement, so the observations may not be physiologically relevant due to disruption of immune synapse dynamics. Regardless of the mechanism, our work showed that inhibitory superagonists can be generated against receptors like PD-1.

8.2 The hPD-1KI mouse model has the immunological features of WT C57BL/6 mice

Insertion of a transgene into the mouse genome may result in various disruptions of the animal's physiology. Therefore, a detailed characterization of the transgenic mice was required before starting the experimental procedures. Our results showed that a healthy humanized PD-1 knock-in mouse model can be generated by replacing exon 2 of mouse PD-1 with its human counterpart. The high level of homology between mouse and human PD-1 [370] allows such a change to be made and the mice do not display any sign of PD-1 signalling deficiency. This supported our hypothesis that replacing the extracellular region of mouse PD-1 would not impair PD-1 signalling since human PD-1 can interact with the mouse PD-1 ligands and this interaction would transmit inhibitory signals through the chimeric form of PD-1. Initially, we confirmed that the modified PD-1 was upregulated to the same degree and at the same time as PD-1 in WT C57BL/6 mice upon TCR stimulation. Together these experiments indicated that the humanized

PD-1 gene is regulated normally and that the humanized protein is properly assembled, folded and trafficked to the cell surface.

Another finding was that the PD-1 antibodies did not recognize mouse PD-1. The lack of an inter-species cross reaction justified the use of a humanized mouse model for testing the effects of anti-human PD-1 antibody treatment. Since it seemed likely that it would be a useful model, further investigation of the possible negative effects of the modified PD-1 on the development of the naïve lymphocyte pool was undertaken. When the thymic and splenic parameters of 8-12 weeks old naïve WT C57BL/6 mice were compared with age-matched naïve hPD-1KI mice, no significant difference was detected. This indicates that there is no overt developmental abnormality in the lymphocyte population of hPD-1KI mice. Having also demonstrated that heterozygous and homozygous hPD-1KI mice are able to mount normal immune responses, we concluded that the hPD-1KI mouse model is an approriate model for analysing the effects of anti-human PD-1 antibody agonists.

Nishimura et al. demonstrated signs of glomerulonephritis and arthritis through the histological examination of PD-1 deficient C57BL/6 mice which were older than 6 months of age whereas they did not detect any signs of either pathology in age matched WT C57BL/6 controls or in younger PD-1 deficient C57BL/6 mice [102]. Therefore, in the C57BL/6 background, PD-1 deficiency manifests as a mild lupus like disease in older mice. This thesis does not address the question of there being a histological difference between the glomeruli and the joints of the aged hPD-1KI and WT C57BL/6 mice. However, a detailed physical examination was performed for the aged mice and no signs of arthritis were observed. Likewise, inspection of the gross anatomy of the aged homozygous hPD-1KI mice did not suggest any autoimmune processes were occuring since the sizes of peripheral lymhoid organs were found to be comparable with those of heterozygous hPD-1KI and WT C57BL/6 littermates. One way to rule out systemic

autoimmunity in hPD-1KI mice would be to check for anti-nuclear antibody (ANA) positivity and/or evidence of renal and other pathology.

8.3 Inhibition of the in vitro allogeneic response by clone 19

Using an in vitro MLR-based assay, we showed that soluble PD-1 agonists can inhibit immune activation. The reason why the agonists against a monomeric receptor did not require immobilization [175] and were active in solution may be explained by the possible capture of the antibodies by Fc receptors [371] that are present on APCs of the allogeneic strain. This may also provide a basis for the activity of the soluble antibodies in vivo [372]. It was interesting that the inhibitory effect required very high concentrations of PD-1 agonists (100 µg/ml) probably because we could only achieve optimum capture of the antibodies at these high concentrations.

The dose of mitomycin-C (MMC) used for preventing the activation and proliferation of alloegeneic antigen presenting cells was found to be crucial for generating an optimal one-way MLR reaction. The MMC doses above 50 µg/ml abrogated the MLR completely, probably due to MMC transferring from the allogeneic cells although they had already been washed extensively before culturing. The doses below 50 µg/ml were also unsuccessful in preventing antigen presenting cell proliferation, therefore we could not detect any inhibition probably due to the proliferation of both the effectors and stimulators and the release of stimulatory cytokines. This could have been solved by fixing the stimulator APCs prior to culture. When inhibition was observed, the allogeneic antigen presenting cells were found to have almost disappeared, and the positive control displayed proliferation of 5-10% for $CD4^+$ T cells and 25-30% for effector $CD8^+$ T cells.

Finally, in contrast to our observation that the top-binding, fast off-rate clone 10 exerted the strongest inhibition on human PBMCs, the mouse MLR-based assay showed that only the slow off-rate, membrane-proximally binding clone 19 induced significant inhibition. Lack of such an effect with the other slow off-rate antibody (clone 2), which targets a membrane distal epitope similar to clone 10, further supports the general hypothesis that the proximity of the epitope to the membrane may influence the potency of the agonistic activity in vivo. One explanation for why clone 19 is then more effective is that it is capable of inhibiting the $CD4^+$ and $CD8^+$ T cells simultaneously. This requires follow up and more experimentation.

8.4 Effects of stimulating the PD-1 pathway during the germinal centre reaction

In our study, we demonstrated that the primary germinal centre response can be modulated by PD-1 agonists. Of the paramaters we analyzed, Tfh cells and activated T cells were found to be significantly fewer in clone 19 treated animals. This effect was accompanied by a decrease in the specific anti-immunogen (SRBC) antibody response, which suggested that PD-1 agonism may down-modulate the humoral parameters of germinal centre responses as well. Using PD-1- and PD-L1/2-deficient mice, Good-Jacobson et al. demonstrated that PD-1 controls the development and function of Tfh cells and thus regulates the GC B cell response and antibody production [200]. Consistent with the findings of Good-Jacobson et al., but rather using hPD-1KI mice and PD-1 agonists, we showed that PD-1 negatively regulates the numbers of Tfh cells and the production of IgM and IgG classes of antibodies during a primary GC reaction. We also demonstrated that the numbers of isotype switched B cells and GC B cells were unaffected by PD-1 stimulation during the primary GC response. However, the time frame of our observations differed from that of Good-Jacobson et al., who did not detect changes in PD-1 deficient mice until at least day 15 post-NP injection whereas we observed changes on day 9 post-SRBC

immunization. Based on their findings, Good-Jacobson et al. concluded that PD-1 has no effect on GC formation since their results suggested that PD-1 starts functioning during the late phase of the GC response when the primary response has started subsiding. In contrast, our findings suggest that the PD-1 pathway is already active during the early phase of the GC response as the anti-PD-1 antibodies have been circulating in the blood of hPD-1KI mice for a week when the effects were observed at the time of the peak primary GC response. These differences might be accounted for by the experimental protocols. The earlier study made its conclusions on the basis of studies in a germline PD-1 deficient mouse strain, whereas we carried out our studies by stimulating the PD-1 pathway in essentially normal hPD-1KI mice using agonistic antibodies. Another explanation would lie with the ability of different immunogens to induce meaningful differences in time frames, with SRBCs being very robust immunogens.

Contrary to our in vitro findings where clone 19 was less potent, clone 19 exerted the strongest activity in this $CD4^+$ T cell driven humoral immune response. This could be due to the superagonistic action of clone 19 since treatment with the other high affinity (clone 2) antibody, which binds to a membrane distal epitope on PD-1, did not affect GC cell numbers. The differences between clone 19 and clone 2 also tended to exclude the possible role of antibody mediated cell depletion or cytotoxicity in the loss of the $PD\text{-}1^+$ cells. This was unlikely anyway because the mIgG1 isotype has very low potential for complement fixation and opsonisation [373].

Although we demonstrated a reduction in the number of Tfh cells, the in vivo study did not show how this agonistic effect influenced the Tfh cell numbers mechanistically. There could be several possible mechanisms for the regulatory action of PD-1 in the GCs, including the intrinsic inhibitory mechanism in the Tfh cells through PD-1 signalling or an extrinsic regulatory mechanism through stimulation of the expansion/activity of a $Foxp3^+$ regulatory Tfh cell population. Since PD-1 has recently been shown to induce the peripheral conversion of naïve

$CD4^+$ T cells into Tregs [192], we asked if such a conversion could be induced in the GC setting upon administration of PD-1 agonists and showed that the PD-1 agonist antibody treatment did not expand the regulatory Tfh cell population in vivo. We therefore speculated that the negative regulatory effect of the PD-1 agonists on Tfh cells was probably through a Tfh cell intrinsic mechanism. However, the lack of expansion in the regulatory Tfh cell population could also simply be due to the origin of those cells. In two separate studies the regulatory Tfh cells have been proposed to originate from thymus-derived natural Tregs [346, 374]. Therefore, regulatory Tfh cells may not comprise an induced population of Tregs at all and this may explain why this population was not induced by stimulation of PD-1. Further investigations can be carried out into the mechanism of Tfh cell regulation by sorting Tfh cells with PD-1 agonists in vitro and analysing the consequences of PD-1 agonism in those cells.

8.5 Inhibitory effects of PD-1 agonists on $CD8^+$ T cell driven immune responses

Through ex vivo stimulation of the cells from mice treated with heat inactivated MVA and clone 19 or clone 10 antibody, we demonstrated that clone 19 treatment is inhibitory in this model of $CD8^+$ T cell driven primary immune responses. Consistent with our observation that clone 19 down-modulates the germinal centre response, this data also suggests that clone 19 induces better inhibition, and is a better superagonist than clone 10, which targets a membrane-distal epitope. It has been shown that the PD-1 pathway plays an important role in the memory reprogramming of $CD8^+$ T cells following an acute response against an inactivated vaccinia virus [349]. Further confirmation of the effect of clone 19 treatment on the memory $CD8^+$ T cell responses should be undertaken in the secondary immune response setting.

An interesting observation providing a basis for the putative PD-1 agonistic action of all three antibodies was the inhibition of the MVA-OVA specific TCR transgenic $CD8^+$ T cell response. In

contrast to our in vivo data showing the significant down-modulation of the GC response and MVA-driven response by clone 19 only, clone 10 and clone 2 also exerted significant inhibition on T cells in this model. This suggests that all three antibodies have some degree of agonistic potential under certain conditions. This may have several explanations. One possibility is the varying contribution of $CD4^+$ T cell help in the in vivo studies. Differential effects of antibodies on cells from different subsets may explain the balance of positive and negative effects. One possibility is that, due to the high sensitivity of $CD8^+$ T cells to PD-1 stimulation [375], even weak PD-1 stimuli such as from clone 2 can pass the threshold for PD-1 signalling and induce inhibition. If this is true the comparable effects of an agonist and a superagonist may only be explained by the ability of $CD8^+$ T cells to generate an all or none response to stimuli that pass a PD-1 signalling threshold. Different PD-1 signalling thresholds may also provide some insight into why clone 2 does not display any agonistic activity in most settings. It may simply be because clone 2 does not induce a signal strong enough to pass the PD-1 signalling threshold of $CD4^+$ T cells. In summary, intrinsic differences between the PD-1 signalling thresholds of $CD4^+$ and $CD8^+$ T cells may account for conditional superagonism. This hypothesis may further be tested in OVA specific TCR transgenic $CD4^+$ T cell responses.

8.6 Tolerogenic effect of PD-1 agonists by induction of regulatory T cells

In order to complement our in vivo findings showing that PD-1 agonists inhibit primary $CD4^+$ and $CD8^+$ T cell driven immune responses, we asked if an indirect, Treg related mechanism is involved in the down-modulation of immune responses. Our bead-bound antibody-based assays provided consistent and reproducible evidence for a Treg inducing effect of PD-1 agonists in vitro. In fact, all three anti-PD-1 antibodies were found to enhance Treg formation similar to the native ligand PD-L1. In the work of Francisco et al., wherein PD-L1 was first shown to induce

Treg formation, the rate of cell death was not noted as a confounding factor [192]. However, when we duplicated their assays by using bead bound antibodies at a high bead to cell ratio, we found that PD-L1 treatment increased the fraction of Tregs largely due to the increased death of effector cells. Our data also strengthened the case for the agonistic activity of all of the anti-PD-1 antibodies since they all displayed a Treg inducing effect comparable to that of PD-L1. Furthermore, either in the absence or at relatively low levels of TGF-β, clone 19 dislayed a greater inducing effect, which suggests that this in vitro setting may provide ideal conditions for clone 19 to display superagonistic effects.

The expansion of Tregs has long been a therapeutic objective in the fields of autoimmunity and transplantation tolerance. Although Treg formation is possible through ex vivo conversion of naïve $CD4^+$ T cells in the presence of antigenic stimuli and TGF-β also, strategies that synergize with these effects will be of considerable interest since they may have the potential to increase the absolute as well as relative yield of cells. The difference between enrichment, as a relative measurement, and a true rise in the absolute count of Tregs was one item highlighted by this study. In fact, our data showing the in vitro Treg inducing effect of PD-1 agonists suggests the value of using PD-1 targeting strategies as previously shown by Francisco et al. for PD-L1 [192]. However, the main question for Treg inducing therapies is whether or not they can enhance Treg formation in vivo. It has been shown that continuous administration of subimmunogenic doses of antigen into the circulation of antigen specific TCR transgenic mice induces Treg formation in vivo [376]. By crossing the hPD-1KI-Foxp3-GFP mice with TCR transgenic mice, such as OT-II mice, which express a TCR specific for a MHC-II restricted peptide, it may be possible to elucidate the in vivo role of the PD-1 agonists in peripheral Treg formation. Consistent with our previous data, this data also suggests that the co-localization of PD-1 and TCR is not required for effective PD-1 signalling in Treg cells.

8.7 Use of PD-1 agonists in models of autoimmunity

Having demonstrated Treg inducing effects in vitro and the modulatory effects of the antibodies in models of immunity in vivo we hypothesised that the PD-1 agonists may be of therapeutic value. To test our hypothesis, we selected MOG/CFA induced EAE as our initial model of autoimmunity since the disease can easily be induced by administration of the encephalitogenic antigen and the disease process is short compared to that of spontaneous models of autoimmunity [377]. On the other hand, due to the severity of this model, we kept our sample size small and conducted our initial experiments with only clone 19, since this displayed a better inhibitory effect compared to other clones in most of the previous models we tested.

Despite its strong inhibitory potential in the models of immunity, the initial EAE trials demonstrated a disease-exacerbating role for clone 19. This effect might be explained by the fact that clone 19 treatment modulates the surface expression of PD-1, as shown for the TCR previously [378], and might therefore attenuate the inhibitory signal before the immune response is underway. But, why does the PD-1 stripping effect obscure the inhibitory effect only in the EAE setting? Early injection of clone 19 may result in PD-1 internalization before PD-1 reaches an optimum surface level, since clone 19 has already been distributed in the body at the time of EAE induction. Therefore, clone 19 treatment could itself lead to a resting condition that is similar to PD-1 deficiency, or that is analogous to a blocking antibody against PD-1 [238]. In the models of immunity, clone 19 was administered 24 hours after immunisation, which may have allowed PD-1 reach a threshold surface level capable of signalling before being internalized. Our last EAE trial lent some support for this theory since allowing some time for PD-1 upregulation removed the disease-exacerbating effect of clone 19 to some extent. Importantly the PD-1 down modulating effect of clone 10 treatment was found to be lower compared to clone 19, which suggests that the degree of PD-1 internalization/stripping may correlate with

affinity. Therefore, engineering clone 19 for lower affinity may eliminate the disease exacerbating potential of clone 19 and make it a better inhibitor.

Finally, we must also consider the possible role of antibody mediated cell depletion/cytotoxicity in the reduction in the number of PD-1^+ cells. However, this seems an unlikely complication as the mIgG1 isotype has very low potential for causing cell depletion/cytotoxicity [379-380]. Another reason why we do not favor this possibility is that PD-1 expression is also a marker of cell activation. This means that if the PD-1 expressing cells were depleted the final outcome would be an amelioration, not an exacerbation, of disease.

8.8 Mechanism of PD-1 triggering

Monoclonal antibodies against TCR and the costimulatory molecules are the most common tools that are used as surrogates of natural ligands for studying receptor downstream events [381]. Therefore, PD-1 agonists have the potential to provide valuable information about how the inhibitory co-receptor PD-1 and, in general, the tyrosine motif containing receptors that are dependent on extrinsic tyrosine kinases are triggered. This thesis mainly examines the relation of epitope location to the strength of the signal generated in the context of PD-1 stimulation. The PD-1 agonist antibody that has the membrane proximal epitope has been shown to be advantageous for obtaining a stronger signal in many of the settings tested. This suggests that antibody superagonism may play a role [173] and size dependent re-organization of the membrane-associated enzymes, which had previously been proposed for the triggering of TCR and CD28, may also be the key event for PD-1 triggering. This would support the notion that the kinetic-segregation model applies generally to the triggering of tyrosine motif-containing T cell receptors [175, 337]. On the other hand, the differences observed in the strength of PD-1 stimulation may not fully reflect the effect of the epitope location since the antibody off-rates are

variable. Different off-rate variants of the current PD-1 agonists could be used as controls to rule out the confounding effect of the off-rate. Also, the conclusions that have been reached so far are deduced from the modulatory effects of the PD-1 agonists on immune responses and there is no direct evidence for the re-organization of the signaling elements. Likewise, strictly speaking, the current data do not exclude the other models for receptor triggering such as conformational change [303]. Therefore, further investigation could be centered around how the kinase/phosphatase balance changes upon binding of PD-1 agonists and whether the effects can be modified by elongated PD-1 constructs [175]. Studying the effects of the agonists using longer PD-1 transfectants would provide direct evidence for the mode of action of the proposed inhibitory antibody superagonists.

8.9 Potential uses of hPD-1KI mice

PD-1 is a negative regulator of T cells which is detected at high levels in the context of chronic immune activation such as autoimmunity, chronic viral infections and immune responses against tumors [152]. Blockade of PD-1 has been shown to reverse the exhausted phenotype on virus specific and tumor infiltrating T cells [210, 382] and stimulation of PD-1 dampens the immune response during autoimmune processes [151, 383]. Therefore, therapeutics targeting PD-1 would be helpful in treating those conditions.

Developing new therapeutics is a time consuming process since extensive preclinical and clinical studies are required for obtaining consistent results about the efficacy and the adverse effects of new drugs. Using animal models that are genetically humanized for the target, this process can be accelerated as the specific agents can directly be tested in in vivo models without any need to change their specificity. The expression of PD-1 ligands has been found on a wide variety of hematologic malignancies and solid tumors [152] and a strong correlation has

been demonstrated between the expression of PD-1 ligands and poor prognosis [384-386]. The current strategy to test the efficacy of the blocking monoclonal antibodies against PD-1 involves grouping the patients according to certain parameters such as type and stage of the tumor and age and sex of the patient [387-388]. Although this kind of grouping allows investigators to make interpretations about the safety and efficacy, there are many other variables that may have an impact on the overall result such as genetic background of the patient. Use of humanized mice would help minimize the effect of individual variation and provide a quicker approach to characterize different agents in different tumor models. Similarly, new blocking antibodies against PD-1 could be serially tested using models of chronic infection in the hPD-1KI background [389] . hPD-1KI mice can also be used for characterizing the therapeutic potential of new PD-1 agonists in models of autoimmunity. Moreover, complexities in PD-1 biology would be illuminated using PD-1 specific agents in models of immunity and disease models.

8.10 Potential uses of PD-1 agonists

The biology of PD-1 is still largely unexplored and there are many questions waiting to be answered such as the type(s) of cytosolic phosphatases recruited under physiologic conditions and the function of PD-1 in fully differentiated primary T cell subsets [178, 183, 390]. The PD-1 agonists characterized in this thesis may be used to study PD-1 biology in depth. Although PD-1 is widely recognized as an inhibitory co-receptor, recent studies have pointed to some controversies about the role of PD-1. Using PD-1 knock-out mice, Sage et al. studied the role of PD-1 in humoral immune responses with respect to follicular helper T cells [391]. They showed that PD-1, which is a marker of follicular helper and follicular regulatory T cells [344, 346] , inhibits follicular regulatory T cells and accentuates humoral immune responses through increasing the activity of follicular helper T cells. Therefore, PD-1 agonists may help in

understanding the function of PD-1 in humoral immunity in wild type mice. This may provide more physiological insights through eliminating the confounding effect of the factors released differently between knock-out and wild type mice. Moreover, germ-line deficiency of PD-1 may create an unexpected developmental defect in the immune system of knock-out mice. So, use of PD-1 agonists may offer a different perspective in studies investigating the importance of PD-1 activity in humoral as well as cellular immunity. There is also an earlier report proposing that the binding of PD-1 agonist antibodies generates positive costimulatory signals and activates T cells [392]. However, that study was problematic since it did not consider the possibility that the PD-1 agonists also blocked PD-1 signalling. Relying on the observation that PD-L1 may have a dual role [393-394] they claimed that stimulation of PD-1 may have both positive and negative costimulatory outcomes. However, later studies showed that PD-L1 may deliver positive costimulatory signals through an independent receptor [395-397].

The data presented in this thesis suggests that PD-1 acts as a negative regulator of the immune responses and the inhibition it provides is generally mild. To date, most of the immunosuppression strategies used for controlling autoimmunity cripple the immune system [398] and therefore, strategies targeting PD-1 may be useful in establishing a fine balance between regulating autoreactivity and maintaining the ability of immune system to fight against pathogens. The data presented in this thesis provides encouraging evidence that inhibitory superagonists against PD-1 could be produced which could be used as a potential therapeutics targeting PD-1. According to our data, it is also possible that the degree of inhibition can be varied by changing the off-rate of the inhibitory agonists. This observation may pave the way for the development of customized inhibitory agonists as immunosuppressive therapeutics with varying potency.

BIBLIOGRAPHY

1. Cooper, M.D. and B.R. Herrin, *How did our complex immune system evolve?* Nat Rev Immunol, 2010. **10**(1): p. 2-3.
2. Darwin, C., *On the origin of species*. 1859, London.
3. Janeway, C.A., Travers, P., Walport, M., *Immunobiology: The Immune System in Health and Disease*. 5 ed. 2001.
4. Mushegian, A. and R. Medzhitov, *Evolutionary perspective on innate immune recognition.* J Cell Biol, 2001. **155**(5): p. 705-10.
5. Cooper, M.D. and M.N. Alder, *The evolution of adaptive immune systems.* Cell, 2006. **124**(4): p. 815-22.
6. Janeway, C.A., Jr. and R. Medzhitov, *Innate immune recognition.* Annu Rev Immunol, 2002. **20**: p. 197-216.
7. Kumar, H., T. Kawai, and S. Akira, *Pathogen recognition by the innate immune system.* Int Rev Immunol, 2011. **30**(1): p. 16-34.
8. Takeuchi, O. and S. Akira, *Pattern recognition receptors and inflammation.* Cell, 2010. **140**(6): p. 805-20.
9. Kumar, H., T. Kawai, and S. Akira, *Pathogen recognition in the innate immune response.* Biochem J, 2009. **420**(1): p. 1-16.
10. Kawai, T. and S. Akira, *The role of pattern-recognition receptors in innate immunity: update on Toll-like receptors.* Nat Immunol, 2010. **11**(5): p. 373-84.
11. Abbas, A.A., Lichtman, A.H., Pillai, S., *Cellular and Molecular Immunology*. 6 ed. 2010.
12. Medzhitov, R., *Recognition of microorganisms and activation of the immune response.* Nature, 2007. **449**(7164): p. 819-26.
13. Litvack, M.L. and N. Palaniyar, *Review: Soluble innate immune pattern-recognition proteins for clearing dying cells and cellular components: implications on exacerbating or resolving inflammation.* Innate Immun, 2010. **16**(3): p. 191-200.
14. Ting, J.P. and B.K. Davis, *CATERPILLER: a novel gene family important in immunity, cell death, and diseases.* Annu Rev Immunol, 2005. **23**: p. 387-414.
15. Kobayashi, K.S., et al., *Nod2-dependent regulation of innate and adaptive immunity in the intestinal tract.* Science, 2005. **307**(5710): p. 731-4.
16. Inohara, et al., *NOD-LRR proteins: role in host-microbial interactions and inflammatory disease.* Annu Rev Biochem, 2005. **74**: p. 355-83.
17. Fritz, J.H., et al., *Nod1-mediated innate immune recognition of peptidoglycan contributes to the onset of adaptive immunity.* Immunity, 2007. **26**(4): p. 445-59.
18. Fritz, J.H., et al., *Nod-like proteins in immunity, inflammation and disease.* Nat Immunol, 2006. **7**(12): p. 1250-7.
19. Lanier, L.L., *NK cell recognition.* Annu Rev Immunol, 2005. **23**: p. 225-74.
20. Smith, K.M., et al., *Ly-49D and Ly-49H associate with mouse DAP12 and form activating receptors.* J Immunol, 1998. **161**(1): p. 7-10.
21. Barten, R., et al., *Divergent and convergent evolution of NK-cell receptors.* Trends Immunol, 2001. **22**(1): p. 52-7.
22. Barclay, A.N. and D. Hatherley, *The counterbalance theory for evolution and function of paired receptors.* Immunity, 2008. **29**(5): p. 675-8.
23. Pegram, H.J., et al., *Activating and inhibitory receptors of natural killer cells.* Immunol Cell Biol, 2011. **89**(2): p. 216-24.

24. Orr, M.T., W.J. Murphy, and L.L. Lanier, *'Unlicensed' natural killer cells dominate the response to cytomegalovirus infection.* Nat Immunol, 2010. **11**(4): p. 321-7.
25. Borrego, F., et al., *Recognition of human histocompatibility leukocyte antigen (HLA)-E complexed with HLA class I signal sequence-derived peptides by CD94/NKG2 confers protection from natural killer cell-mediated lysis.* J Exp Med, 1998. **187**(5): p. 813-8.
26. Lee, N., et al., *HLA-E surface expression depends on binding of TAP-dependent peptides derived from certain HLA class I signal sequences.* J Immunol, 1998. **160**(10): p. 4951-60.
27. Ito, M., et al., *Killer cell lectin-like receptor G1 binds three members of the classical cadherin family to inhibit NK cell cytotoxicity.* J Exp Med, 2006. **203**(2): p. 289-95.
28. Cowin, P., T.M. Rowlands, and S.J. Hatsell, *Cadherins and catenins in breast cancer.* Curr Opin Cell Biol, 2005. **17**(5): p. 499-508.
29. Jamieson, A.M., et al., *The role of the NKG2D immunoreceptor in immune cell activation and natural killing.* Immunity, 2002. **17**(1): p. 19-29.
30. Wu, J., et al., *An activating immunoreceptor complex formed by NKG2D and DAP10.* Science, 1999. **285**(5428): p. 730-2.
31. Lanier, L.L., *Up on the tightrope: natural killer cell activation and inhibition.* Nat Immunol, 2008. **9**(5): p. 495-502.
32. Westwood, J.A., et al., *Cutting edge: novel priming of tumor-specific immunity by NKG2D-triggered NK cell-mediated tumor rejection and Th1-independent CD4+ T cell pathway.* J Immunol, 2004. **172**(2): p. 757-61.
33. McQueen, K.L. and P. Parham, *Variable receptors controlling activation and inhibition of NK cells.* Curr Opin Immunol, 2002. **14**(5): p. 615-21.
34. Brown, M.H., et al., *2B4, the natural killer and T cell immunoglobulin superfamily surface protein, is a ligand for CD48.* J Exp Med, 1998. **188**(11): p. 2083-90.
35. Vaidya, S.V., et al., *Targeted disruption of the 2B4 gene in mice reveals an in vivo role of 2B4 (CD244) in the rejection of B16 melanoma cells.* J Immunol, 2005. **174**(2): p. 800-7.
36. Wang, J., et al., *An essential role of sialylated O-linked sugar chains in the recognition of mouse CD99 by paired Ig-like type 2 receptor (PILR).* J Immunol, 2008. **180**(3): p. 1686-93.
37. Hoebe, K., E. Janssen, and B. Beutler, *The interface between innate and adaptive immunity.* Nat Immunol, 2004. **5**(10): p. 971-4.
38. McKenna, K., A.S. Beignon, and N. Bhardwaj, *Plasmacytoid dendritic cells: linking innate and adaptive immunity.* J Virol, 2005. **79**(1): p. 17-27.
39. Steinman, R.M. and K. Inaba, *Myeloid dendritic cells.* J Leukoc Biol, 1999. **66**(2): p. 205-8.
40. Iwasaki, A. and R. Medzhitov, *Toll-like receptor control of the adaptive immune responses.* Nat Immunol, 2004. **5**(10): p. 987-95.
41. Iwasaki, A. and R. Medzhitov, *Regulation of adaptive immunity by the innate immune system.* Science, 2010. **327**(5963): p. 291-5.
42. Blander, J.M. and R. Medzhitov, *Toll-dependent selection of microbial antigens for presentation by dendritic cells.* Nature, 2006. **440**(7085): p. 808-12.
43. Takeuchi, O. and S. Akira, *Innate immunity to virus infection.* Immunol Rev, 2009. **227**(1): p. 75-86.
44. Aoshi, T., et al., *Innate and adaptive immune responses to viral infection and vaccination.* Curr Opin Virol, 2011. **1**(4): p. 226-32.
45. Schmid, D. and C. Munz, *Innate and adaptive immunity through autophagy.* Immunity, 2007. **27**(1): p. 11-21.
46. Palm, N.W. and R. Medzhitov, *Pattern recognition receptors and control of adaptive immunity.* Immunol Rev, 2009. **227**(1): p. 221-33.

47. Ganesh, K. and M.S. Neuberger, *The relationship between hypothesis and experiment in unveiling the mechanisms of antibody gene diversification.* FASEB J, 2011. **25**(4): p. 1123-32.
48. Jerne, N.K., *The Natural-Selection Theory of Antibody Formation.* Proc Natl Acad Sci U S A, 1955. **41**(11): p. 849-57.
49. Burnet, F.M., *A modification of Jerne's theory of antibody production using the concept of clonal selection.* Aust. J. Sci. , 1957(20): p. 67–69.
50. Nossal, G.J. and J. Lederberg, *Antibody production by single cells.* Nature, 1958. **181**(4620): p. 1419-20.
51. Jordan, M.A. and A.G. Baxter, *Quantitative and qualitative approaches to GOD: the first 10 years of the clonal selection theory.* Immunol Cell Biol, 2008. **86**(1): p. 72-9.
52. Talmage, D.W., *Immunological specificity, unique combinations of selected natural globulins provide an alternative to the classical concept.* Science, 1959. **129**(3364): p. 1643-8.
53. Miller, J.F., *Events that led to the discovery of T-cell development and function--a personal recollection.* Tissue Antigens, 2004. **63**(6): p. 509-17.
54. Miller, J.F. and G.F. Mitchell, *The thymus and the precursors of antigen reactive cells.* Nature, 1967. **216**(5116): p. 659-63.
55. Mitchell, G.F. and J.F. Miller, *Immunological activity of thymus and thoracic-duct lymphocytes.* Proc Natl Acad Sci U S A, 1968. **59**(1): p. 296-303.
56. Miller, J.F. and J. Sprent, *Thymus-derived cells in mouse thoracic duct lymph.* Nat New Biol, 1971. **230**(17): p. 267-70.
57. Miller, J.F. and G.F. Mitchell, *Cell to cell interaction in the immune response. I. Hemolysin-forming cells in neonatally thymectomized mice reconstituted with thymus or thoracic duct lymphocytes.* J Exp Med, 1968. **128**(4): p. 801-20.
58. Mitchell, G.F. and J.F. Miller, *Cell to cell interaction in the immune response. II. The source of hemolysin-forming cells in irradiated mice given bone marrow and thymus or thoracic duct lymphocytes.* J Exp Med, 1968. **128**(4): p. 821-37.
59. Zinkernagel, R.M. and P.C. Doherty, *Restriction of in vitro T cell-mediated cytotoxicity in lymphocytic choriomeningitis within a syngeneic or semiallogeneic system.* Nature, 1974. **248**(450): p. 701-2.
60. Weiss, A., *Discovering the TCR beta-chain by subtraction.* J Immunol, 2005. **175**(5): p. 2769-70.
61. Tonegawa, S., *Somatic generation of antibody diversity.* Nature, 1983. **302**(5909): p. 575-81.
62. Brandt, V.L. and D.B. Roth, *G.O.D.'s Holy Grail: discovery of the RAG proteins.* J Immunol, 2008. **180**(1): p. 3-4.
63. Allison, J.P., B.W. McIntyre, and D. Bloch, *Tumor-specific antigen of murine T-lymphoma defined with monoclonal antibody.* J Immunol, 1982. **129**(5): p. 2293-300.
64. Meuer, S.C., et al., *Clonotypic structures involved in antigen-specific human T cell function. Relationship to the T3 molecular complex.* J Exp Med, 1983. **157**(2): p. 705-19.
65. Haskins, K., et al., *The major histocompatibility complex-restricted antigen receptor on T cells. I. Isolation with a monoclonal antibody.* J Exp Med, 1983. **157**(4): p. 1149-69.
66. Bjorkman, P.J., et al., *The foreign antigen binding site and T cell recognition regions of class I histocompatibility antigens.* Nature, 1987. **329**(6139): p. 512-8.
67. Davis, M.M. and P.J. Bjorkman, *T-cell antigen receptor genes and T-cell recognition.* Nature, 1988. **334**(6181): p. 395-402.
68. Mak, T.W., et al., *Genes encoding the T-cell antigen receptor.* J Invest Dermatol, 1985. **85**(1 Suppl): p. 107s-109s.
69. Van Parijs, L. and A.K. Abbas, *Homeostasis and self-tolerance in the immune system: turning lymphocytes off.* Science, 1998. **280**(5361): p. 243-8.

70. Sprent, J. and C.D. Surh, *Normal T cell homeostasis: the conversion of naive cells into memory-phenotype cells.* Nat Immunol, 2011. **12**(6): p. 478-84.
71. Gorelik, L., et al., *Normal B cell homeostasis requires B cell activation factor production by radiation-resistant cells.* J Exp Med, 2003. **198**(6): p. 937-45.
72. Medzhitov, R. and C.A. Janeway, Jr., *Innate immunity: impact on the adaptive immune response.* Curr Opin Immunol, 1997. **9**(1): p. 4-9.
73. McAdam, A.J., et al., *Mouse inducible costimulatory molecule (ICOS) expression is enhanced by CD28 costimulation and regulates differentiation of CD4+ T cells.* J Immunol, 2000. **165**(9): p. 5035-40.
74. Cherukuri, A., P.C. Cheng, and S.K. Pierce, *The role of the CD19/CD21 complex in B cell processing and presentation of complement-tagged antigens.* J Immunol, 2001. **167**(1): p. 163-72.
75. Gonzalez, S.F., et al., *Complement-dependent transport of antigen into B cell follicles.* J Immunol, 2010. **185**(5): p. 2659-64.
76. Elgueta, R., et al., *Molecular mechanism and function of CD40/CD40L engagement in the immune system.* Immunol Rev, 2009. **229**(1): p. 152-72.
77. Gimmi, C.D., et al., *Human T-cell clonal anergy is induced by antigen presentation in the absence of B7 costimulation.* Proc Natl Acad Sci U S A, 1993. **90**(14): p. 6586-90.
78. Chikuma, S., et al., *PD-1-mediated suppression of IL-2 production induces CD8+ T cell anergy in vivo.* J Immunol, 2009. **182**(11): p. 6682-9.
79. Greenwald, R.J., et al., *CTLA-4 regulates induction of anergy in vivo.* Immunity, 2001. **14**(2): p. 145-55.
80. Sloan-Lancaster, J., B.D. Evavold, and P.M. Allen, *Induction of T-cell anergy by altered T-cell-receptor ligand on live antigen-presenting cells.* Nature, 1993. **363**(6425): p. 156-9.
81. Matzinger, P., *Tolerance, danger, and the extended family.* Annu Rev Immunol, 1994. **12**: p. 991-1045.
82. Goodnow, C.C., et al., *Altered immunoglobulin expression and functional silencing of self-reactive B lymphocytes in transgenic mice.* Nature, 1988. **334**(6184): p. 676-82.
83. Mueller, D.L., *Mechanisms maintaining peripheral tolerance.* Nat Immunol, 2010. **11**(1): p. 21-7.
84. Greenwald, R.J., G.J. Freeman, and A.H. Sharpe, *The B7 family revisited.* Annu Rev Immunol, 2005. **23**: p. 515-48.
85. Van Parijs, L. and A.K. Abbas, *Role of Fas-mediated cell death in the regulation of immune responses.* Curr Opin Immunol, 1996. **8**(3): p. 355-61.
86. Suda, T., et al., *Expression of the Fas ligand in cells of T cell lineage.* J Immunol, 1995. **154**(8): p. 3806-13.
87. Sadlack, B., et al., *Ulcerative colitis-like disease in mice with a disrupted interleukin-2 gene.* Cell, 1993. **75**(2): p. 253-61.
88. Willerford, D.M., et al., *Interleukin-2 receptor alpha chain regulates the size and content of the peripheral lymphoid compartment.* Immunity, 1995. **3**(4): p. 521-30.
89. Sakaguchi, S., F. Powrie, and R.M. Ransohoff, *Re-establishing immunological self-tolerance in autoimmune disease.* Nat Med, 2012. **18**(1): p. 54-8.
90. Gregersen, P.K. and T.W. Behrens, *Genetics of autoimmune diseases--disorders of immune homeostasis.* Nat Rev Genet, 2006. **7**(12): p. 917-28.
91. Ramsey, C., et al., *Aire deficient mice develop multiple features of APECED phenotype and show altered immune response.* Hum Mol Genet, 2002. **11**(4): p. 397-409.
92. Pugliese, A., et al., *The insulin gene is transcribed in the human thymus and transcription levels correlated with allelic variation at the INS VNTR-IDDM2 susceptibility locus for type 1 diabetes.* Nat Genet, 1997. **15**(3): p. 293-7.

93. Sakaguchi, N., et al., *Altered thymic T-cell selection due to a mutation of the ZAP-70 gene causes autoimmune arthritis in mice.* Nature, 2003. **426**(6965): p. 454-60.
94. Wang, H., et al., *ZAP-70: an essential kinase in T-cell signaling.* Cold Spring Harb Perspect Biol, 2010. **2**(5): p. a002279.
95. Piccirillo, C.A. and E.M. Shevach, *Naturally-occurring CD4+CD25+ immunoregulatory T cells: central players in the arena of peripheral tolerance.* Semin Immunol, 2004. **16**(2): p. 81-8.
96. Sakaguchi, S., K. Wing, and T. Yamaguchi, *Dynamics of peripheral tolerance and immune regulation mediated by Treg.* Eur J Immunol, 2009. **39**(9): p. 2331-6.
97. Thornton, A.M. and E.M. Shevach, *CD4+CD25+ immunoregulatory T cells suppress polyclonal T cell activation in vitro by inhibiting interleukin 2 production.* J Exp Med, 1998. **188**(2): p. 287-96.
98. Francisco, L.M., P.T. Sage, and A.H. Sharpe, *The PD-1 pathway in tolerance and autoimmunity.* Immunol Rev, 2010. **236**: p. 219-42.
99. Guo, F., et al., *CD28 controls differentiation of regulatory T cells from naive CD4 T cells.* J Immunol, 2008. **181**(4): p. 2285-91.
100. d'Hennezel, E., et al., *The immunogenetics of immune dysregulation, polyendocrinopathy, enteropathy, X linked (IPEX) syndrome.* J Med Genet, 2012. **49**(5): p. 291-302.
101. Khattri, R., et al., *Lymphoproliferative disorder in CTLA-4 knockout mice is characterized by CD28-regulated activation of Th2 responses.* J Immunol, 1999. **162**(10): p. 5784-91.
102. Nishimura, H., et al., *Development of lupus-like autoimmune diseases by disruption of the PD-1 gene encoding an ITIM motif-carrying immunoreceptor.* Immunity, 1999. **11**(2): p. 141-51.
103. Nishimura, H., et al., *Autoimmune dilated cardiomyopathy in PD-1 receptor-deficient mice.* Science, 2001. **291**(5502): p. 319-22.
104. Lafferty, K.J. and A.J. Cunningham, *A new analysis of allogeneic interactions.* Aust J Exp Biol Med Sci, 1975. **53**(1): p. 27-42.
105. Beyersdorf, N., et al., *Superagonistic anti-CD28 antibodies: potent activators of regulatory T cells for the therapy of autoimmune diseases.* Ann Rheum Dis, 2005. **64 Suppl 4**: p. iv91-5.
106. Chan, A.C. and P.J. Carter, *Therapeutic antibodies for autoimmunity and inflammation.* Nat Rev Immunol, 2010. **10**(5): p. 301-16.
107. Finck, B.K., P.S. Linsley, and D. Wofsy, *Treatment of murine lupus with CTLA4Ig.* Science, 1994. **265**(5176): p. 1225-7.
108. Anderson, D.E., A.H. Sharpe, and D.A. Hafler, *The B7-CD28/CTLA-4 costimulatory pathways in autoimmune disease of the central nervous system.* Curr Opin Immunol, 1999. **11**(6): p. 677-83.
109. Bachmaier, K., et al., *Induction of autoimmunity in the absence of CD28 costimulation.* J Immunol, 1996. **157**(4): p. 1752-7.
110. Tada, Y., et al., *CD28-deficient mice are highly resistant to collagen-induced arthritis.* J Immunol, 1999. **162**(1): p. 203-8.
111. Peterson, K.E., et al., *B7.2 has opposing roles during the activation versus effector stages of experimental autoimmune thyroiditis.* J Immunol, 1999. **162**(3): p. 1859-67.
112. Shi, F.D., et al., *Differential requirements for CD28 and CD40 ligand in the induction of experimental autoimmune myasthenia gravis.* Eur J Immunol, 1998. **28**(11): p. 3587-93.
113. Girvin, A.M., et al., *A critical role for B7/CD28 costimulation in experimental autoimmune encephalomyelitis: a comparative study using costimulatory molecule-deficient mice and monoclonal antibody blockade.* J Immunol, 2000. **164**(1): p. 136-43.
114. Salomon, B. and J.A. Bluestone, *Complexities of CD28/B7: CTLA-4 costimulatory pathways in autoimmunity and transplantation.* Annu Rev Immunol, 2001. **19**: p. 225-52.
115. Stuart, R.W. and M.K. Racke, *Targeting T cell costimulation in autoimmune disease.* Expert Opin Ther Targets, 2002. **6**(3): p. 275-89.

116. Perrin, P.J., et al., *Differential requirements of naive and memory T cells for CD28 costimulation in autoimmune pathogenesis.* Histol Histopathol, 1999. **14**(4): p. 1269-76.
117. Beyersdorf, N., et al., *CD28 superagonists put a break on autoimmunity by preferentially activating CD4+CD25+ regulatory T cells.* Autoimmun Rev, 2006. **5**(1): p. 40-5.
118. Hunig, T., *The storm has cleared: lessons from the CD28 superagonist TGN1412 trial.* Nat Rev Immunol, 2012. **12**(5): p. 317-8.
119. Eastwood, D., et al., *Monoclonal antibody TGN1412 trial failure explained by species differences in CD28 expression on CD4+ effector memory T-cells.* Br J Pharmacol, 2010. **161**(3): p. 512-26.
120. Miller, S.D., et al., *Blockade of CD28/B7-1 interaction prevents epitope spreading and clinical relapses of murine EAE.* Immunity, 1995. **3**(6): p. 739-45.
121. Vanderlugt, C.L., et al., *Treatment with intact anti-B7-1 mAb during disease remission enhances epitope spreading and exacerbates relapses in R-EAE.* J Neuroimmunol, 1997. **79**(2): p. 113-8.
122. Orabona, C., et al., *CD28 induces immunostimulatory signals in dendritic cells via CD80 and CD86.* Nat Immunol, 2004. **5**(11): p. 1134-42.
123. Grohmann, U., et al., *CTLA-4-Ig regulates tryptophan catabolism in vivo.* Nat Immunol, 2002. **3**(11): p. 1097-101.
124. Lenschow, D.J., et al., *Differential effects of anti-B7-1 and anti-B7-2 monoclonal antibody treatment on the development of diabetes in the nonobese diabetic mouse*. J Exp Med, 1995. **181**(3): p. 1145-55.
125. Butte, M.J., et al., *Interaction of human PD-L1 and B7-1.* Mol Immunol, 2008. **45**(13): p. 3567-72.
126. Riley, J.L. and C.H. June, *The CD28 family: a T-cell rheostat for therapeutic control of T-cell activation.* Blood, 2005. **105**(1): p. 13-21.
127. Alegre, M.L. and F. Fallarino, *Mechanisms of CTLA-4-Ig in tolerance induction.* Curr Pharm Des, 2006. **12**(2): p. 149-60.
128. Riella, L.V., et al., *Deleterious effect of CTLA4-Ig on a Treg-dependent transplant model.* Am J Transplant, 2012. **12**(4): p. 846-55.
129. Tang, A.L., et al., *CTLA4 expression is an indicator and regulator of steady-state CD4+ FoxP3+ T cell homeostasis.* J Immunol, 2008. **181**(3): p. 1806-13.
130. Alvarez-Quiroga, C., et al., *CTLA-4-Ig therapy diminishes the frequency but enhances the function of Treg cells in patients with rheumatoid arthritis.* J Clin Immunol, 2011. **31**(4): p. 588-95.
131. Ko, H.J., et al., *CTLA4-Ig modifies dendritic cells from mice with collagen-induced arthritis to increase the CD4+CD25+Foxp3+ regulatory T cell population.* J Autoimmun, 2010. **34**(2): p. 111-20.
132. van Gelder, M., E.P. Kinwel-Bohre, and D.W. van Bekkum, *Treatment of experimental allergic encephalomyelitis in rats with total body irradiation and syngeneic BMT.* Bone Marrow Transplant, 1993. **11**(3): p. 233-41.
133. Cross, A.H., et al., *Long-term inhibition of murine experimental autoimmune encephalomyelitis using CTLA-4-Fc supports a key role for CD28 costimulation.* J Clin Invest, 1995. **95**(6): p. 2783-9.
134. Wallace, P.M., et al., *CTLA4Ig treatment ameliorates the lethality of murine graft-versus-host disease across major histocompatibility complex barriers.* Transplantation, 1994. **58**(5): p. 602-10.
135. Zimmerman, R., et al., *Advances in the treatment of lupus nephritis.* Annu Rev Med, 2001. **52**: p. 63-78.
136. Racke, M.K., et al., *Distinct roles for B7-1 (CD-80) and B7-2 (CD-86) in the initiation of experimental allergic encephalomyelitis.* J Clin Invest, 1995. **96**(5): p. 2195-203.
137. Martin Mola, E., et al., *Abatacept use in rheumatoid arthritis: Evidence review and recommendations.* Reumatol Clin, 2012.

138. Pilat, N., M.H. Sayegh, and T. Wekerle, *Costimulatory pathways in transplantation.* Semin Immunol, 2011. **23**(4): p. 293-303.
139. Hwang, K.W., et al., *Cutting edge: targeted ligation of CTLA-4 in vivo by membrane-bound anti-CTLA-4 antibody prevents rejection of allogeneic cells.* J Immunol, 2002. **169**(2): p. 633-7.
140. Fife, B.T., et al., *Inhibition of T cell activation and autoimmune diabetes using a B cell surface-linked CTLA-4 agonist.* J Clin Invest, 2006. **116**(8): p. 2252-61.
141. Walunas, T.L., et al., *CTLA-4 can function as a negative regulator of T cell activation.* Immunity, 1994. **1**(5): p. 405-13.
142. Hutloff, A., et al., *ICOS is an inducible T-cell co-stimulator structurally and functionally related to CD28.* Nature, 1999. **397**(6716): p. 263-6.
143. Grimbacher, B., et al., *Homozygous loss of ICOS is associated with adult-onset common variable immunodeficiency.* Nat Immunol, 2003. **4**(3): p. 261-8.
144. Bossaller, L., et al., *ICOS deficiency is associated with a severe reduction of CXCR5+CD4 germinal center Th cells.* J Immunol, 2006. **177**(7): p. 4927-32.
145. Moore, T.V., et al., *Protective effector memory CD4 T cells depend on ICOS for survival.* PLoS One, 2011. **6**(2): p. e16529.
146. Tajima, N., et al., *JTA-009, a fully human antibody against human AILIM/ICOS, ameliorates graft-vs-host reaction in SCID mice grafted with human PBMCs.* Exp Hematol, 2008. **36**(11): p. 1514-23.
147. Mollweide, A., et al., *Only therapeutic ICOS:ICOSL blockade alleviates acute graft versus host disease.* Klin Padiatr, 2009. **221**(6): p. 344-50.
148. Hu, Y.L., et al., *B7RP-1 blockade ameliorates autoimmunity through regulation of follicular helper T cells.* J Immunol, 2009. **182**(3): p. 1421-8.
149. Carlesso, G. *Depletion of Inducible Co-Stimulator (ICOS) Bearing T Cells Inhibits Expansion of T Follicular Helper Cells (TFH) and Prevents Disease in a Graft Versus Host Mouse Model of Scleroderma*. in *ACR/ARHP Annual Scientific Meeting*. 2009. Philedelphia: Arthritis Rheum.
150. Okazaki, T. and T. Honjo, *PD-1 and PD-1 ligands: from discovery to clinical application.* Int Immunol, 2007. **19**(7): p. 813-24.
151. Hirata, S., et al., *Prevention of experimental autoimmune encephalomyelitis by transfer of embryonic stem cell-derived dendritic cells expressing myelin oligodendrocyte glycoprotein peptide along with TRAIL or programmed death-1 ligand.* J Immunol, 2005. **174**(4): p. 1888-97.
152. Jin, H.T., Ahmed, R., Okazaki, T., *Role of PD-1 in regulating T cell immunity*, in *Negative Co-Receptors and Ligands*, R. Ahmed, Honjo, T., Editor. 2011.
153. Chapoval, A.I., et al., *B7-H3: a costimulatory molecule for T cell activation and IFN-gamma production.* Nat Immunol, 2001. **2**(3): p. 269-74.
154. Suh, W.K., et al., *The B7 family member B7-H3 preferentially down-regulates T helper type 1-mediated immune responses.* Nat Immunol, 2003. **4**(9): p. 899-906.
155. Prasad, D.V., et al., *Murine B7-H3 is a negative regulator of T cells.* J Immunol, 2004. **173**(4): p. 2500-6.
156. Wang, L., et al., *B7-H3 promotes acute and chronic allograft rejection.* Eur J Immunol, 2005. **35**(2): p. 428-38.
157. McGrath, M.M. and N. Najafian, *The role of coinhibitory signaling pathways in transplantation and tolerance.* Front Immunol, 2012. **3**: p. 47.
158. Prasad, D.V., et al., *B7S1, a novel B7 family member that negatively regulates T cell activation.* Immunity, 2003. **18**(6): p. 863-73.
159. Sica, G.L., et al., *B7-H4, a molecule of the B7 family, negatively regulates T cell immunity.* Immunity, 2003. **18**(6): p. 849-61.

160. Kryczek, I., et al., *Cutting edge: induction of B7-H4 on APCs through IL-10: novel suppressive mode for regulatory T cells.* J Immunol, 2006. **177**(1): p. 40-4.
161. Wang, X., et al., *Early treatment of NOD mice with B7-H4 reduces the incidence of autoimmune diabetes.* Diabetes, 2011. **60**(12): p. 3246-55.
162. Gonzalez, L.C., et al., *A coreceptor interaction between the CD28 and TNF receptor family members B and T lymphocyte attenuator and herpesvirus entry mediator.* Proc Natl Acad Sci U S A, 2005. **102**(4): p. 1116-21.
163. Cai, G., et al., *CD160 inhibits activation of human CD4+ T cells through interaction with herpesvirus entry mediator.* Nat Immunol, 2008. **9**(2): p. 176-85.
164. Murphy, T.L. and K.M. Murphy, *Slow down and survive: Enigmatic immunoregulation by BTLA and HVEM.* Annu Rev Immunol, 2010. **28**: p. 389-411.
165. Mauri, D.N., et al., *LIGHT, a new member of the TNF superfamily, and lymphotoxin alpha are ligands for herpesvirus entry mediator.* Immunity, 1998. **8**(1): p. 21-30.
166. Oya, Y., et al., *Development of autoimmune hepatitis-like disease and production of autoantibodies to nuclear antigens in mice lacking B and T lymphocyte attenuator.* Arthritis Rheum, 2008. **58**(8): p. 2498-510.
167. Deppong, C., et al., *Cutting edge: B and T lymphocyte attenuator and programmed death receptor-1 inhibitory receptors are required for termination of acute allergic airway inflammation.* J Immunol, 2006. **176**(7): p. 3909-13.
168. Steinberg, M.W., et al., *A crucial role for HVEM and BTLA in preventing intestinal inflammation.* J Exp Med, 2008. **205**(6): p. 1463-76.
169. Lin, S.C., C.C. Kuo, and C.H. Chan, *Association of a BTLA gene polymorphism with the risk of rheumatoid arthritis.* J Biomed Sci, 2006. **13**(6): p. 853-60.
170. Cheung, T.C., et al., *Unconventional ligand activation of herpesvirus entry mediator signals cell survival.* Proc Natl Acad Sci U S A, 2009. **106**(15): p. 6244-9.
171. Albring, J.C., et al., *Targeting of B and T lymphocyte associated (BTLA) prevents graft-versus-host disease without global immunosuppression.* J Exp Med, 2010. **207**(12): p. 2551-9.
172. Tacke, M., et al., *CD28-mediated induction of proliferation in resting T cells in vitro and in vivo without engagement of the T cell receptor: evidence for functionally distinct forms of CD28.* Eur J Immunol, 1997. **27**(1): p. 239-47.
173. Luhder, F., et al., *Topological requirements and signaling properties of T cell-activating, anti-CD28 antibody superagonists.* J Exp Med, 2003. **197**(8): p. 955-66.
174. Evans, E.J., et al., *Crystal structure of a soluble CD28-Fab complex.* Nat Immunol, 2005. **6**(3): p. 271-9.
175. Davis, S.J. and P.A. van der Merwe, *The kinetic-segregation model: TCR triggering and beyond.* Nat Immunol, 2006. **7**(8): p. 803-9.
176. Ishida, Y., et al., *Induced expression of PD-1, a novel member of the immunoglobulin gene superfamily, upon programmed cell death.* EMBO J, 1992. **11**(11): p. 3887-95.
177. Freeman, G.J., et al., *Engagement of the PD-1 immunoinhibitory receptor by a novel B7 family member leads to negative regulation of lymphocyte activation.* J Exp Med, 2000. **192**(7): p. 1027-34.
178. Latchman, Y., et al., *PD-L2 is a second ligand for PD-1 and inhibits T cell activation.* Nat Immunol, 2001. **2**(3): p. 261-8.
179. Zhang, X., et al., *Structural and functional analysis of the costimulatory receptor programmed death-1.* Immunity, 2004. **20**(3): p. 337-47.
180. Long, E.O., *Regulation of immune responses through inhibitory receptors.* Annu Rev Immunol, 1999. **17**: p. 875-904.

181. Sidorenko, S.P. and E.A. Clark, *The dual-function CD150 receptor subfamily: the viral attraction.* Nat Immunol, 2003. **4**(1): p. 19-24.
182. Lazar-Molnar, E., et al., *Crystal structure of the complex between programmed death-1 (PD-1) and its ligand PD-L2.* Proc Natl Acad Sci U S A, 2008. **105**(30): p. 10483-8.
183. Okazaki, T., et al., *PD-1 immunoreceptor inhibits B cell receptor-mediated signaling by recruiting src homology 2-domain-containing tyrosine phosphatase 2 to phosphotyrosine.* Proc Natl Acad Sci U S A, 2001. **98**(24): p. 13866-71.
184. Sheppard, K.A., et al., *PD-1 inhibits T-cell receptor induced phosphorylation of the ZAP70/CD3zeta signalosome and downstream signaling to PKCtheta.* FEBS Lett, 2004. **574**(1-3): p. 37-41.
185. Yokosuka, T., et al., *Programmed cell death 1 forms negative costimulatory microclusters that directly inhibit T cell receptor signaling by recruiting phosphatase SHP2.* J Exp Med, 2012. **209**(6): p. 1201-17.
186. Parry, R.V., et al., *CTLA-4 and PD-1 receptors inhibit T-cell activation by distinct mechanisms.* Mol Cell Biol, 2005. **25**(21): p. 9543-53.
187. Chuang, E., et al., *The CD28 and CTLA-4 receptors associate with the serine/threonine phosphatase PP2A.* Immunity, 2000. **13**(3): p. 313-22.
188. Rudd, C.E. and H. Schneider, *Unifying concepts in CD28, ICOS and CTLA4 co-receptor signalling.* Nat Rev Immunol, 2003. **3**(7): p. 544-56.
189. Yokosuka, T., et al., *Spatiotemporal basis of CTLA-4 costimulatory molecule-mediated negative regulation of T cell activation.* Immunity, 2010. **33**(3): p. 326-39.
190. Yokosuka, T. and T. Saito, *The immunological synapse, TCR microclusters, and T cell activation.* Curr Top Microbiol Immunol, 2010. **340**: p. 81-107.
191. Qureshi, O.S., et al., *Trans-endocytosis of CD80 and CD86: a molecular basis for the cell-extrinsic function of CTLA-4.* Science, 2011. **332**(6029): p. 600-3.
192. Francisco, L.M., et al., *PD-L1 regulates the development, maintenance, and function of induced regulatory T cells.* J Exp Med, 2009. **206**(13): p. 3015-29.
193. Bishop, K.D., et al., *Depletion of the programmed death-1 receptor completely reverses established clonal anergy in CD4(+) T lymphocytes via an interleukin-2-dependent mechanism.* Cell Immunol, 2009. **256**(1-2): p. 86-91.
194. Kuipers, H., et al., *Contribution of the PD-1 ligands/PD-1 signaling pathway to dendritic cell-mediated CD4+ T cell activation.* Eur J Immunol, 2006. **36**(9): p. 2472-82.
195. Butte, M.J., et al., *Programmed death-1 ligand 1 interacts specifically with the B7-1 costimulatory molecule to inhibit T cell responses.* Immunity, 2007. **27**(1): p. 111-22.
196. Nishimura, H., T. Honjo, and N. Minato, *Facilitation of beta selection and modification of positive selection in the thymus of PD-1-deficient mice.* J Exp Med, 2000. **191**(5): p. 891-8.
197. Blank, C., et al., *Absence of programmed death receptor 1 alters thymic development and enhances generation of CD4/CD8 double-negative TCR-transgenic T cells.* J Immunol, 2003. **171**(9): p. 4574-81.
198. Raimondi, G., et al., *Regulated compartmentalization of programmed cell death-1 discriminates CD4+CD25+ resting regulatory T cells from activated T cells.* J Immunol, 2006. **176**(5): p. 2808-16.
199. Yu, D. and C.G. Vinuesa, *The elusive identity of T follicular helper cells.* Trends Immunol, 2010. **31**(10): p. 377-83.
200. Good-Jacobson, K.L., et al., *PD-1 regulates germinal center B cell survival and the formation and affinity of long-lived plasma cells.* Nat Immunol, 2010. **11**(6): p. 535-42.
201. Keir, M.E., et al., *PD-1 and its ligands in tolerance and immunity.* Annu Rev Immunol, 2008. **26**: p. 677-704.

202. Pittet, C.L., et al., *The majority of infiltrating CD8 T lymphocytes in multiple sclerosis lesions is insensitive to enhanced PD-L1 levels on CNS cells.* Glia, 2011. **59**(5): p. 841-56.
203. Zhong, X., et al., *PD-L2 expression extends beyond dendritic cells/macrophages to B1 cells enriched for V(H)11/V(H)12 and phosphatidylcholine binding.* Eur J Immunol, 2007. **37**(9): p. 2405-10.
204. Messal, N., et al., *PD-L2 is expressed on activated human T cells and regulates their function.* Mol Immunol, 2011. **48**(15-16): p. 2214-9.
205. Lesterhuis, W.J., H. Steer, and R.A. Lake, *PD-L2 is predominantly expressed by Th2 cells.* Mol Immunol, 2011. **49**(1-2): p. 1-3.
206. Keir, M.E., et al., *Programmed death-1 (PD-1):PD-ligand 1 interactions inhibit TCR-mediated positive selection of thymocytes.* J Immunol, 2005. **175**(11): p. 7372-9.
207. Oestreich, K.J., et al., *NFATc1 regulates PD-1 expression upon T cell activation.* J Immunol, 2008. **181**(7): p. 4832-9.
208. Cho, H.Y., et al., *Interferon-sensitive response element (ISRE) is mainly responsible for IFN-alpha-induced upregulation of programmed death-1 (PD-1) in macrophages.* Biochim Biophys Acta, 2008. **1779**(12): p. 811-9.
209. Wherry, E.J. and R. Ahmed, *Memory CD8 T-cell differentiation during viral infection.* J Virol, 2004. **78**(11): p. 5535-45.
210. Barber, D.L., et al., *Restoring function in exhausted CD8 T cells during chronic viral infection.* Nature, 2006. **439**(7077): p. 682-7.
211. Velu, V., et al., *Enhancing SIV-specific immunity in vivo by PD-1 blockade.* Nature, 2009. **458**(7235): p. 206-10.
212. Day, C.L., et al., *PD-1 expression on HIV-specific T cells is associated with T-cell exhaustion and disease progression.* Nature, 2006. **443**(7109): p. 350-4.
213. Boettler, T., et al., *Expression of the interleukin-7 receptor alpha chain (CD127) on virus-specific CD8+ T cells identifies functionally and phenotypically defined memory T cells during acute resolving hepatitis B virus infection.* J Virol, 2006. **80**(7): p. 3532-40.
214. Urbani, S., et al., *PD-1 expression in acute hepatitis C virus (HCV) infection is associated with HCV-specific CD8 exhaustion.* J Virol, 2006. **80**(22): p. 11398-403.
215. Streeck, H., et al., *Antigen load and viral sequence diversification determine the functional profile of HIV-1-specific CD8+ T cells.* PLoS Med, 2008. **5**(5): p. e100.
216. Muthumani, K., et al., *Human immunodeficiency virus type 1 Nef induces programmed death 1 expression through a p38 mitogen-activated protein kinase-dependent mechanism.* J Virol, 2008. **82**(23): p. 11536-44.
217. Yao, Z.Q., et al., *T cell dysfunction by hepatitis C virus core protein involves PD-1/PDL-1 signaling.* Viral Immunol, 2007. **20**(2): p. 276-87.
218. Ha, S.J., et al., *Enhancing therapeutic vaccination by blocking PD-1-mediated inhibitory signals during chronic infection.* J Exp Med, 2008. **205**(3): p. 543-55.
219. Porichis, F., et al., *Responsiveness of HIV-specific CD4 T cells to PD-1 blockade.* Blood, 2011. **118**(4): p. 965-74.
220. Macatangay, B.J. and C.R. Rinaldo, *PD-1 blockade: A promising immunotherapy for HIV?* Cellscience, 2009. **5**(4): p. 61-65.
221. Raziorrouh, B., et al., *The immunoregulatory role of CD244 in chronic hepatitis B infection and its inhibitory potential on virus-specific CD8+ T-cell function.* Hepatology, 2010. **52**(6): p. 1934-47.
222. Jin, H.T., et al., *Cooperation of Tim-3 and PD-1 in CD8 T-cell exhaustion during chronic viral infection.* Proc Natl Acad Sci U S A, 2010. **107**(33): p. 14733-8.
223. Blackburn, S.D., et al., *Coregulation of CD8+ T cell exhaustion by multiple inhibitory receptors during chronic viral infection.* Nat Immunol, 2009. **10**(1): p. 29-37.

224. Ahmadzadeh, M., et al., *Tumor antigen-specific CD8 T cells infiltrating the tumor express high levels of PD-1 and are functionally impaired.* Blood, 2009. **114**(8): p. 1537-44.
225. Curiel, T.J., et al., *Blockade of B7-H1 improves myeloid dendritic cell-mediated antitumor immunity.* Nat Med, 2003. **9**(5): p. 562-7.
226. Iwai, Y., et al., *Involvement of PD-L1 on tumor cells in the escape from host immune system and tumor immunotherapy by PD-L1 blockade.* Proc Natl Acad Sci U S A, 2002. **99**(19): p. 12293-7.
227. Blank, C., et al., *PD-L1/B7H-1 inhibits the effector phase of tumor rejection by T cell receptor (TCR) transgenic CD8+ T cells.* Cancer Res, 2004. **64**(3): p. 1140-5.
228. Iwai, Y., S. Terawaki, and T. Honjo, *PD-1 blockade inhibits hematogenous spread of poorly immunogenic tumor cells by enhanced recruitment of effector T cells.* Int Immunol, 2005. **17**(2): p. 133-44.
229. He, Y.F., et al., *Blocking programmed death-1 ligand-PD-1 interactions by local gene therapy results in enhancement of antitumor effect of secondary lymphoid tissue chemokine.* J Immunol, 2004. **173**(8): p. 4919-28.
230. Terawaki, S., et al., *Specific and high-affinity binding of tetramerized PD-L1 extracellular domain to PD-1-expressing cells: possible application to enhance T cell function.* Int Immunol, 2007. **19**(7): p. 881-90.
231. Borkner, L., et al., *RNA interference targeting programmed death receptor-1 improves immune functions of tumor-specific T cells.* Cancer Immunol Immunother, 2010. **59**(8): p. 1173-83.
232. Garber, K., *Beyond ipilimumab: new approaches target the immunological synapse.* J Natl Cancer Inst, 2011. **103**(14): p. 1079-82.
233. Liang, S.C., et al., *Regulation of PD-1, PD-L1, and PD-L2 expression during normal and autoimmune responses.* Eur J Immunol, 2003. **33**(10): p. 2706-16.
234. Ansari, M.J., et al., *The programmed death-1 (PD-1) pathway regulates autoimmune diabetes in nonobese diabetic (NOD) mice*. J Exp Med, 2003. **198**(1): p. 63-9.
235. Cheng, X., et al., *The PD-1/PD-L pathway is up-regulated during IL-12-induced suppression of EAE mediated by IFN-gamma.* J Neuroimmunol, 2007. **185**(1-2): p. 75-86.
236. Schreiner, B., et al., *PD-1 ligands expressed on myeloid-derived APC in the CNS regulate T-cell responses in EAE.* Eur J Immunol, 2008. **38**(10): p. 2706-17.
237. Magnus, T., et al., *Microglial expression of the B7 family member B7 homolog 1 confers strong immune inhibition: implications for immune responses and autoimmunity in the CNS.* J Neurosci, 2005. **25**(10): p. 2537-46.
238. Salama, A.D., et al., *Critical role of the programmed death-1 (PD-1) pathway in regulation of experimental autoimmune encephalomyelitis.* J Exp Med, 2003. **198**(1): p. 71-8.
239. Zhu, B., et al., *Differential role of programmed death-ligand 1 [corrected] and programmed death-ligand 2 [corrected] in regulating the susceptibility and chronic progression of experimental autoimmune encephalomyelitis.* J Immunol, 2006. **176**(6): p. 3480-9.
240. Latchman, Y.E., et al., *PD-L1-deficient mice show that PD-L1 on T cells, antigen-presenting cells, and host tissues negatively regulates T cells.* Proc Natl Acad Sci U S A, 2004. **101**(29): p. 10691-6.
241. Linthicum, D.S., J.J. Munoz, and A. Blaskett, *Acute experimental autoimmune encephalomyelitis in mice. I. Adjuvant action of Bordetella pertussis is due to vasoactive amine sensitization and increased vascular permeability of the central nervous system.* Cell Immunol, 1982. **73**(2): p. 299-310.
242. Bruckener, K.E., et al., *Permeabilization in a cerebral endothelial barrier model by pertussis toxin involves the PKC effector pathway and is abolished by elevated levels of cAMP.* J Cell Sci, 2003. **116**(Pt 9): p. 1837-46.
243. Cassan, C., et al., *Pertussis toxin reduces the number of splenic Foxp3+ regulatory T cells.* J Immunol, 2006. **177**(3): p. 1552-60.

244. Chen, X., et al., *Pertussis toxin as an adjuvant suppresses the number and function of CD4+CD25+ T regulatory cells.* Eur J Immunol, 2006. **36**(3): p. 671-80.
245. Wang, C., et al., *Down-modulation of programmed death 1 alters regulatory T cells and promotes experimental autoimmune encephalomyelitis.* J Neurosci Res, 2010. **88**(1): p. 7-15.
246. Weber, M.S., et al., *Repetitive pertussis toxin promotes development of regulatory T cells and prevents central nervous system autoimmune disease.* PLoS One, 2010. **5**(12): p. e16009.
247. Liu, Y., et al., *Neuron-mediated generation of regulatory T cells from encephalitogenic T cells suppresses EAE.* Nat Med, 2006. **12**(5): p. 518-25.
248. Chen, L., et al., *Constitutive neuronal expression of the immune regulator, programmed death 1 (PD-1), identified during experimental autoimmune uveitis.* Ocul Immunol Inflamm, 2009. **17**(1): p. 47-55.
249. Totsuka, T., et al., *Regulation of murine chronic colitis by CD4+CD25- programmed death-1+ T cells.* Eur J Immunol, 2005. **35**(6): p. 1773-85.
250. Totsuka, T., et al., *Immunosenescent colitogenic CD4(+) T cells convert to regulatory cells and suppress colitis.* Eur J Immunol, 2008. **38**(5): p. 1275-86.
251. Wang, G., et al., *The effects of PDL-Ig on collagen-induced arthritis.* Rheumatol Int, 2011. **31**(4): p. 513-9.
252. Prokunina, L., et al., *A regulatory polymorphism in PDCD1 is associated with susceptibility to systemic lupus erythematosus in humans.* Nat Genet, 2002. **32**(4): p. 666-9.
253. Nielsen, C., et al., *Association of a putative regulatory polymorphism in the PD-1 gene with susceptibility to type 1 diabetes.* Tissue Antigens, 2003. **62**(6): p. 492-7.
254. Lee, S.H., et al., *Association of the programmed cell death 1 (PDCD1) gene polymorphism with ankylosing spondylitis in the Korean population.* Arthritis Res Ther, 2006. **8**(6): p. R163.
255. Lin, S.C., et al., *Association of a programmed death 1 gene polymorphism with the development of rheumatoid arthritis, but not systemic lupus erythematosus.* Arthritis Rheum, 2004. **50**(3): p. 770-5.
256. Wang, S.C., et al., *Ligands for programmed cell death 1 gene in patients with systemic lupus erythematosus.* J Rheumatol, 2007. **34**(4): p. 721-5.
257. Hayashi, M., et al., *Association of an A/C single nucleotide polymorphism in programmed cell death-ligand 1 gene with Graves' disease in Japanese patients.* Eur J Endocrinol, 2008. **158**(6): p. 817-22.
258. Sandner, S.E., et al., *Role of the programmed death-1 pathway in regulation of alloimmune responses in vivo.* J Immunol, 2005. **174**(6): p. 3408-15.
259. Tao, R., et al., *Differential effects of B and T lymphocyte attenuator and programmed death-1 on acceptance of partially versus fully MHC-mismatched cardiac allografts.* J Immunol, 2005. **175**(9): p. 5774-82.
260. Ozkaynak, E., et al., *Programmed death-1 targeting can promote allograft survival.* J Immunol, 2002. **169**(11): p. 6546-53.
261. Habicht, A., et al., *Striking dichotomy of PD-L1 and PD-L2 pathways in regulating alloreactive CD4(+) and CD8(+) T cells in vivo.* Am J Transplant, 2007. **7**(12): p. 2683-92.
262. Tanaka, K., et al., *PDL1 is required for peripheral transplantation tolerance and protection from chronic allograft rejection.* J Immunol, 2007. **179**(8): p. 5204-10.
263. Ito, T., et al., *Analysis of the role of negative T cell costimulatory pathways in CD4 and CD8 T cell-mediated alloimmune responses in vivo.* J Immunol, 2005. **174**(11): p. 6648-56.
264. Koga, N., et al., *Blockade of the interaction between PD-1 and PD-L1 accelerates graft arterial disease in cardiac allografts.* Arterioscler Thromb Vasc Biol, 2004. **24**(11): p. 2057-62.

265. Kitazawa, Y., et al., *Involvement of the programmed death-1/programmed death-1 ligand pathway in CD4+CD25+ regulatory T-cell activity to suppress alloimmune responses.* Transplantation, 2007. **83**(6): p. 774-82.
266. Blazar, B.R., et al., *Blockade of programmed death-1 engagement accelerates graft-versus-host disease lethality by an IFN-gamma-dependent mechanism.* J Immunol, 2003. **171**(3): p. 1272-7.
267. Yang, J., et al., *The novel costimulatory programmed death ligand 1/B7.1 pathway is functional in inhibiting alloimmune responses in vivo.* J Immunol, 2011. **187**(3): p. 1113-9.
268. Ullrich, A. and J. Schlessinger, *Signal transduction by receptors with tyrosine kinase activity.* Cell, 1990. **61**(2): p. 203-12.
269. van der Merwe, P.A. and O. Dushek, *Mechanisms for T cell receptor triggering.* Nat Rev Immunol, 2011. **11**(1): p. 47-55.
270. Sykulev, Y., et al., *Evidence that a single peptide-MHC complex on a target cell can elicit a cytolytic T cell response.* Immunity, 1996. **4**(6): p. 565-71.
271. Palmer, E. and D. Naeher, *Affinity threshold for thymic selection through a T-cell receptor-co-receptor zipper.* Nat Rev Immunol, 2009. **9**(3): p. 207-13.
272. Madrenas, J., R.H. Schwartz, and R.N. Germain, *Interleukin 2 production, not the pattern of early T-cell antigen receptor-dependent tyrosine phosphorylation, controls anergy induction by both agonists and partial agonists.* Proc Natl Acad Sci U S A, 1996. **93**(18): p. 9736-41.
273. Morris, G.P. and P.M. Allen, *How the TCR balances sensitivity and specificity for the recognition of self and pathogens.* Nat Immunol, 2012. **13**(2): p. 121-8.
274. Arstila, T.P., et al., *A direct estimate of the human alphabeta T cell receptor diversity.* Science, 1999. **286**(5441): p. 958-61.
275. Casrouge, A., et al., *Size estimate of the alpha beta TCR repertoire of naive mouse splenocytes.* J Immunol, 2000. **164**(11): p. 5782-7.
276. Ratcliffe, M.J., et al., *T cell receptor aggregation, but not dimerization, induces increased cytosolic calcium concentrations and reveals a lack of stable association between CD4 and the T cell receptor.* J Immunol, 1992. **148**(6): p. 1643-51.
277. Abastado, J.P., et al., *Dimerization of soluble major histocompatibility complex-peptide complexes is sufficient for activation of T cell hybridoma and induction of unresponsiveness.* J Exp Med, 1995. **182**(2): p. 439-47.
278. Cooper, J.A. and H. Qian, *A mechanism for SRC kinase-dependent signaling by noncatalytic receptors.* Biochemistry, 2008. **47**(21): p. 5681-8.
279. Delon, J., et al., *CD8 expression allows T cell signaling by monomeric peptide-MHC complexes.* Immunity, 1998. **9**(4): p. 467-73.
280. Salter, R.D., et al., *A binding site for the T-cell co-receptor CD8 on the alpha 3 domain of HLA-A2.* Nature, 1990. **345**(6270): p. 41-6.
281. Jameson, S.C. and M.J. Bevan, *T cell receptor antagonists and partial agonists.* Immunity, 1995. **2**(1): p. 1-11.
282. Locksley, R.M., et al., *Helper T cells without CD4: control of leishmaniasis in CD4-deficient mice.* Science, 1993. **261**(5127): p. 1448-51.
283. O'Rourke, A.M., J. Rogers, and M.F. Mescher, *Activated CD8 binding to class I protein mediated by the T-cell receptor results in signalling.* Nature, 1990. **346**(6280): p. 187-9.
284. Mittler, R.S., et al., *T-cell receptor-CD4 physical association in a murine T-cell hybridoma: induction by antigen receptor ligation.* Proc Natl Acad Sci U S A, 1989. **86**(21): p. 8531-5.
285. Davis, S.J., et al., *The nature of molecular recognition by T cells.* Nat Immunol, 2003. **4**(3): p. 217-24.
286. Davis, S.J. and P.A. van der Merwe, *TCR triggering: co-receptor-dependent or -independent?* Trends Immunol, 2003. **24**(12): p. 624-6; author reply 626-7.

287. Irvine, D.J., et al., *Direct observation of ligand recognition by T cells.* Nature, 2002. **419**(6909): p. 845-9.
288. Krogsgaard, M., et al., *Agonist/endogenous peptide-MHC heterodimers drive T cell activation and sensitivity.* Nature, 2005. **434**(7030): p. 238-43.
289. James, J.R., et al., *The T cell receptor triggering apparatus is composed of monovalent or monomeric proteins.* J Biol Chem, 2011. **286**(37): p. 31993-2001.
290. Varma, R., et al., *T cell receptor-proximal signals are sustained in peripheral microclusters and terminated in the central supramolecular activation cluster.* Immunity, 2006. **25**(1): p. 117-27.
291. James, J.R. and R.D. Vale, *Biophysical mechanism of T-cell receptor triggering in a reconstituted system.* Nature, 2012. **487**(7405): p. 64-9.
292. Kjer-Nielsen, L., et al., *A structural basis for the selection of dominant alphabeta T cell receptors in antiviral immunity.* Immunity, 2003. **18**(1): p. 53-64.
293. Beddoe, T., et al., *Antigen ligation triggers a conformational change within the constant domain of the alphabeta T cell receptor.* Immunity, 2009. **30**(6): p. 777-88.
294. Call, M.E. and K.W. Wucherpfennig, *The T cell receptor: critical role of the membrane environment in receptor assembly and function.* Annu Rev Immunol, 2005. **23**: p. 101-25.
295. Kuhns, M.S., M.M. Davis, and K.C. Garcia, *Deconstructing the form and function of the TCR/CD3 complex.* Immunity, 2006. **24**(2): p. 133-9.
296. Kuhns, M.S., et al., *Evidence for a functional sidedness to the alphabetaTCR.* Proc Natl Acad Sci U S A, 2010. **107**(11): p. 5094-9.
297. Martinez-Martin, N., et al., *Cooperativity between T cell receptor complexes revealed by conformational mutants of CD3epsilon.* Sci Signal, 2009. **2**(83): p. ra43.
298. Wang, Y., et al., *A conserved CXXC motif in CD3epsilon is critical for T cell development and TCR signaling.* PLoS Biol, 2009. **7**(12): p. e1000253.
299. Mohan, S., et al., *Association energetics of cross-reactive and specific antibodies.* Biochemistry, 2009. **48**(6): p. 1390-8.
300. Fernandes, R.A., et al., *T cell receptors are structures capable of initiating signaling in the absence of large conformational rearrangements.* J Biol Chem, 2012. **287**(16): p. 13324-35.
301. Gil, D., et al., *Recruitment of Nck by CD3 epsilon reveals a ligand-induced conformational change essential for T cell receptor signaling and synapse formation.* Cell, 2002. **109**(7): p. 901-12.
302. Risueno, R.M., W.W. Schamel, and B. Alarcon, *T cell receptor engagement triggers its CD3epsilon and CD3zeta subunits to adopt a compact, locked conformation.* PLoS One, 2008. **3**(3): p. e1747.
303. Xu, C., et al., *Regulation of T cell receptor activation by dynamic membrane binding of the CD3epsilon cytoplasmic tyrosine-based motif.* Cell, 2008. **135**(4): p. 702-13.
304. Deford-Watts, L.M., et al., *The cytoplasmic tail of the T cell receptor CD3 epsilon subunit contains a phospholipid-binding motif that regulates T cell functions.* J Immunol, 2009. **183**(2): p. 1055-64.
305. Kuhns, M.S. and M.M. Davis, *The safety on the TCR trigger.* Cell, 2008. **135**(4): p. 594-6.
306. O'Shea, J.J., et al., *Activation of human peripheral blood T lymphocytes by pharmacological induction of protein-tyrosine phosphorylation.* Proc Natl Acad Sci U S A, 1992. **89**(21): p. 10306-10.
307. Secrist, J.P., et al., *Stimulatory effects of the protein tyrosine phosphatase inhibitor, pervanadate, on T-cell activation events.* J Biol Chem, 1993. **268**(8): p. 5886-93.
308. Imbert, V., et al., *Induction of tyrosine phosphorylation and T-cell activation by vanadate peroxide, an inhibitor of protein tyrosine phosphatases.* Biochem J, 1994. **297 (Pt 1)**: p. 163-73.
309. Fernandes, R.A., et al., *What controls T cell receptor phosphorylation?* Cell, 2010. **142**(5): p. 668-9.

310. Burroughs, N.J., Z. Lazic, and P.A. van der Merwe, *Ligand detection and discrimination by spatial relocalization: A kinase-phosphatase segregation model of TCR activation.* Biophys J, 2006. **91**(5): p. 1619-29.
311. Hopfield, J.J., *Kinetic proofreading: a new mechanism for reducing errors in biosynthetic processes requiring high specificity.* Proc Natl Acad Sci U S A, 1974. **71**(10): p. 4135-9.
312. McKeithan, T.W., *Kinetic proofreading in T-cell receptor signal transduction.* Proc Natl Acad Sci U S A, 1995. **92**(11): p. 5042-6.
313. Lin, J. and A. Weiss, *The tyrosine phosphatase CD148 is excluded from the immunologic synapse and down-regulates prolonged T cell signaling.* J Cell Biol, 2003. **162**(4): p. 673-82.
314. Bunnell, S.C., et al., *T cell receptor ligation induces the formation of dynamically regulated signaling assemblies.* J Cell Biol, 2002. **158**(7): p. 1263-75.
315. Irles, C., et al., *CD45 ectodomain controls interaction with GEMs and Lck activity for optimal TCR signaling.* Nat Immunol, 2003. **4**(2): p. 189-97.
316. Sicheri, F. and J. Kuriyan, *Structures of Src-family tyrosine kinases.* Curr Opin Struct Biol, 1997. **7**(6): p. 777-85.
317. Stepanek, O., et al., *Regulation of Src family kinases involved in T cell receptor signaling by protein-tyrosine phosphatase CD148.* J Biol Chem, 2011. **286**(25): p. 22101-12.
318. Choudhuri, K., et al., *T-cell receptor triggering is critically dependent on the dimensions of its peptide-MHC ligand.* Nature, 2005. **436**(7050): p. 578-82.
319. Choudhuri, K., et al., *Peptide-major histocompatibility complex dimensions control proximal kinase-phosphatase balance during T cell activation.* J Biol Chem, 2009. **284**(38): p. 26096-105.
320. Geppert, T.D. and P.E. Lipsky, *Accessory cell independent proliferation of human T4 cells stimulated by immobilized monoclonal antibodies to CD3.* J Immunol, 1987. **138**(6): p. 1660-6.
321. Ma, Z., et al., *Surface-anchored monomeric agonist pMHCs alone trigger TCR with high sensitivity.* PLoS Biol, 2008. **6**(2): p. e43.
322. James, S.E., et al., *Antigen sensitivity of CD22-specific chimeric TCR is modulated by target epitope distance from the cell membrane.* J Immunol, 2008. **180**(10): p. 7028-38.
323. Bluemel, C., et al., *Epitope distance to the target cell membrane and antigen size determine the potency of T cell-mediated lysis by BiTE antibodies specific for a large melanoma surface antigen.* Cancer Immunol Immunother, 2010. **59**(8): p. 1197-209.
324. Horejsi, V., *Lipid rafts and their roles in T-cell activation.* Microbes Infect, 2005. **7**(2): p. 310-6.
325. Lingwood, D. and K. Simons, *Lipid rafts as a membrane-organizing principle.* Science, 2010. **327**(5961): p. 46-50.
326. Gaus, K., et al., *Condensation of the plasma membrane at the site of T lymphocyte activation.* J Cell Biol, 2005. **171**(1): p. 121-31.
327. Zech, T., et al., *Accumulation of raft lipids in T-cell plasma membrane domains engaged in TCR signalling.* EMBO J, 2009. **28**(5): p. 466-76.
328. Harder, T. and D. Sangani, *Plasma membrane rafts engaged in T cell signalling: new developments in an old concept.* Cell Commun Signal, 2009. **7**: p. 21.
329. Glebov, O.O. and B.J. Nichols, *Lipid raft proteins have a random distribution during localized activation of the T-cell receptor.* Nat Cell Biol, 2004. **6**(3): p. 238-43.
330. Hashimoto-Tane, A., et al., *T-cell receptor microclusters critical for T-cell activation are formed independently of lipid raft clustering.* Mol Cell Biol, 2010. **30**(14): p. 3421-9.
331. Pizzo, P., et al., *Lipid rafts and T cell receptor signaling: a critical re-evaluation.* Eur J Immunol, 2002. **32**(11): p. 3082-91.
332. Alonso, A., et al., *Protein tyrosine phosphatases in the human genome.* Cell, 2004. **117**(6): p. 699-711.

333. Van Wauwe, J.P., J.R. De Mey, and J.G. Goossens, *OKT3: a monoclonal anti-human T lymphocyte antibody with potent mitogenic properties.* J Immunol, 1980. **124**(6): p. 2708-13.
334. Siefken, R., R. Kurrle, and R. Schwinzer, *CD28-mediated activation of resting human T cells without costimulation of the CD3/TCR complex.* Cell Immunol, 1997. **176**(1): p. 59-65.
335. Broeren, C.P., et al., *Costimulation light: activation of CD4+ T cells with CD80 or CD86 rather than anti-CD28 leads to a Th2 cytokine profile.* J Immunol, 2000. **165**(12): p. 6908-14.
336. Riley, J.L., et al., *Modulation of TCR-induced transcriptional profiles by ligation of CD28, ICOS, and CTLA-4 receptors.* Proc Natl Acad Sci U S A, 2002. **99**(18): p. 11790-5.
337. Viola, A., et al., *T lymphocyte costimulation mediated by reorganization of membrane microdomains.* Science, 1999. **283**(5402): p. 680-2.
338. Bromley, S.K., et al., *The immunological synapse and CD28-CD80 interactions.* Nat Immunol, 2001. **2**(12): p. 1159-66.
339. Mestas, J. and C.C. Hughes, *Of mice and not men: differences between mouse and human immunology.* J Immunol, 2004. **172**(5): p. 2731-8.
340. He, X., et al., *Anti-human tissue factor antibody ameliorated intestinal ischemia reperfusion-induced acute lung injury in human tissue factor knock-in mice.* PLoS One, 2008. **3**(1): p. e1527.
341. Kuhn, C., et al., *Human CD3 transgenic mice: preclinical testing of antibodies promoting immune tolerance.* Sci Transl Med, 2011. **3**(68): p. 68ra10.
342. Lute, K.D., et al., *Human CTLA4 knock-in mice unravel the quantitative link between tumor immunity and autoimmunity induced by anti-CTLA-4 antibodies.* Blood, 2005. **106**(9): p. 3127-33.
343. Lin, D.Y., et al., *The PD-1/PD-L1 complex resembles the antigen-binding Fv domains of antibodies and T cell receptors.* Proc Natl Acad Sci U S A, 2008. **105**(8): p. 3011-6.
344. Crotty, S., *Follicular helper CD4 T cells (TFH).* Annu Rev Immunol, 2011. **29**: p. 621-63.
345. Dorfman, D.M., et al., *Programmed death-1 (PD-1) is a marker of germinal center-associated T cells and angioimmunoblastic T-cell lymphoma.* Am J Surg Pathol, 2006. **30**(7): p. 802-10.
346. Linterman, M.A., et al., *Foxp3+ follicular regulatory T cells control the germinal center response.* Nat Med, 2011. **17**(8): p. 975-82.
347. Brown, K.E., et al., *Role of PD-1 in regulating acute infections.* Curr Opin Immunol, 2010. **22**(3): p. 397-401.
348. Fuse, S., et al., *Recall responses by helpless memory CD8+ T cells are restricted by the up-regulation of PD-1.* J Immunol, 2009. **182**(7): p. 4244-54.
349. Allie, S.R., et al., *Programmed death 1 regulates development of central memory CD8 T cells after acute viral infection.* J Immunol, 2011. **186**(11): p. 6280-6.
350. Watson, M.P., A.J. George, and D.F. Larkin, *Differential effects of costimulatory pathway modulation on corneal allograft survival.* Invest Ophthalmol Vis Sci, 2006. **47**(8): p. 3417-22.
351. Kronenberg, M. and A. Rudensky, *Regulation of immunity by self-reactive T cells.* Nature, 2005. **435**(7042): p. 598-604.
352. Sakaguchi, S., et al., *Regulatory T cells and immune tolerance.* Cell, 2008. **133**(5): p. 775-87.
353. Tang, Q., et al., *Cutting edge: CD28 controls peripheral homeostasis of CD4+CD25+ regulatory T cells.* J Immunol, 2003. **171**(7): p. 3348-52.
354. Fontenot, J.D., M.A. Gavin, and A.Y. Rudensky, *Foxp3 programs the development and function of CD4+CD25+ regulatory T cells.* Nat Immunol, 2003. **4**(4): p. 330-6.
355. Hori, S., T. Nomura, and S. Sakaguchi, *Control of regulatory T cell development by the transcription factor Foxp3.* Science, 2003. **299**(5609): p. 1057-61.
356. Chen, W., et al., *Conversion of peripheral CD4+CD25- naive T cells to CD4+CD25+ regulatory T cells by TGF-beta induction of transcription factor Foxp3.* J Exp Med, 2003. **198**(12): p. 1875-86.

357. Coombes, J.L., et al., *A functionally specialized population of mucosal CD103+ DCs induces Foxp3+ regulatory T cells via a TGF-beta and retinoic acid-dependent mechanism.* J Exp Med, 2007. **204**(8): p. 1757-64.
358. Fantini, M.C., et al., *Cutting edge: TGF-beta induces a regulatory phenotype in CD4+CD25- T cells through Foxp3 induction and down-regulation of Smad7.* J Immunol, 2004. **172**(9): p. 5149-53.
359. Rubtsov, Y.P. and A.Y. Rudensky, *TGFbeta signalling in control of T-cell-mediated self-reactivity.* Nat Rev Immunol, 2007. **7**(6): p. 443-53.
360. Engelhardt, B. and R.M. Ransohoff, *The ins and outs of T-lymphocyte trafficking to the CNS: anatomical sites and molecular mechanisms.* Trends Immunol, 2005. **26**(9): p. 485-95.
361. Rebenko-Moll, N.M., et al., *Chemokines, mononuclear cells and the nervous system: heaven (or hell) is in the details.* Curr Opin Immunol, 2006. **18**(6): p. 683-9.
362. Villares, R., et al., *CCR6 regulates EAE pathogenesis by controlling regulatory CD4+ T-cell recruitment to target tissues.* Eur J Immunol, 2009. **39**(6): p. 1671-81.
363. Kroner, A., et al., *Accelerated course of experimental autoimmune encephalomyelitis in PD-1-deficient central nervous system myelin mutants.* Am J Pathol, 2009. **174**(6): p. 2290-9.
364. Carter, L.L., et al., *PD-1/PD-L1, but not PD-1/PD-L2, interactions regulate the severity of experimental autoimmune encephalomyelitis.* J Neuroimmunol, 2007. **182**(1-2): p. 124-34.
365. Ravetch, J.V. and S. Bolland, *IgG Fc receptors.* Annu Rev Immunol, 2001. **19**: p. 275-90.
366. Iruretagoyena, M.I., et al., *Activating and inhibitory Fcgamma receptors can differentially modulate T cell-mediated autoimmunity.* Eur J Immunol, 2008. **38**(8): p. 2241-50.
367. Ghiotto, M., et al., *PD-L1 and PD-L2 differ in their molecular mechanisms of interaction with PD-1.* Int Immunol, 2010. **22**(8): p. 651-60.
368. Valitutti, S., et al., *Serial triggering of many T-cell receptors by a few peptide-MHC complexes.* Nature, 1995. **375**(6527): p. 148-51.
369. Chodorge, M., et al., *A series of Fas receptor agonist antibodies that demonstrate an inverse correlation between affinity and potency.* Cell Death Differ, 2012. **19**(7): p. 1187-95.
370. Carreno, B.M. and M. Collins, *The B7 family of ligands and its receptors: new pathways for costimulation and inhibition of immune responses.* Annu Rev Immunol, 2002. **20**: p. 29-53.
371. Raghavan, M. and P.J. Bjorkman, *Fc receptors and their interactions with immunoglobulins.* Annu Rev Cell Dev Biol, 1996. **12**: p. 181-220.
372. Chames, P., et al., *Therapeutic antibodies: successes, limitations and hopes for the future.* Br J Pharmacol, 2009. **157**(2): p. 220-33.
373. Michaelsen, T.E., et al., *The four mouse IgG isotypes differ extensively in bactericidal and opsonophagocytic activity when reacting with the P1.16 epitope on the outer membrane PorA protein of Neisseria meningitidis.* Scand J Immunol, 2004. **59**(1): p. 34-9.
374. Wollenberg, I., et al., *Regulation of the germinal center reaction by Foxp3+ follicular regulatory T cells.* J Immunol, 2011. **187**(9): p. 4553-60.
375. Carter, L., et al., *PD-1:PD-L inhibitory pathway affects both CD4(+) and CD8(+) T cells and is overcome by IL-2.* Eur J Immunol, 2002. **32**(3): p. 634-43.
376. Daniel, C., et al., *Enhancement of antigen-specific Treg vaccination in vivo.* Proc Natl Acad Sci U S A, 2010. **107**(37): p. 16246-51.
377. Emerson, M.R., et al., *Enhancing the ability of experimental autoimmune encephalomyelitis to serve as a more rigorous model of multiple sclerosis through refinement of the experimental design.* Comp Med, 2009. **59**(2): p. 112-28.
378. Minami, Y., L.E. Samelson, and R.D. Klausner, *Internalization and cycling of the T cell antigen receptor. Role of protein kinase C.* J Biol Chem, 1987. **262**(27): p. 13342-7.
379. Nimmerjahn, F. and J.V. Ravetch, *Divergent immunoglobulin g subclass activity through selective Fc receptor binding.* Science, 2005. **310**(5753): p. 1510-2.

380. Nimmerjahn, F. and J.V. Ravetch, *Fcgamma receptors: old friends and new family members.* Immunity, 2006. **24**(1): p. 19-28.
381. Corse, E., R.A. Gottschalk, and J.P. Allison, *Strength of TCR-peptide/MHC interactions and in vivo T cell responses.* J Immunol, 2011. **186**(9): p. 5039-45.
382. Sakuishi, K., et al., *Targeting Tim-3 and PD-1 pathways to reverse T cell exhaustion and restore anti-tumor immunity.* J Exp Med, 2010. **207**(10): p. 2187-94.
383. Ding, H., et al., *Delivering PD-1 inhibitory signal concomitant with blocking ICOS co-stimulation suppresses lupus-like syndrome in autoimmune BXSB mice.* Clin Immunol, 2006. **118**(2-3): p. 258-67.
384. Thompson, R.H., et al., *Costimulatory B7-H1 in renal cell carcinoma patients: Indicator of tumor aggressiveness and potential therapeutic target.* Proc Natl Acad Sci U S A, 2004. **101**(49): p. 17174-9.
385. Wu, C., et al., *Immunohistochemical localization of programmed death-1 ligand-1 (PD-L1) in gastric carcinoma and its clinical significance.* Acta Histochem, 2006. **108**(1): p. 19-24.
386. Hamanishi, J., et al., *Programmed cell death 1 ligand 1 and tumor-infiltrating CD8+ T lymphocytes are prognostic factors of human ovarian cancer.* Proc Natl Acad Sci U S A, 2007. **104**(9): p. 3360-5.
387. Brahmer, J.R., et al., *Phase I study of single-agent anti-programmed death-1 (MDX-1106) in refractory solid tumors: safety, clinical activity, pharmacodynamics, and immunologic correlates.* J Clin Oncol, 2010. **28**(19): p. 3167-75.
388. Berger, R., et al., *Phase I safety and pharmacokinetic study of CT-011, a humanized antibody interacting with PD-1, in patients with advanced hematologic malignancies.* Clin Cancer Res, 2008. **14**(10): p. 3044-51.
389. Yi, J.S., M.A. Cox, and A.J. Zajac, *T-cell exhaustion: characteristics, causes and conversion.* Immunology, 2010. **129**(4): p. 474-81.
390. Riley, J.L., *PD-1 signaling in primary T cells.* Immunol Rev, 2009. **229**(1): p. 114-25.
391. Sage, P.T., et al., *The receptor PD-1 controls follicular regulatory T cells in the lymph nodes and blood.* Nat Immunol, 2012. **14**(2): p. 152-61.
392. del Rio, M.L., et al., *Antibody-mediated signaling through PD-1 costimulates T cells and enhances CD28-dependent proliferation.* Eur J Immunol, 2005. **35**(12): p. 3545-60.
393. Dong, H., et al., *B7-H1, a third member of the B7 family, co-stimulates T-cell proliferation and interleukin-10 secretion.* Nat Med, 1999. **5**(12): p. 1365-9.
394. Tamura, H., et al., *B7-H1 costimulation preferentially enhances CD28-independent T-helper cell function.* Blood, 2001. **97**(6): p. 1809-16.
395. Shin, T., et al., *Cooperative B7-1/2 (CD80/CD86) and B7-DC costimulation of CD4+ T cells independent of the PD-1 receptor.* J Exp Med, 2003. **198**(1): p. 31-8.
396. Dong, H. and X. Chen, *Immunoregulatory role of B7-H1 in chronicity of inflammatory responses.* Cell Mol Immunol, 2006. **3**(3): p. 179-87.
397. Liu, X., et al., *B7DC/PDL2 promotes tumor immunity by a PD-1-independent mechanism.* J Exp Med, 2003. **197**(12): p. 1721-30.
398. Sfriso, P., et al., *Infections and autoimmunity: the multifaceted relationship.* J Leukoc Biol, 2010. **87**(3): p. 385-95.